AD_____

Award Number: DAMD17-99-1-9564 Volume I

TITLE: Role of Angiogenesis in the Etiology and Prevention of Ovarian Cancer

I: Effect of Angiogenesis Inhibitors in Preventing Ovarian Cancer Growth

PRINCIPAL INVESTIGATOR: Sundaram Ramakrishnan, Ph.D.

CONTRACTING ORGANIZATION: University of Minnesota
Minneapolis, MN 55455-2070

REPORT DATE: October 2003

TYPE OF REPORT: Annual

PREPARED FOR: U.S. Army Medical Research and Materiel Command
Fort Detrick, Maryland 21702-5012

REPORT DOCUMENTATION PAGE

Form Approved
OMB No. 074-0188

1. AGENCY USE ONLY (Leave blank)	2. REPORT DATE	3. REPORT TYPE AND DATES COVERED
	October 2003	Annual (1 Oct 2002 - 30 Sep 2003)

4. TITLE AND SUBTITLE
Role of Angiogenesis in the Etiology and Prevention of Ovarian Cancer
I: Effect of Angiogenesis Inhibitors in Preventing Ovarian Cancer Growth

5. FUNDING NUMBERS
DAMD17-99-1-9564

6. AUTHOR(S)
Sundaram Ramakrishnan, Ph.D.

7. PERFORMING ORGANIZATION NAME(S) AND ADDRESS(ES)
University of Minnesota
Minneapolis, MN 55455-2070

E-Mail: sunda001@tc.umn.edu

8. PERFORMING ORGANIZATION REPORT NUMBER

9. SPONSORING / MONITORING AGENCY NAME(S) AND ADDRESS(ES)
U.S. Army Medical Research and Materiel Command
Fort Detrick, Maryland 21702-5012

10. SPONSORING / MONITORING AGENCY REPORT NUMBER

11. SUPPLEMENTARY NOTES
This is Volume I of IV
Original contains color plates: ALL DTIC reproductions will be in black and white

12a. DISTRIBUTION / AVAILABILITY STATEMENT
Approved for Public Release; Distribution Unlimited

12b. DISTRIBUTION CODE

13. ABSTRACT (Maximum 200 Words)

Primary growth of ovarian cancer and its spreading in the peritoneal cavity as micrometastases are dependent on angiogenesis. Therefore, angiogenesis inhibitors can be used in the prevention and treatment of ovarian cancers. One of the objectives of Project 1 is the development of a genetically reengineered angiostatic protein, endostatin. A mutant endostatin containing a single amino acid substitution at position 125 (P125A-endostatin) was found to be more active than the native protein. P125A endostatin was further modified to incorporate vascular targeting sequence, RGD, so that the bioavailability can be increased at the tumor vasculature. Modified endostatins were evaluated for antiangiogenic and antitumor activities in model systems. Genetic modifications significantly improved the biological activity of endostatin. Synthetic peptides corresponding to the mutation site were made to characterize the mechanism of enhanced antiangiogenic activity.

14. SUBJECT TERMS
Ovarian Cancer

15. NUMBER OF PAGES
110

16. PRICE CODE

17. SECURITY CLASSIFICATION OF REPORT	18. SECURITY CLASSIFICATION OF THIS PAGE	19. SECURITY CLASSIFICATION OF ABSTRACT	20. LIMITATION OF ABSTRACT
Unclassified	Unclassified	Unclassified	Unlimited

Table of Contents

(4) INTRODUCTION:

Establishment of new blood supply (angiogenesis) is necessary for ovarian cancers to grow and spread inside the peritoneum (1 –3). Angiognesis is a complex process involving growth factors and matrix degrading proteases (4) . Angiogenesis can also be inhibited by a number of proteolytic fragments of the coagulation cascade. One of the well-studied antiangiogenic molecule is endostatin, which, is produced by the proteolysis of collagen type XVIII that is selectively expressed on vascular basement membrane (5,6). We have earlier shown that a mouse endostatin is effective in inhibiting ovarian cancer growth in athymic mice (7). Furthermore, endostatin treatment delayed the appearance of malignant lesions in a transgenic mouse line, which has been genetically modified to develop mammary adenocarcinomas (8). These studies demonstrated the potential of using antiangiogenic molecules to prevent and treat ovarian cancer. While native endostatin was effective in inhibiting cancer growth, its biological activity can be further improved by genetically redesigning the molecule to enhance bioavailability, tumor homing and potency. Structure-function studies are necessary to accomplish this goal. Endostatin binds to integrins and glypicans expressed on endothelial cell surface (9,10). Regions of endostatin involved in binding these molecules are not completely understood. During expression cloning of human endostatin, we identified a mutant protein containing a substitution of proline to an alanine (P125A) . Pro_{125}, is located immediately upstream to Asn-Gly-Arg (NGR) sequence. NGR containing peptides target tumor vasculature and inhibit endothelial membrane associated aminopeptidase N activity. Therefore investigations were carried out with the mutant endostatin and the native protein.

(5) BODY :

Hypothesis and Purpose : Ovarian cancer growth and peritoneal spread is dependent on neovascularization. Furthermore, angiogenic growth factors such as VEGF play an important role in the development of malignant ascites. Therefore, inhibition angiogenesis will have a significant impact on the development of ovarian cancer. The purpose of the present study is to determine the effect of angiogenesis inhibitors on ovarian cancer growth.

Task 1 : Large-scale production of angiostatin and endostatin. Evaluate their efficacy in ovarian cancer model systems. This task has been completed. Fermentation conditions have been optimized to make large-scale production of endostatin in yeast. Major findings from this study are that mutant endostatin containing a single amino acid substitution, P125A endostatin was prepared and characterized. P125A-endostatin is better in inhibiting ovarian and breast cancer growth. Endostatin treatment inhibits angiogenesis related gene expression at the tumor site.

Task # 2 : Alternate methods to improve antitumor activity of angiostatin and endostatin. Angiogenic inhibitors in combination with chemotherapy for example are

likely to be synergistic in inhibiting ovarian cancer growth. Two strategies were proposed ; a) combination treatment with chemotherapy and an angiogenesis inhibitor and b) genetic modification of endostatin to improve its bioavailability and potency. For the later approach, endostatin was modified with specific vascular targeting motifs. Construction and preliminary characterization of these constructs began in year two instead of year three as originally proposed .

Results Related to the Task # 2 completed in Year 4 :

A number of chemotherapeutic drugs were tested for differential effects on endothelial cells. Interestingly, carboplatin, maphosphamide, methotrexate, melphalan and chlorambucil induced survival signals in endothelial cells by producing VEGF. VEGF secretion was transcriptionally upregulated upon treatment and protected endothelial cells from apoptosis. Neutralization of VEGF by antibodies sensitized endothelial cells to chemotherapeutic drugs. Based on these observations, in vivo studies were carried out using human ovarian cancer xenografts in mice. Treatment of ovarian cancer bearing mice with carboplatin and anti=VEGF antibodies synergistically inhibited tumor growth. Endothelial cell survival signal therefore offers a mechanistic understanding for combining antiangiogenic and chemotherapy for better clinical outcome (manuscript under review, attached).

Ongoing studies include, the effect of endostatin plus carboplatin on ovarian cancer growth. These studies will be completed during the current year (no-cost-extension).

Task # 3. Investigate genetically engineered endostatin to inhibit ovarian cancer growth. Since P125A-endostatin showed improved antiangiogenic activities, it was important to understand the mechanism of action. Both mutant and native endostatin did not affect the amino peptidase activity indicating that this enzyme may not be the target for endostatin. Two synthetic peptides were made on containing the mutation and the other corresponding to the native sequence. Both peptides are then characterized for their ability to inhibit endothelial cell proliferation in vitro. Summary of these studies are communicated to the Br. J. Cancer (manuscript attached).

RGD addition to P125A-endostatin enhanced the biological activity even further. Carboxyl terminus modification produced better activity when compared to the amino terminus mutation. Presence of RGD increased the amount of endostatin that can localize onto tumor vasculature . P125A-endostatin was then microencapsulated into alginate beads for slow release. Slow release preparations vastly improved inhibition of tumor growth (Manuscript communicated to Clin. Cancer Res., attached).

(6) KEY RESEARCH ACCOMPLISHMENTS IN YEAR 4:

- P125A-endostatin mediated antiangiogenic effect was characterized.

- Vascular targeting sequence, RGD, addition to mutant endostatin (P125A) improved its tumor homing properties.
- Endostatin-RGD was more effective in inhibiting ovarian cancer growth .
- As an alternate to protein delivery, gene therapy vectors were constructed.
- These constructs will be evaluated in prevention trials using transgenic mouse models.
-

(7) **REPORTABLE OUTCOMES** :

Manuscripts :

1. Robert Wild, Ruud P.M. Dings, I. V. Subramanian and S. Ramakrishnan. Carboplatin selectively induces the VEGF stress response in endothelial cells : Synergistic inhibition of tumor growth by combination treatment with antibody to VEGF. (Int. J. Cancer . revised).

2. Yumi Yokoyama and S. Ramakrishnan. Substitution of a single amino acid residue in human endostatin potentiates inhibition of cancer growth. (communicated to Brit. J. Cancer 2003).

3. Yumi Yokoyama and S. Ramakrishnan. Addition of integrin binding sequence to a mutant endostatin improves inhibition of tumor growth. (communicated to Clin. Cancer Res., 2003).

(9) **CONCLUSIONS** :

We conclude from the studies carried out in Year 4 that human endostatin can be genetically modified to improve its biological activity. Point mutation at position 125 suggests that this region may hold important functional information determining biological activity. Addition of vascular targeting sequence to endostatin offers potential therapeutic benefit by improving bioavailability at the tumor site. Based on these studies, we believe that long term delivery of second generation endostatins will have clinical utility in secondary prevention of ovarian cancer.

(10) **REFERENCES** :

1. O'Reilly, M.S., T. Boehm, Y. Shing, N. Fukai, G. Vasios, W.S. Lane, E. Flynn, J.R. Birkhead, B.R. Olsen, and J. Folkman. 1997. Endostatin: an endogenous inhibitor of angiogenesis and tumor growth. *Cell*. 88:277-285.

2. Dhanabal, M., R. Ramchandran, R. Volk, I.E. Stillman, M. Lombardo, M.L. Iruela-Arispe, M. Simons, and V.P. Sukhatme. 1999. Endostatin: yeast production, mutants, and antitumor effect in renal cell carcinoma. *Cancer Res.* 59:189-197.

3. Boehm, T., J. Folkman, T. Browder, and M.S. O'Reilly. 1997. Antiangiogenic therapy of experimental cancer does not induce acquired drug resistance. *Nature.* 390:404-407.

4. Boehm, T., S. O'Reilly M, K. Keough, J. Shiloach, R. Shapiro, and J. Folkman. 1998. Zinc-binding of endostatin is essential for its antiangiogenic activity. *Biochem Biophys Res Commun.* 252:190-194.

5. Yamaguchi, N., B. Anand-Apte, M. Lee, T. Sasaki, N. Fukai, R. Shapiro, I. Que, C. Lowik, R. Timpl, and B.R. Olsen. 1999. Endostatin inhibits VEGF-induced endothelial cell migration and tumor growth independently of zinc binding. *Embo J.* 18:4414-4423.

6. Sasaki, T., H. Larsson, J. Kreuger, M. Salmivirta, L. Claesson-Welsh, U. Lindahl, E. Hohenester, and R. Timpl. 1999. Structural basis and potential role of heparin/heparan sulfate binding to the angiogenesis inhibitor endostatin. *Embo J.* 18:6240-6248.

7. Rehn, M., T. Veikkola, E. Kukk-Valdre, H. Nakamura, M. Ilmonen, C. Lombardo, T. Pihlajaniemi, K. Alitalo, and K. Vuori. 2001. Interaction of endostatin with integrins implicated in angiogenesis. *Proc Natl Acad Sci U S A.* 98:1024-1029.

8. Karumanchi, S.A., V. Jha, R. Ramchandran, A. Karihaloo, L. Tsiokas, B. Chan, M. Dhanabal, J.I. Hanai, G. Venkataraman, Z. Shriver, N. Keiser, R. Kalluri, H. Zeng, D. Mukhopadhyay, R.L. Chen, A.D. Lander, K. Hagihara, Y. Yamaguchi, R. Sasisekharan, L. Cantley, and V.P. Sukhatme. 2001. Cell surface glypicans are low-affinity endostatin receptors. *Mol Cell.* 7:811-822.

9. Dhanabal, M., R. Ramchandran, M.J. Waterman, H. Lu, B. Knebelmann, M. Segal, and V.P. Sukhatme. 1999. Endostatin induces endothelial cell apoptosis. *J Biol Chem.* 274:11721-11726.

10. Shichiri, M., and Y. Hirata. 2001. Antiangiogenesis signals by endostatin. *Faseb J.* 15:1044-1053.

(11) **APPENDICES** :

1. Robert Wild, Ruud P.M. Dings, I. V. Subramanian and S. Ramakrishnan. Carboplatin selectively induces the VEGF stress response in endothelial cells : Synergistic inhibition of tumor growth by combination treatment with antibody to VEGF. (Int. J. Cancer . revised).

2. Yumi Yokoyama and S. Ramakrishnan. Substitution of a single amino acid residue in human endostatin potentiates inhibition of cancer growth. (communicated to Brit. J. Cancer 2003).

3. Yumi Yokoyama and S. Ramakrishnan. Addition of integrin binding sequence to a mutant endostatin improves inhibition of tumor growth. (communicated to Clin. Cancer Res., 2003).

Journal: International Journal of Cancer
Article Type: Research paper
Category: Cancer Cell Biology
File: Wild carbo et al.doc
Date: 22 June 2003

Carboplatin selectively induces the VEGF stress response in endothelial cells: synergistic inhibition of tumor growth by combination treatment with antibody to VEGF

Robert Wild[1$], Ruud P.M. Dings[1] and S. Ramakrishnan[1,2*]
Departments of [1]Pharmacology, [2]Obstetrics/Gynecology, Comprehensive Cancer Center
University of Minnesota Medical School, Minneapolis, MN 55455, USA

Running Title: Carboplatin and VEGF antibody combination treatment

Total number of pages: 23
Total number of figures: 5
Total number of tables: 1

*Address correspondence to:
Dr. S. Ramakrishnan, Department of Pharmacology. University of Minnesota 6-120 Jackson Hall, 321 Church Street SE, Minneapolis, MN 55455
Phone: (612) 626-6461; Fax : (612) 625-8408; E-mail: sunda001@umn.edu
$Present address: Pharmaceutical Research Institute,
Bristol-Myers Squibb, Princeton, NJ USA

ABSTRACT

Vascular Endothelial Growth Factor (VEGF) functions as a key regulator in tumor angiogenesis. In addition, VEGF is an important survival factor for endothelial cells under chemical or physical stress. In this report, we show that treatment of endothelial cells with the chemotherapeutic agent, carboplatin, significantly increased the expression of VEGF. Furthermore, neutralization of secreted VEGF with antibodies sensitized endothelial cells to carboplatin and increased apoptosis several-fold. Interestingly, carboplatin treatment did not alter VEGF expression in tumor cells. Similarly, antibody to VEGF did not change the chemosensitivity of tumor cells to the drug. Most importantly, tumor-bearing animals treated with carboplatin showed an increase in VEGF immunoreactivity in the vasculature, confirming the *in vitro* studies. Based on these observations, we determined whether neutralization of VEGF could enhance the anti-tumor activity of carboplatin in an *in vivo* model system. A combination therapy consisting of a suboptimal dose of carboplatin and VEGF antibody synergistically inhibited solid tumor growth and included multiple complete responses. These findings suggest that VEGF is a critical endothelial cell specific survival factor that is induced by carboplatin and contributes to the protection of tumor vasculature during chemotherapy. These results provide evidence for the mechanism of why chemotherapy combined with anti-VEGF antibodies results in improved anti-tumor effect. This combination therapy should be potentially applicable to many types of malignancies since VEGF expression was differentially induced in tumor vasculature and not in tumor cells..

Key Words: angiogenesis; antibody; carboplatin; chemotherapy; VEGF.

Abbreviations: H&E, hematoxilyn and eosin; HUVEC, human umbilical vein endothelial cells; PBS, phosphate buffered saline; TCID, tissue culture inhibitory dose; VEGF, vascular endothelial growth factor.

INTRODUCTION

Ovarian cancer is the leading cause of death among gynecological malignancies.[Berek, 1999 #317] The current standard treatment regimen consists of surgical debulking of primary tumors followed by platinum-based chemotherapy. However, major limitations are associated with this approach. Insufficient delivery of drugs to tumor tissues is accompanied by major, intolerable toxicity of current chemotherapeutic agents. In addition, the heterogeneity of cancer tissues and the development of drug resistance complicate cancer therapy. As a consequence, even new combination therapies (i.e. carboplatin and taxol) displayed only marginal improvements in overall response rates in ovarian cancer patients.[Ozols, 1998 #318; Ozols, 1999 #319; ICON, 2002 #72] Clearly, there is a need for a better understanding of chemotherapy-induced cancer cell resistance. More importantly, improved treatment modalities are necessary.

Recent studies have shown that tumor angiogenesis may be an alternate target for cancer therapy.[Folkman, 1992 #320; Folkman, 1997 #321] Angiogenesis, the development of new blood vessels from pre-existing vasculature, is one of the processes linked to tumor growth and its metastatic spread. In the absence of neovascularization tumor cells undergo apoptosis and fail to expand.[Folkman, 1997 #321] Tumor angiogenesis is mediated by both tumor cells themselves and the stromal cells creating a unique microenvironment. Several growth factors have been identified as potential regulators of angiogenesis. However, VEGF and its tyrosine kinase receptors, VEGF-R1 (Flt-1) and VEGFR-2 (KDR/Flk-1), have been implicated as key components in the vascularization of a tumor.[Neufeld, 1999 #286] Direct proof for this hypothesis comes from a multitude of experiments, where the disruption of the VEGF signaling pathway inhibited angiogenesis *in vitro* and solid tumor growth *in vivo*.[Kim, 1993 #322; Witte, 1998 #323; Prewett, 1999 #324; Goldman, 1998 #325; Lin, 1998 #55; Lin, 1998 #326; Oku, 1998 #327; Im, 1999 #328; Fong, 1999 #67; Ramakrishnan, 1996 #293; Olson, 1997 #294]

In addition to its central role in regulating tumor angiogenesis, VEGF is also a survival factor for endothelial cells. VEGF expression is induced by hypoxia, which was shown to rescue newly formed endothelial cells in the retina that were exposed to low

oxygen environment.[Alon, 1995 #329] VEGF is also able to save newly formed tumor vessels from undergoing apoptosis.[Benjamin, 1997 #330; Jain, 1998 #331] Moreover, VEGF was shown to inhibit endothelial cell apoptosis induced by tumor necrosis factor-alpha and anchorage disruption.[Spyridopoulos, 1997 #332; Watanabe, 1997 #333] Therefore, VEGF seems to play an important dual role in the progression of a cancer, which include the direct stimulation of neovascularization and the concomitant protection of tumor vessels.

Various reports have shown that antiangiogenic therapies potentiate cytotoxic anticancer therapies in several *in vivo* model systems.[Teicher, 1992 #334; Teicher, 1996 #302; Dings, 2003 #257] Particularly, carboplatin-based therapies were responsive to combination treatment with either the antiangiogenic agents anginex or TNP-470, potent inhibitors of endothelial cell proliferation and migration.[Dings, 2003 #257][Herbst, 1998 #335] However, the exact mechanism of action of this combination strategy is not fully understood. In this report, we show that carboplatin significantly increases the expression of VEGF in endothelial cells *in vitro* and in tumor vessels *in vivo*. Neutralization of VEGF by specific antibodies significantly increased the sensitivity of endothelial cells to Carboplatin. In contrast, antibody to VEGF did not augment the chemosensitivity of tumor cells *in vitro*. We also show that a combination therapy consisting of carboplatin and VEGF antibody produced a more than additive antitumor effect with multiple complete responses in an ovarian cancer model system. Our findings suggest that carboplatin treatment induces the VEGF stress response in tumor vessels and by blocking this survival mechanism, synergistic inhibition of tumor growth can be achieved.

MATERIALS AND METHODS

Cell Culture

Human umbilical vein endothelial cells (HUVEC), were kindly provided by Dr. G. Vercellotti (University of Minnesota, Minneapolis, MN), and maintained in EGM medium (Clonetics, San Diego, CA) in tissue culture flasks pre-coated with 0.1% gelatin (Sigma, St. Louis, MO). HUVEC cultures were used between the second and fourth passage for experiments. MA148, a human epithelial ovarian carcinoma cell line, was

maintained in RPMI 1640 medium (Life Technologies, Grand Island, NY) supplemented with 10% fetal bovine serum (FBS, Cellgro, Mediatech, Washington, DC) and penicillin/streptomycin (Cellgro, Mediatech, Washington, DC). MA148 cultures were split 1:3 every 3 days. All cell lines were maintained at 37 ^{0}C and 5% CO_2.

Anti-VEGF antibody

Polyclonal anti-VEGF antiserum was developed in rabbits by a hyperimmunization protocol using recombinant human VEGF165 as previously described.[Olson, 1996 #337] The antibodies were purified from the serum by affinity chromatography using a Protein A agarose column (Sigma, St. Louis, MO). Similarly, control antibody was obtained from the serum of non-immunized rabbits and purified by Protein A affinity chromatography. Purified IgG fractions were dialyzed in phosphate buffered saline (PBS, pH 7.6) and concentrated to 20 mg/ml by ultrafiltration using a YM-30 membrane (Millipore, Bedford, MA). Antibody samples were then filter sterilized by a 0.2 μm filter (Millipore, Bedford, MA) and stored in aliquots at –20 ^{0}C. Antibody purity was assessed by SDS-PAGE. ELISA and Western Blots were used to determine specificity of the antibody preparations .[Olson, 1996 #337; Olson, 1997 #294]

Measurement of VEGF levels

MA148 or HUVEC were plated at a density of 3 x 10^5 cells/well in a 6-well plate, allowed to attach overnight, and exposed to various concentrations of carboplatin (Sigma, St. Louis, MO). HUVEC were seeded on plates pre-treated with 0.1% gelatin. At 24 and 48 hours time points after carboplatin treatment, VEGF levels in the conditioned media were measured by ELISA (Cytimmune, College Park, MD) and normalized to viable cell number as determined by Trypan Blue exclusion (Sigma, St. Louis, MO).

Cell proliferation assays

Cells (HUVEC or MA148) were seeded at a density of 1x10^4 cells/well into 96-well plates and allowed to attach overnight. Carboplatin and/or antibodies were then prepared in different dilutions using the appropriate culture medium and added to the cells. Forty-eight hours after treatment, cells were treated with MTT (Sigma, St. Louis, MO) at 0.5

mg/ml for four hours. Medium was then removed and 100 µl dimethyl sulfoxide (Sigma, St. Louis, MO) was added to each wells. Absorbance was measured at 560 nm with 650 nm background readings subtracted.

Apoptosis assay

Cells (HUVEC/MA148) were seeded at a density of $3x10^4$ cells/well into 8-well chamber slides (Nalge Nunc, Naperville, IL) and allowed to attach overnight. Carboplatin and/or antibodies were then added to the wells. Samples were incubated for forty-eight hours and then analyzed for apoptosis by TUNEL assay (Boehringer Mannheim, Germany). Digital images were acquired using a fluorescence microscope equipped with an Optronics (TEC 470) single chip cooled camera. Metamorph image analysis software (Image 1, Westchester, PA) was used to store the images as TIFF files. Fields were chosen randomly to ensure objectivity of sampling. The files were then opened in Adobe Photoshop (Adobe Inc., Mountain View, CA) and the apoptotic index was estimated by counting the number of TUNEL positive pixels per field using a histogram analysis.

Tumor model

Exponentially growing MA148, a human epithelial ovarian carcinoma cell line, was harvested by trypsinization, washed twice with Hanks' balanced salt solution (Cellgro, Mediatech, Washington, DC) and resuspended at 2×10^7 cells/ml in serum free RPMI 1640 medium. One hundred µl of the suspension was then injected subcutaneously into the flanks of 6 – 8 week old female, athymic, nu/nu mice (National Cancer Institute, Bethesda, MD) and the tumors were allowed to establish. On day ten, the animals were randomized and treatment was initiated. Carboplatin was administered in a sub-optimal dose (32.5 mg/kg) by i.p. injections once every three days for five doses. Anti-VEGF IgG or pre-immune control IgG treatment (2 mg/dose) was given i.p. once every three days for a total of ten injections. Control animals received equal amounts of sterile PBS. Tumor growth was monitored by caliper measurements and tumor volumes were calculated by the formula (tumor volume (mm^3) = $a \times b^2 \times \pi/6$), where 'a' represents the larger diameter and 'b' represents the smaller diameter of the tumor.

For histological examination of the tissues, animals were sacrificed and tumor specimens were harvested at either the conclusion of the carboplatin treatment regimen (day 22) or anti-VEGF IgG treatment schedule (day 40) as indicated.

Histology and immunohistochemistry

Hematoxilyn and eosin (H&E) stainings of paraffin embedded tissue sections were used for general histological examination of the tissue specimens. Frozen sections were prepared for the staining of VEGF and tumor blood vessels in carboplatin treated specimens versus PBS control animals. Harvested tumor tissues were embedded in tissue freezing medium (Miles Inc, Elkhart, IN), snap frozen in liquid nitrogen and subsequently cut into 10 μm thick sections. Next, tissue specimens were slowly brought to room temperature, air dried and subsequently fixed in cold acetone for ten minutes. The slides were then allowed to air dried for one hour and washed three times for 5 minutes in PBS, pH 7.5. The samples were then blocked with PBS containing 0.1% bovine serum albumin for thirty minutes at room temperature. The tissue sections were stained for VEGF with a mouse monoclonal anti-VEGF antibody (VEGF Ab-3 (JH121), Neomarkers, Fremont, CA; 1:20 dilution) which reacted to VEGF preparations from different species for one hour at room temperature. Next, the sections were washed in PBS and incubated with FITC-labeled rabbit anti-mouse IgG antibody (Sigma, St. Louis, MO, 1:20 dilution) for one hour at room temperature. In addition, we simultaneously incubated the slides with phycoerythrin (PE) conjugated to a monoclonal antibody to PECAM-1 (PE conjugated anti-mouse CD31, 1:50 dilution, Pharmingen, San Diego, CA) to stain for blood vessels. The slides were washed three times with PBS, pH 7.5 and immediately imaged in an Olympus BX-60 fluorescence microscope.

Statistical analysis

Statistical significance between treatment groups was determined by one-way ANOVA or the Student's *t*-test.

RESULTS

Differential sensitivity of tumor cells versus endothelial cells to carboplatin

Carboplatin is a potent chemotherapeutic drug used in the treatment of ovarian cancer. In a series of experiments, the *in vitro* sensitivity of ovarian carcinoma cells (MA148) and endothelial cells (HUVEC) to carboplatin was evaluated. MA148 cells were about 100 fold more sensitive to carboplatin than HUVEC (Fig. 1*a*). The tumor cells showed a $TCID_{50}$ of roughly 0.7 μg/ml compared to a $TCID_{50}$ of 50-70 μg/ml for HUVEC. Therefore, endothelial cell populations appear to be less sensitive to carboplatin than tumor cells.

Carboplatin differentially up-regulates VEGF expression in endothelial cells

To further elucidate the apparent resistance of endothelial cells to carboplatin treatment, we investigated the role of Vascular Endothelial Growth Factor (VEGF), a known endothelial cell survival factor, under these conditions. Both ovarian and endothelial cell cultures were treated with their respective $TCID_{50}$ concentration of carboplatin and VEGF levels in the conditioned media were measured by ELISA. Carboplatin treatment did not alter the level of VEGF secreted by the tumor cell line at both 24 and 48 hours time points (Fig. 2*a*). VEGF concentrations ranged between 47.8 and 58.4 pg/1x10^6 cells. However, treatment of HUVEC with carboplatin resulted in a five-fold increase of VEGF levels at 24 hours (22.8 pg/1x10^6 cells for control versus 129.4 pg/1x10^6 cells for carboplatin treated cultures). An even more pronounced effect was seen at the 48 hour time point with a twelve-fold increase in VEGF levels in carboplatin treated HUVEC (17.9 pg/1x10^6 cells for control cells versus 224.2 pg/1x10^6 cells for carboplatin treated cells). These values were statistically significant as determined by the Student's *t*-test ($p < 0.038$).

Antibody to VEGF potentiates the inhibitory activity of carboplatin on endothelial cells

To further verify the above-mentioned hypothesis, we next tested whether the addition of specific antibodies to VEGF could neutralize the growth factor dependent rescue. Carboplatin induced cytotoxicity was determined in the presence or absence of anti-VEGF IgG (30 μg/ml). The addition of anti-VEGF antibody to carboplatin-treated HUVEC significantly increased the cytotoxicity of the chemotherapeutic by 12.58% ($p < 0.014$, Student's *t*-test; Fig. 2*b*). This effect was specific since a corresponding pre-

immune control IgG treatment (30 μg/ml) did not significantly increase the inhibitory effect of the drug ($p > 0.34$). In contrast to endothelial cells, anti-VEGF IgG did not influence the chemosensitivity of tumor cells. In fact, the inhibitory activity of carboplatin was decreased by 10 % with the addition of anti-VEGF IgG and by 3.7% with the use of pre-immune control IgG. However, these changes were not statistically significant ($p > 0.057$ for both points).

We also assessed the effect of exogenous addition of recombinant $VEGF_{165}$ [Mohanraj, 1995 #34] to carboplatin-treated HUVEC. VEGF partially rescued endothelial cells at concentrations between 10-100 ng/ml (data not shown). In contrast, the human ovarian carcinoma cell line did not respond to the exogenous addition of VEGF (data not shown).

Antibody to VEGF increases apoptosis in carboplatin treated endothelial cells

To determine whether carboplatin induced expression of VEGF rescues endothelial cells from apoptosis a TUNEL assay was performed. Addition of the chemotherapeutic drug to HUVEC increased the apoptotic index nine-fold compared to medium control (Fig. 2*c*). More importantly, a combination treatment of carboplatin with anti-VEGF IgG (50 μg/ml) resulted in an additional 1.85-fold increase in apoptotic index versus carboplatin alone treated samples ($p < 0.03$, Student's *t*-test). This effect corresponded to a 17.4-fold increase in apoptosis when compared to medium control. Again, the specificity of this effect was verified with the addition of pre-immune IgG (50 μg/ml), which did not augment the apoptotic response to carboplatin treatment. In comparison, equal concentrations of anti-VEGF or pre-immune antibodies alone did not change the apoptotic index, which was similar to medium control.

Carboplatin specifically up-regulates VEGF expression in tumor vessels in vivo

To determine whether carboplatin could induce VEGF expression *in vivo*, a nude mouse model was employed. MA148 tumor cells, the same carcinoma cell line used for the *in vitro* experiments, were transplanted s.c. into the flanks of female, athymic nude mice. After ten days, small palpable tumors were established and treatment was initiated. A low dose of carboplatin (32.5 mg/kg) [Dings, 2003 #257] was then administered every

three days for five doses, at which point the animals were sacrificed and tumor tissues were harvested. Sections were prepared and immunochemically stained for VEGF and CD31. PBS treated control animals showed a consistent but low expression of VEGF in the tumor tissue (Fig. 3*a*). In contrast, carboplatin treated animals displayed localized increase in the expression of VEGF (Fig. 3*b*). Staining of the tissues with specific antibodies to the endothelial cell marker CD31 was used to identify vascular structures in the tumor tissue (Fig. 3*c* and 3*d*). A subsequent overlay of the images showed a clear co-localization of VEGF in the tumor vasculature of carboplatin treated animals, as identified by the yellow coloring (Fig. 3*f*). In contrast, no significant co-localization was seen in the PBS treated control tissue (Fig. 3*e*).

Antibody to VEGF significantly improves the anti-tumor effects of carboplatin

Subsequently, experiments were carried out to determine the therapeutic benefit of anti-VEGF antibodies during carboplatin chemotherapy. MA148 cells were inoculated s.c. into the flanks of athymic, nude mice and tumors were allowed to establish for ten days. Animals were then randomized and divided into four treatment groups. Tumor growth was then monitored by caliper measurements and the experiments were terminated once tumor volumes reached about 3,000 mm^3.

By the end of the treatment regimen (day 40), administration of low dose carboplatin inhibited the tumor growth by approximately 35% compared control animals (Fig. 4*a*). Similarly, anti-VEGF antibody alone treated mice displayed an inhibition of tumor growth of approximately 25% compared to control animals (Fig. 4*a*). In contrast, the administration of carboplatin in combination with anti-VEGF antibody showed tumor growth inhibition of approximately 75% compared to PBS treated mice. Moreover, combination treatment significantly inhibited tumor growth throughout the entire course of the experiment ($p < 0.04$ for all time as determined by the Student's *t*-test). Most importantly, three mice (23%) of all combination treated animals (cumulative of three experiments) displayed a complete response and remained tumor free for the entire period of observation.

A one-way ANOVA with treatment as the between-subjects factor with 4 levels was used to analyze the combined effects of the three individual experiments. On day 22 (end

of carboplatin treatment) both carboplatin and anti-VEGF IgG did not significantly inhibit tumor growth ($p = 0.0718$ for carboplatin, $p = 0.6324$ for anti-VEGF IgG), whereas combination therapy showed a significant difference in tumor volume compared to PBS ($p = 0.0016$). Similarly, on day 40 (end of antibody treatment) only the combination treatment of carboplatin with anti-VEGF IgG displayed a significant inhibition of tumor growth ($p = 0.0003$, $p = 0.1533$ for carboplatin alone, $p = 0.731$ for anti-VEGF IgG alone). More importantly, tumor volumes from the combination treatment group were also significantly lower than both monotherapies ($p = 0.0229$ compared to carboplatin, $p = 0.0016$ compared to anti-VEGF IgG).

Treatment of tumor bearing animals with non-specific pre-immune IgG (2 mg/dose every three days for ten injections) did not affect the *in vivo* tumor growth rate of MA148 either alone or in combination with carboplatin (Fig. 4*b*). Data points are expressed as a mean relative to mean tumor volume of carboplatin treated animals ($V/V_{carboplatin}$). The results illustrate that the addition of pre-immune control IgG did not significantly alter the inhibitory activity of carboplatin treatment. However, the addition of specific anti-VEGF IgG showed a statistically significant increase in anti-tumor activity when compared to carboplatin monotherapy.

To further determine the overall extend of the combined treatment effect of carboplatin with anti-VEGF IgG, we analyzed the fractional tumor volumes relative to untreated controls. Combination therapy showed a multiplicative effect at both day 22 and day 40 of observation (approximately 2.3-fold higher for both time points; Table 1).

Carboplatin/anti-VEGF antibody combination treatment results in extensive tumor cell apoptosis and necrosis

Human xenograft tumors were surgically removed from the animals by the end of the treatment regimen (day 40) and paraffin embedded for the preparation of tissue sections. Histological analysis demonstrated dramatic differences in tumors from carboplatin/anti-VEGF antibody combination treated animals compared to PBS control or individual drug treatment groups.

A TUNEL assay was used to detect apoptotic cells. Carboplatin or anti-VEGF antibody alone treated animals displayed no difference in apoptosis when compared to

PBS treated control tissues (data not shown). In contrast, animals that received a combination treatment regimen presented an increase in apoptotic cells (data not shown). Similarly, these effects were also seen in H&E stained tissue sections (Fig. 5). Here, carboplatin (Fig. 5*b*) or anti-VEGF antibody (Fig. 5*c*) monotherapy samples displayed a slight increase in apoptotic and necrotic cells (picnotic nuclei) when compared to PBS control (Fig. 5*a*). However, an enormous decrease in cellularity and large areas of necrosis were observed in tissues from combination treated animals (Fig. 5*d*). In addition, a marked increase in fibrous tissue was detected in these samples. Most importantly, histological examination of a tumor sample from a complete responder (Fig. 5*e*) showed that the entire tumor tissue was replaced by fibrous matrix, indicating full remission by combination therapy.

DISCUSSION

Despite significant efforts to produce new and improved treatments, the outcome for patients with ovarian cancer remains poor.[Ozols, 1999 #319] The application of the chemotherapeutic drug, carboplatin, either alone or in combination with paclitaxel, has become the front line therapy for this disease.[Harries, 2001 #27][Tattersall, 2002 #71] However, it is still far from being curative and the development of chemoresistance poses a major challenge. In a recent study, single-agent carboplatin proved to be just as effective as carboplatin plus paclitaxel in women requiring chemotherapy for ovarian cancer. The favorable toxicity profile of carboplatin alone suggested that this is a reasonable option as a single-agent chemotherapeutic.[ICON, 2002 #72] An additional advantage of carboplatin is that, in contrast to other agents such as taxanes, cyclophosphamide and vincristine, it is not an anti-angiogenic by itself.[Dings, 2003 #257] Recent efforts have focused on the application of various combination treatment regimens that include cytotoxic and anti-angiogenic agents. Such combinations have shown to significantly improve the overall anti-tumor response *in vivo*.[Teicher, 1992 #77][Teicher, 1996 #302][Dings, 2003 #257] However, the mechanism underlying this additive effect has not been fully elucidated.

In this report, we show that tumor cells are by far more sensitive to carboplatin than endothelial cells. This differential chemosensitivity could be explained by several factors.

For instance, the proliferative status of target cells can substantially influence its sensitivity to DNA cross-linking drugs. Tumor cells are actively proliferating as indicated by several-fold higher ^{3}H-thymidine incorporation when compared to endothelial cells[1]. Secondly, drug uptake mechanisms could be differentially regulated in tumor cells versus endothelial cells. In addition, DNA repair mechanisms could be substantially different in these two cell types, which could at least in part contribute to the differential chemosensitivity. Lastly, specific cell survival factors could influence the chemosensitivity of various cell types to this drug therapy.

This report provides evidence for the later possibility. The results demonstrate that carboplatin substantially induces the expression of VEGF in endothelial cells *in vitro*. This seems a common response of the endothelial cells upon treatment with chemotherapy[1]. VEGF has been shown to function as an important endothelial cell-specific survival factor that prevents apoptotic cell death. As a consequence, up-regulation of VEGF directly increases cell viability and decreases the overall chemosensitivity of endothelial cells to carboplatin. Proof of principal comes from our experiments where the concomitant neutralization of VEGF by specific antibodies significantly increased the drug-induced cytotoxicity as well as the overall apoptotic response in endothelial cells. Very interestingly, individual administration of the antibody did not result in any endothelial cell death or increased apoptosis. Therefore, our data suggests that carboplatin sensitizes the cells to VEGF and illustrates the necessity of this survival factor under such conditions. In contrast, VEGF levels in the tumor cell line were not altered by carboplatin treatment. In addition, the tumor cells did not respond to either exogenous addition of VEGF or its respective antibodies. As a consequence, the up-regulation of VEGF induced by carboplatin appears to be unique to the endothelial cell population. This is a novel finding, since the predominant notion in the angiogenesis field was that VEGF functions as a paracrine mediator of endothelial cell activity. However, we report here, that this factor also contributes an important autocrine function to this system. It remains to be seen whether carboplatin directly influences the expression of VEGF at the transcriptional (i.e. induction of the VEGF promoter) or

[1] R. Wild and S. Ramakrishnan unpublished data

perhaps at the post-transcriptional level (i.e. increased mRNA stability). Investigations are currently underway to identify such possibilities.

In addition to the implications of carboplatin induced expression of VEGF *in vitro*, we provide evidence for the potential clinical implications of this phenomenon with our *in vivo* experiments. We show that low dose carboplatin treatment to tumor bearing mice significantly up-regulates the expression of VEGF in tumor vessels *in vivo*. This experiment provides evidence that even though both tumor cells and blood vessels are exposed to similar concentrations of carboplatin, a selective increase of VEGF expression was found in the vasculature. Increased levels of this survival factor could potentially save tumor blood vessels from apoptosis, which directly translates into an enhanced overall tumor cell survival. As a consequence, concomitant neutralization of this growth factor with specific anti-VEGF antibodies significantly improved the cytotoxic effects of carboplatin and increased the anti-tumor effect several fold. Similarly, previous studies have shown that ionizing radiation combined with VEGF specific antibodies could improve anti-tumor effects *in vivo,*[Gorski, 1999 #338] possible through the same mechanism.[Kermani, 2001 #341]

Histological analysis of tissue samples provides further evidence for the therapeutic benefit of a carboplatin/anti-VEGF antibody combination therapy. The complete remission in some of the treated animals and the overall increase in apoptotic activity in tumor tissue clearly support the combination regimen. More importantly, improved anti-tumor effects were possible at significantly lower doses of the chemotherapeutic drug, thereby eliminating apparent toxicity.[Dings, 2003 #257]

Finally, the role of VEGF as an endothelial cell specific survival factor could have implications that are even more profound in solid tumor therapy in general. Multiple reports have shown that the combination of antiangiogenic drugs with several different cytotoxic therapeutics can significantly increase the antitumor effects *in vivo*. For instance, the addition of the angiogenesis inhibitor TNP-470/Minocycline to the treatment with paclitaxel and carboplatin resulted in increased antitumor activity and efficacy in non-small-cell lung cancer and breast cancer.[Herbst, 1998 #335] Antiangiogenic modulators also markedly increased the cytotoxicity of cyclophosphamide toward FSaIIC tumor cells.[Teicher, 1993 #339] Similarly,

minocycline significantly increased the growth delay of Lewis lung carcinoma after treatment with the cytotoxic drugs cis-diamminedichloroplatinum(II), melphalan, cyclophosphamide, adriamycin and bleomycin.[Teicher, 1992 #77] Similarly, the neutralization of VEGF in combination with the cytotoxic agent doxorubicin resulted in a more than additive inhibition of tumor cell induced angiogenesis in a dorsal skinfold chamber assay.[Borgstrom, 1999 #340] Therefore, it is conceivable that other chemotherapeutic drugs act similarly on endothelial cells and induce the expression of VEGF. As a consequence, combining conventional chemotherapeutic drugs with agents that are interfering with the VEGF stress response system could be a widely applicable treatment regimen with immediate clinical implications.

ACKNOWLEDGMENTS

We thank Dr. K. Ghosh for technical support and Dr. C. Le and R.L. Bliss (Biostatistics Core, University of Minnesota Cancer Center) for their advice and assistance in statistical analysis. We want to acknowledge Dr. J Kersey (University of Minnesota Cancer Center) for his comments and suggestions. This work was supported in part by grants from NIH CA 71803, DAMD 17-99-1-9564 from ASARMY, Gustaves and Louise Pfeiffer Foundation, Sparboe and Women's Health Fund Endowment (to S.R.) and a doctoral dissertation fellowship from the University of Minnesota Graduate School (to R.W.).

REFERENCES

Table 1 - Carboplatin and anti-VEGF antibody combination treatment results in a more than additive anti-tumor response

Day	Fractional Tumor Volume[a]				
	Carboplatin	Anti-VEGF	Combined (expected)[b]	Combined (observed)	Expected/ observed[c]
22	0.65	0.88	0.57	0.24	2.4
40	0.6	0.72	0.43	0.19	2.3

[a] Fractional tumor volume was obtained by dividing the mean volume of treated tumors by the mean volume of untreated PBS control tumors. All three individual experiments were pooled to determine the overall mean volumes.

[b] Expected combined effect if treatment modalities have additive activities. Obtained by multiplying the individual fractional tumor volumes of both treatments.

[c] Fold increase over additive effect as determined by dividing the combined expected fractional tumor volume by the combined observed fractional tumor volume.

FIGURE LEGENDS

Figure 1 - Differential sensitivity of tumor cells versus endothelial cells to carboplatin. The dose response of carboplatin on endothelial cells (HUVEC) and human ovarian carcinoma cells (MA148) was determined by a non-radioactive cell viability assay (MTT). Values of medium control were considered as 100 % viability. Each point is a mean of triplicate cultures from a representative experiment (error bars denote standard deviation; μ HUVEC, λ MA148).

Figure 2 – Blocking the VEGF response induced by carboplatin with antibody to VEGF potentiates the carboplatin inhibitory activity and increases apoptosis in endothelial cells. Endothelial cell cultures and human ovarian carcinoma cells were exposed to their respective $TCID_{50}$ concentration of carboplatin (0.7 μg/ml for MA148, 50 μg/ml for HUVEC) and conditioned medium was harvested. VEGF levels were measured by ELISA and normalized to cell number (*a*; left panel, 24 hours time point; right panel, 48 hours time point; □ no carboplatin (PBS control), ν carboplatin). Cells were treated with their respective $TCID_{50}$ concentration of carboplatin and supplemented with purified anti-VEGF IgG or pre-immune control IgG (*b*). Forty-eight hours after treatment, cell viability was measured by MTT assay. Absorbance associated with carboplatin treatment alone was considered as 100 % inhibition. Results are expressed as % change in inhibition relative to carboplatin treatment alone (ν anti-VEGF IgG treatment, □ pre-immune IgG treatment). HUVEC were treated with carboplatin and/or antibodies and incubated for forty-eight hours and analyzed for apoptosis by a TUNEL assay (*c*). For all panels data are presented as means of three independent experiments with standard deviation as error bars. *statistical significance as determined by the Student's *t*-test ($p < 0.038$ for both points in panel *a*; $p < 0.014$ in panel *b*; $p < 0.03$ in panel *c*) .

Figure 3 - Carboplatin specifically up-regulates VEGF expression in tumor vessels *in vivo*. Shown are representative sections from the PBS control group (*a*, *c* and *e*) and from the carboplatin treated group (*b*, *d* and *f*). Immunohistochemical localization of VEGF (*a* and *b*) and blood vessels (*c* and *d*) is shown. Co-localization of VEGF and blood vessels

is determined by merging respective images (*e* and *f*). Arrows indicate representative VEGF positive tumor blood vessels. Scale bar = 200 μm for all samples.

Figure 4 - Antibody to VEGF significantly improves the anti-tumor effect of carboplatin. The tumor growth curve of human MA148 ovarian carcinoma is shown in athymic mice (*a*). The groups are defined as control (PBS; square), anti-VEGF IgG (circle), carboplatin (triangle-up), carboplatin + anti-VEGF IgG (triangle down). Data points show the mean tumor volume with respective standard error bars (pooled data from three independent experiments, n = 14-16 animals per group). Tumor growth inhibition is enhanced by the addition of anti-VEGF IgG to carboplatin therapy (*b*). Results are expressed as mean tumor volumes relative to mean carboplatin treated volumes ($V/V_{carboplatin}$). Shown is carboplatin (white bar), carboplatin + anti-VEGF IgG (black bar), carboplatin + pre-immune IgG (gray bar) on day 22 (end of carboplatin treatment) and day 40 (end of antibody treatment). * Statistical significance as determined by Student's *t*-test ($p < 0.033$ for both values compared to carboplatin alone treatment).

Figure 5 - Carboplatin/anti-VEGF antibody combination treatment results in extensive tumor necrosis. MA148 tumor tissues were resected at the end of the treatment schedule (day 40), fixed, embedded in paraffin and sectioned onto slides. Representative H&E stained sections are shown for control (PBS; *a*), carboplatin (*b*), anti-VEGF IgG (*c*), carboplatin + anti-VEGF IgG (*d*) and carboplatin + anti-VEGF IgG complete responder (*e*). Scale bar = 100 μm for all samples.

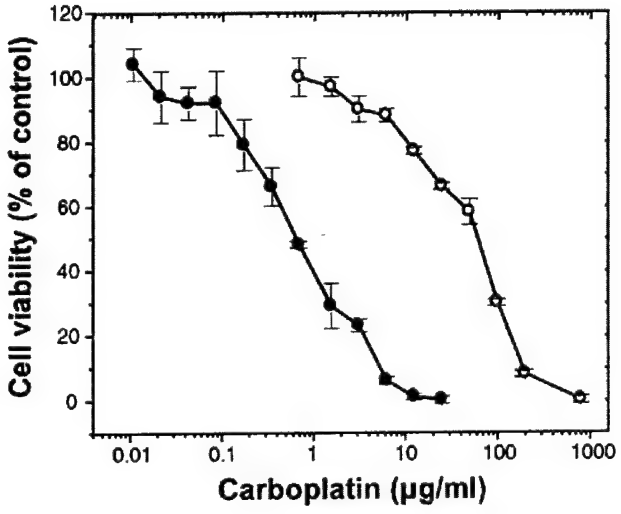
Cell viability (% of control)
120
100
80
60
40
20
0
0.01
0.1
1
10
100
1000
Carboplatin (µg/ml)

Figure 1

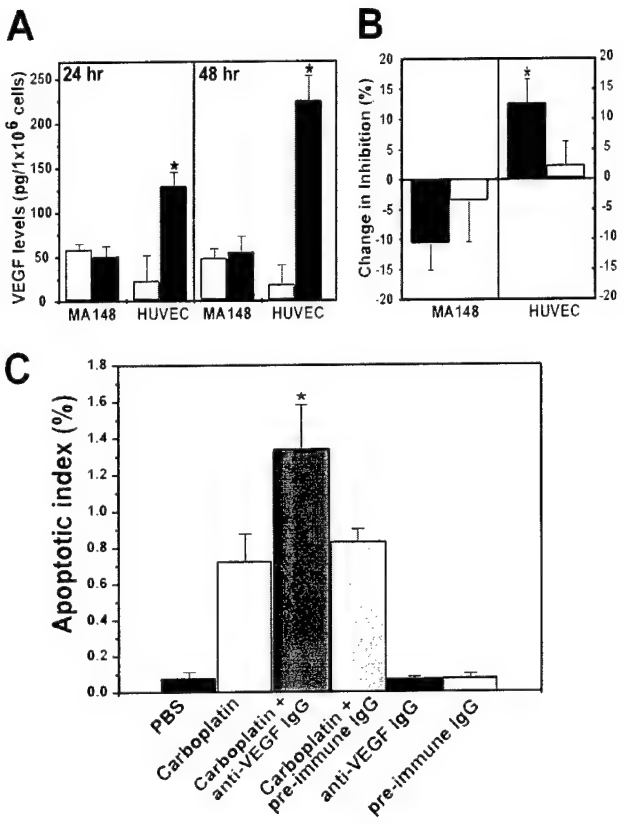
A
24 hr
48 hr
VEGF levels (pg/1x10^6 cells)
250
200
150
100
50
0
MA148
HUVEC
MA148
HUVEC
B
Change in Inhibition (%)
20
15
10
5
0
-5
-10
-15
-20
MA148
HUVEC
C
Apoptotic index (%)
1.8
1.6
1.4
1.2
1.0
0.8
0.6
0.4
0.2
0.0
PBS
Carboplatin
Carboplatin + anti-VEGF IgG
Carboplatin + pre-immune IgG
anti-VEGF IgG
pre-immune IgG

Figure 2

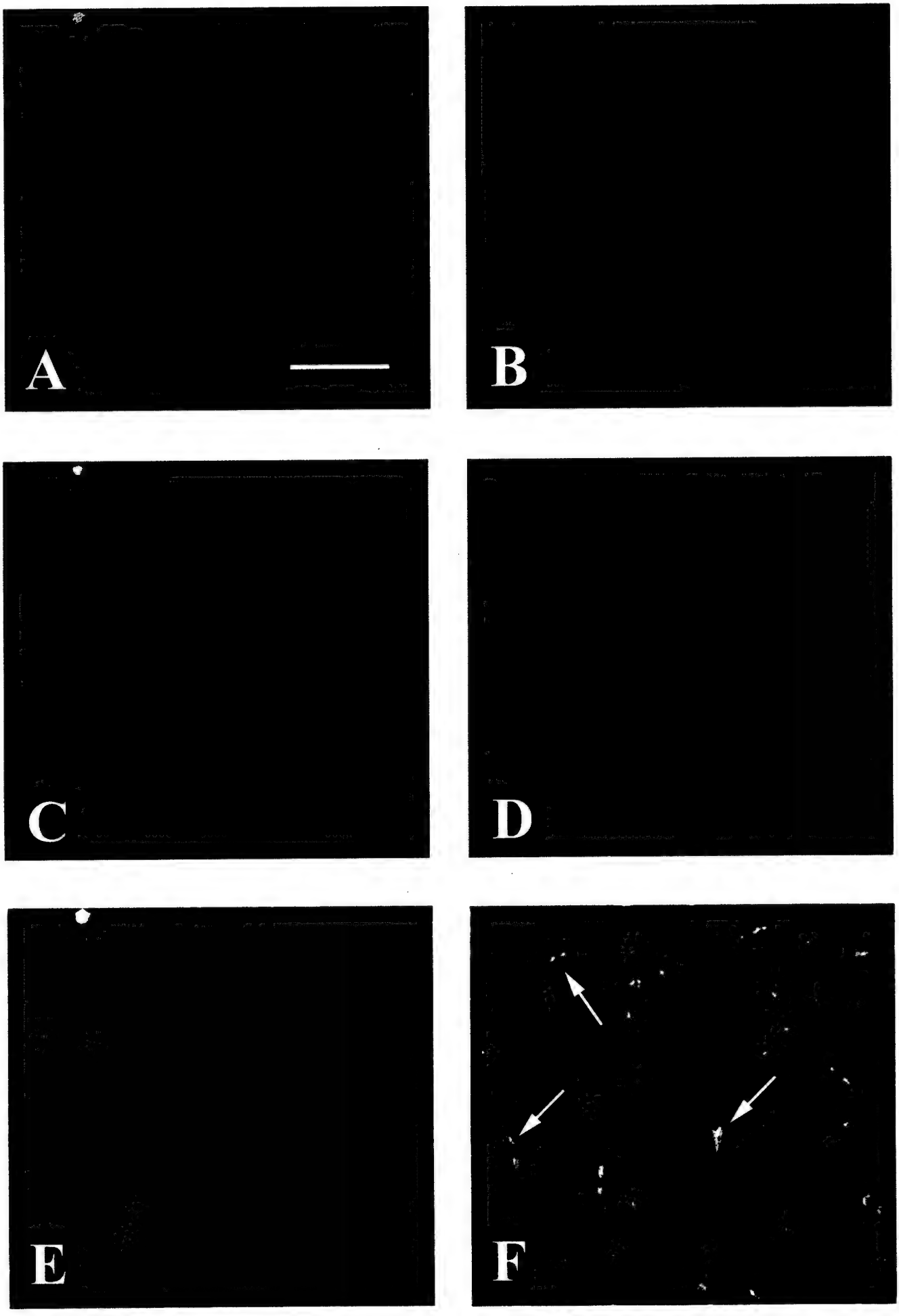

Figure 3

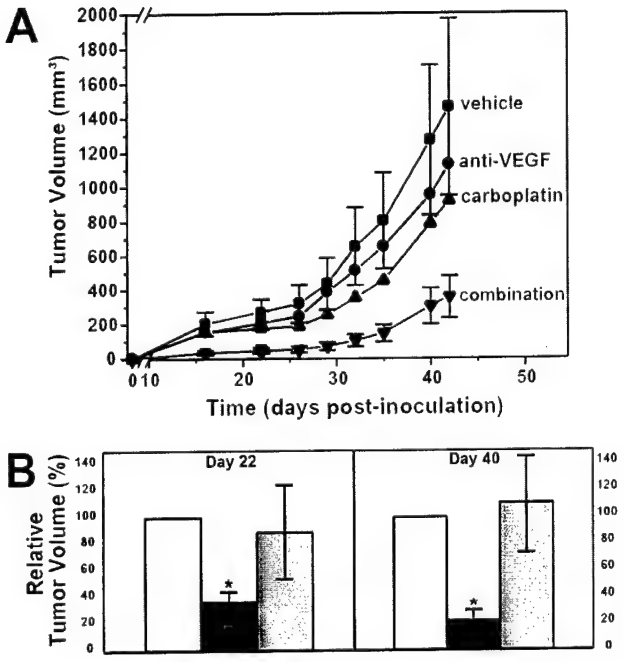
A
Tumor Volume (mm³)
2000
1800
1600
1400
1200
1000
800
600
400
200
0
0 10
20
30
40
50
Time (days post-inoculation)
vehicle
anti-VEGF
carboplatin
combination
B
Relative Tumor Volume (%)
Day 22
Day 40
140
120
100
80
60
40
20
0
*
*

Figure 4

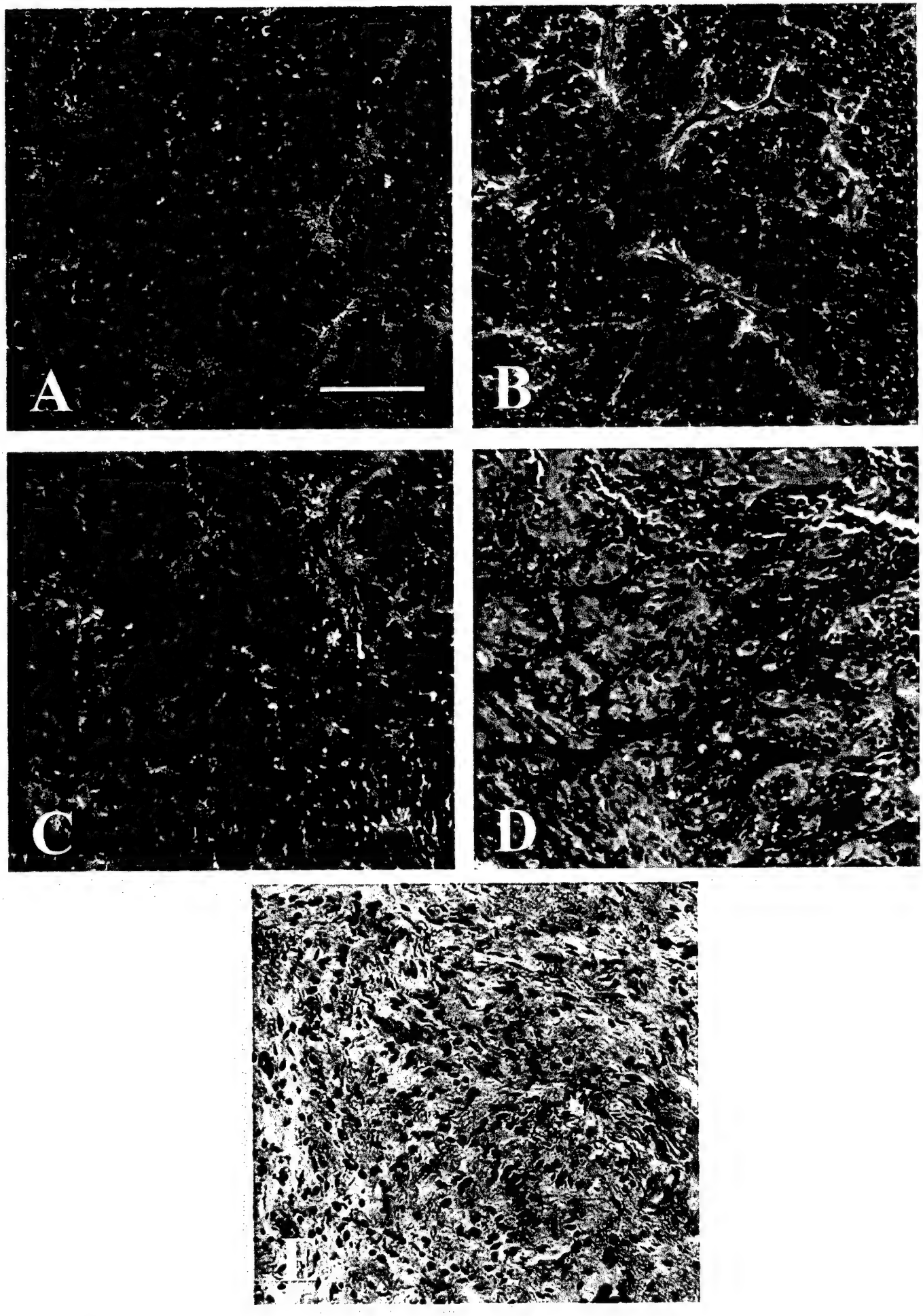

Figure 5

Addition of Integrin Binding Sequence to a Mutant Endostatin Improves Inhibition of Tumor Growth

Yumi Yokoyama[1] and S. Ramakrishnan[1,2,3]

Department of Pharmacology [1], Obstetrics and Gynecology [2], Comprehensive Cancer Center [3], University of Minnesota, Minneapolis, MN,

Running Title: Genetic modification of endostatin

Key Words: endostatin, angiogenesis, RGD, vascular targeting, ovarian cancer.

The abbreviations used are: bFGF, basic fibroblast growth factor; VEGF, vascular endothelial growth factor; RGD-endostatin, amino terminal RGD-modified P125A-endostatin; endostatin-RGD, carboxyl terminal RGD-modified P125A-endostatin.

Corresponding author: S. Ramakrishnan,

6-120 Jackson Hall, 321 Church Street, S.E.,

Department of Pharmacology,

University of Minnesota, Minneapolis, MN 55455

Ph: (612) 624 1461

Fax : (612) 625 8408

Email: sunda001@umn.edu

ABSTRACT

Tumor vasculatures express high levels of $\alpha_v\beta_3$ / $\alpha_v\beta_5$ and $\alpha_5\beta_1$ integrins. Consequently, peptides containing the RGD (Arg-Gly-Asp) sequence, which is present in ligands of integrins, is effective in targeting therapeutic reagents to tumor vascular endothelium. In the present study, we investigated whether the biological activity of endostatin can be improved by the addition of an integrin targeting sequence. RGD sequence was added to either the amino or carboxyl terminus of endostatin containing a point mutation, P125A-endostatin. Earlier we have shown that the P125A mutation did not affect the biological activity of endostatin but in fact improved the antiangiogenic activity when compared to the native molecule. Further modification of P125A-endostatin with the RGD-motif showed specific and increased binding to endothelial cells, relative to unmodified endostatin, and the increased binding coincided with improved antiangiogenic properties. Both amino and carboxyl terminal RGD-modification of P125A-endostatin resulted in greater inhibition of endothelial cell migration and proliferation. RGD-modification increased tumor localization without affecting the circulatory half-life of P125A-endostatin, and RGD-P125A-endostatin was found to be more effective when compared to the P125A-endostatin in inhibiting ovarian and colon cancer growth in athymic mice. Complete inhibition of ovarian tumor growth was observed when P125A-endostatin-RGD was encapsulated into alginate beads. These studies demonstrate that human endostatin can be genetically modified to improve its biological activities.

INTRODUCTION

Establishing a new blood supply, or neovascularization, is important for tumor growth and metastasis (1). Formation of new blood vessels is a complex process involving endothelial cell proliferation, matrix degradation, migration, tube formation and maturation. Tumor cells along with stromal and inflammatory cells collectively create a proangiogenic microenvironment (2, 3). Angiogenic growth factors such as VEGF, FGF and angiopoietins stimulate endothelial cells to proliferate and migrate to form new blood vessels. In addition to growth factor receptor-mediated signaling, interaction between cell surface anchored integrins and extracellular matrix components constitutes an additional pathway necessary for angiogenesis. In fact, two cytokine mediated, integrin dependent angiogenic pathways have been described. One of these pathways is associated with $\alpha_v\beta_3$ integrin, which selectively influences bFGF mediated angiogenic signals (4). A second, non-overlapping pathway is represented by crosstalk between $\alpha_v\beta_5$ integrin and PKC dependent growth factor mediated signaling (VEGF, IGF, TNF-α) (4, 5). Tumor angiogenesis can therefore be inhibited either by blocking the interaction between $\alpha_v\beta_3/\beta_5$ and RGD containing extracellular matrix or by interfering with angiogenic growth factors.

Angiogenesis is regulated by a delicate balance between pro- and anti-angiogenic factors present in the microenvironment of tumor tissues. A number of proteolytic fragments of extracellular matrix (6) and coagulation factors are capable of inhibiting angiogenesis. Endostatin is a proteolytic fragment of a collagen type XVIII (7). Endostatin is believed to be sequestered by glypican and presented to integrins (8). Rehn *et al* (9) recently showed that endostatin interacts with $\alpha_5\beta_1$ and $\alpha_v\beta_3$ integrins on the surface of endothelial cells in an RGD-independent manner.

Another antiangiogenic protein, tumstatin, derived from the NC-1 domain of collagen IV α-3 chain also binds to $\alpha_v\beta_3$ integrins in an RGD independent manner (10).

These studies suggest that endostatin and tumstatin can transduce antiangiogenic signals by binding with integrins present on endothelial cells. However, a number of independent studies have reported that RGD-dependent interactions on the endothelial cell surface can also inhibit angiogenesis. This is consistent with the observation that RGD-peptides and cyclic peptides containing the RGD motif are potent inhibitors of tumor angiogenesis (11). Therefore we hypothesized that by introducing the RGD-sequence into human endostatin we might promote both RGD-dependent and independent signaling via integrins. Such dual binding might potentiate the antiangiogenic activity of endostatin.

To test this hypothesis, human P125A-endostatin (12, 13) was genetically modified to incorporate an RGD sequence and expressed in yeast. P125A-endostatin has a point mutation and is biologically active in inhibiting tumor angiogenesis. *In vitro*, cell-binding studies showed that endothelial cells bound to RGD-modified P125A-endostatin coated plates significantly higher than to plates with unmodified P125A-endostatin. The increased binding was completely blocked by anti $\alpha_v\beta_3$ antibody or RGD peptide. RGD-modified-endostatins were more potent in inhibiting bFGF-induced endothelial cell proliferation and migration when compared to P125A-endostatin. RGD-containing P125A-endostatin was also more effective in inhibiting tumor growth in athymic nude mice. Our studies further show that slow release of alginate beads microencapsulated with RGD-modified endostatin completely inhibited established ovarian cancers in athymic mice. These studies suggest that antiangiogenic activity of endostatin can be improved by adding an RGD-sequence.

MATERIALS AND METHODS

Cell s and Animals. Bovine adrenal gland capillary endothelial cells (BCE) were obtained from Clonetics Inc. (San Diego, CA). Human umbilical vein endothelial cells (HUVEC), passage 2, were kindly provided by Dr. Vercelotti, University of Minnesota. Human colon carcinoma cells, LS174T, were obtained from American Type Culture Collection (ATCC, Rockville, MD). MA148, a human epithelial ovarian carcinoma cell line was established locally at the University of Minnesota from a patient with stage III epithelial ovarian cystadenocarcinoma (14). Human primary melanoma cell line WM35, which expresses $\alpha_v\beta_3$ integrin, was provided by Dr. Joji Iida and Dr. James B. McCarthy (University of Minnesota). Culture conditions of these cell lines have been previously described (15). WM35 cell line was cultured under the same conditions as MA148.

Cloning and Expression of Human Endostatin. The yeast expression system, *Pichia pastoris* was purchased from Invitrogen (San Diego, CA). Restriction enzymes and Taq DNA polymerase were purchased from Boehringer Mannheim (Indianapolis, IN).

We earlier cloned and characterized a mutant endostatin with a single amino acid substitution at the position 125, P125A-endostatin (12, 13). This clone was further modified to incorporate the RGD sequence either at the amino terminus or at the carboxyl terminus. The following sets of primers were used to modify P125A-endostatin by PCR.

1) RGD-human P125A-endostatin

Up [5']: GGGGAATTCAGAGGAGATCACAGCCACCGCGACTTCCAG

Down [3']: GGGGCGGCCGCCTACTTGGAGGCAGTCATGAAGCT

2) human P125A-endostatin-RGD

Up [5']: GGGGAATTCCACAGCCACCGCGACTTCCAG

Down [3']: GGGGCGGCCGCCTAATCTCCTCTCTTGGAGGCAGTCATGAAGCT

Amplified fragments were purified by using a DNA extraction kit (Amicon, Beverly, MA), digested with EcoRI and NotI, and cloned into pPICZα-A vector. DNA sequencing was carried out by Applied Biosystems sequencer (ABI 377 at the Advanced Genetic Analysis Center of the University of Minnesota) to verify the identity. Plasmid DNA was then linearized at the SacI site and electroporated into the yeast host strain X-33 (Invitrogen). Recombinants were selected on Zeocin containing plates and characterized for expression of mutant endostatins. All endostatin constructs used in this study had the P125A substitution.

Purification of Recombinant Proteins. Pichia clones were cultured in baffled shaker flasks and induced by methanol as previously described (15). For large-scale preparations, a fermentation procedure was used. A mouse angiostatin expressing Pichia clone (kindly provided by Dr. V.P. Sukhatme) was cultured under similar conditions. P125A-endostatin and angiostatin were purified following published methods (15).

Cell Attachment Assay. One nmole/well endostatin preparations or RGD peptide [$(H)_4$-$(G)_3$-R-G-D-$(G)_3$-C] or 0.2% gelatin were used to coat 96 well polystyrene plates. The plates were incubated at 4°C overnight, and then blocked with 2 % BSA in PBS at 37°C for 2 hr. HUVEC, MA148 (negative control), or WM35 (positive control for $\alpha_v\beta_3$ integrin expressing cell line) were harvested by suspending in PBS containing 1 mM EDTA, and prelabeled for 10 min at 37°C with 5 μM 5-(and-6)-carboxyfluorescein diacetate, succinimidyl ester (5(6)-CFDA), a vital, fluorescence dye, (Molecular Probes, Eugene, OR). After washing with Hank's balanced salt solution (HBSS), fluorescence labeled cells were resuspended in EGM medium (HUVEC) or RPMI1640 medium

supplemented with 10 % FBS (MA148, WM35). The cells were incubated with or without competitors (1 μg anti-$\alpha_v\beta_3$ integrin monoclonal antibody (LM609, Chemicon, Temecula, CA) or anti-HLA monoclonal antibody (negative control; G46-2.6, BD PharMingen, San Diego, CA), or 25 nmole/well RGDS or RGES peptides (Sigma Chemicals, MO) for 1 hr at 37°C. Cells were added to the wells at a density of 40,000 cells / well (HUVEC and MA148) or 30,000 cells / well (WM35). After an hour-incubation at 37°C, the plates were washed twice with HBSS to remove unbound cells. Cells bound to the wells were assayed by a fluorescence plate reader (Cyto Fluor II; PerSeptive Biosystems, Framigham, MA) (excitation; 485 nm, emission; 530 nm).

Binding of P125A-endostatin and RGD-modified P125A-endostatins to HUVEC was also determined by using [^{125}I]-labeled proteins. [^{125}I]-labeling was carried out by the Iodogen method. HUVEC was harvested in 1 mM EDTA/PBS and was resuspended in 0.1 % BSA/PBS. Five microliters of [^{125}I]-endostatin (27380 cpm/μg) or [^{125}I]-RGD-P125A-endostatin (32908 cpm/μg) were added to 40,000 HUVEC cells in 100 μl of 0.1 % BSA/PBS. Cells were incubated at room temperature for 1 hr, and then washed with 0.1 % BSA/PBS for twice. [^{125}I]-P125A-endostatin and [^{125}I]-RGD-P125A-endostatin bound to HUVEC were detected by a γ-counter (Packard, Meriden, CT).

Endothelial Cell Proliferation Assay. Essentially, the method described by O'Reilly *et al.* was used (7). Proliferating cells were quantified by 5'-bromo-2'-deoxyuridine (BrdU) incorporation (Roche, Indianapolis, IN) according to the manufacturer's instructions.

Endothelial Cell Migration Assay. The migration of endothelial cells was determined by using Boyden chambers (Neuro Probe, Gaithersburg, MD). Polycarbonate filters (pore size; 12 μm) were

coated with 0.2% gelatin for 1 hour at 37°C. HUVEC were harvested in 2 mM EDTA in PBS, and prelabeled with 5 μM 5(6)-CFDA for 10 min at 37°C. Cells were resuspended in 0.5% FBS, M199 medium and then preincubated with P125A-endostatin, RGD-endostatin or endostatin-RGD for 60 min at 37°C. Basic FGF (25 μl of 25 ng/ml 0.5% FBS, M199 medium) was added to the lower chambers. HUVEC (200,000 cells / ml, control and treated) were added to upper chambers. After 4 hours of incubation at 37°C, endothelial cells that had migrated to the bottom side of the membrane were counted in a fluorescence microscope (Olympus) using FITC filters (magnification 200 X). Two independent experiments were carried out.

Detection of Bcl2 and Bax mRNA. HUVEC were treated with P125A-endostatin or RGD-modified endostatins at a concentration of 50 nM. After 48 hr, the cells were trypsinized, and total RNA was extracted by using the RNeasy Mini kit (Qiagen, Valencia, CA) according to the manufacturer's protocol. Reverse transcription was performed with the SuperScript II kit (Invitrogen) using 1 μg of total RNA. DNA of bcl2 or bax was determined by PCR using primers of the Amplifluor Universal Amplification and Detection System (Intergen Company, Purchase, NY). As a control the following human GAPDH primers were used:

Up [5'] : CCACCCATGGCAAATTCCATGGCA,

Down [3'] : TCTACACGGCAGGTCAGGTCCACC

Tumor Localization. LS174T cells were injected subcutaneously in the flanks of female, athymic nude mice (8 wk old). Tumor size reached about 500 mm^3 on day 10. Tumor bearing mice were randomized into 3 groups. P125A-endostatin, RGD-endostatin or endostatin-RGD was injected at a dose of 20 mg/kg subcutaneously. Nineteen hours after injection, tumor tissues and representative

normal tissues were surgically removed. This time point was chosen to minimize overwhelming serum levels from obscuring the tissue bound endostatin. For comparison, serum samples were also collected from the mice at the time of sacrifice. Tissues were snap frozen, and homogenized in RIPA buffer containing proteinase inhibitors (PBS, 1% NP40, 0.5% sodium deoxycholate, 0.1% SDS, 10 μg/ml PMSF), maintained at 4°C for 45 min, and cleared by centrifugation. Human endostatin concentrations in serum and tissue lysates were measured using an enzyme linked immunoassay (Cytimmune, College park, MD) according to the manufacturer's instructions. Endostatin standards were also prepared in RIPA buffer. Statistical significance was determined by Student's t-test.

Half Life. About one million cpm of [^{125}I]-labeled P125A-endostatin or RGD-endostatin was injected intravenously. Mice were bled at different time points from the tail vein and total radioactivity in aliquots of serum samples was determined.

Tumor Growth Inhibition Studies. Female athymic nude mice (6-8-week-old) were obtained from NCI and acclimatized to local conditions for one week. Logarithmically growing human colon carcinoma cells (LS174T) and human ovarian carcinoma cells (MA148) were harvested by trypsinization and suspended in fresh medium at a density of 1 x 10^7 cells/ml (LS174T) or 2 x 10^7 cells/ml (MA148). One hundred μl of the single cell suspension were then subcutaneously injected into the flanks of mice. When the tumors became visible (LS174T; 3 days after inoculation, MA148; 7 days after inoculation), mice were randomized into groups. The mice were treated with P125A-endostatins, RGD- endostatin or endostatin-RGD s.c. at a dose of 20 mg/kg/day for 11 days for LS174T or 21 days for MA148. A control group of mice (n=5) was treated with sterile PBS

under similar conditions. All injections were given subcutaneously near the neck, about 2 cm away from the growing tumor mass. Tumor growth was monitored by periodic caliper measurements. Tumor volume was calculated by the following formula.

Tumor volume (mm^3) = $(a \times b^2)/2$ Where in 'a' = length in mm, 'b' = width in mm, a>b. Statistical significance between control and treated groups was determined by Repeated measurement analysis of variance.

Determination of Vessel Density and Apoptosis. To determine the effect of anti-angiogenic treatments on vessel density and apoptosis, residual tumors were surgically resected and snap frozen. Cryostat sections (10 μm) of tumors were fixed in cold acetone, air dried and then treated with PBS containing 0.1% BSA and 5% human serum to block non-specific binding (background). Sections were then incubated with 1:50 dilution of an anti-CD31 (mouse) monoclonal antibody conjugated to phycoerythrin (MEC 13.3, BD PharMingen, San Diego, CA). Following one hour incubation at room temperature, sections were washed thoroughly with PBS containing 0.1% BSA and 5% human serum followed by washing with PBS and then examined by an Olympus BX-60 fluorescence microscope. Images (7 to 10) were captured by the Metamorph program for analysis. Detection of apoptosis was carried out by using an In Situ Cell Death Detection Kit (Boeringer Mannheim, Indianapolis, IN) following the manufacture's protocol. Parts of the tumor samples were also fixed in 10% neutral buffered formalin and processed for histochemistry.

Microencapsulation of Endostatins into Alginate Beads and Tumor Growth Inhibition Studies. Alginic acid extracted from *Macrocystis pyrifera* was purchased from Sigma Chemicals (St. Louis, MO). A four percent solution of alginic acid in water was sterilized by

autoclave. P125A-endostatins preparations made in 2% alginic acid were dropped gently into 0.1 M $CaCl_2$ solution using a fine needle under aseptic conditions. The beads were kept at 4°C overnight and washed with sterile water before the subcutaneous implantation into tumor bearing mice (MA148 ovarian cancer cell line). A BCA kit was used to determine concentration of protein encapsulated into alginic beads. P125A-endostatins encapsulated in alginate beads were administered four times at a dose of 20 mg/kg/mouse/ once a week.

RESULTS

First we evaluated whether human P125A-endostatin could be modified at either of its termini without compromising its biological activity. Addition of His-Tag or c-Myc Tag did not affect the ability of P125A-endostatin to inhibit endothelial cell proliferation or migration *in vitro* (data not shown). Based on these results P125A-endostatin was modified to incorporate an RGD motif at the amino (designated as RGD-endostatin) or carboxyl (endostatin-RGD) terminus.

RGD-Endostatin Increases Endothelial Cell Attachment *In Vitro*. RGD-peptide is well known for its binding to integrins on the surface of endothelial cells. To determine whether addition of RGD-motif to P125A-endostatin could enhance its binding to endothelial cells, cell attachment assays were performed. As a positive control, 0.2% gelatin coated wells were used. Number of cells attached to gelatin coated wells was considered as 100% to calculate relative binding. HUVEC attached to endostatin coated wells (Fig. 1A). BSA blocked wells were used as a negative control. In this assay system, P125A-endostatin coated wells showed about 60 % cell

attachment, which was further increased by RGD-modification (Fig. 1A). RGD-endostatin ($p < 0.05$) and endostatin-RGD ($p<0.01$) showed about 80 % cell attachment. Parallel experiments with RGD-containing synthetic peptide showed similar binding of HUVEC. Under the experimental conditions used, a preparation of recombinant murine angiostatin (kringle 1-4, expressed in yeast) did not increase endothelial cell attachment over the control values (Fig. 1A).

Cell attachment studies were repeated using human microvascular endothelial cells (MVEC) and bovine adrenal gland capillary endothelial cells (BCE). These studies showed a profile similar to results obtained with HUVEC (data not shown). Then experiments were carried out to determine the specificity of RGD-mediated enhanced binding to endothelial cells (Fig. 1B). Presence of RGD sequence (COOH or NH_2 terminus) increased endothelial cell attachment by 40 % over unmodified endostatin. This was completely blocked by RGD containing synthetic peptide. As an additional control, an epithelial ovarian tumor cell line, MA148, was used in cell attachment assays. Results shown in Fig. 1C suggest that RGD-containing peptide did not facilitate MA148 cell attachment. Human endostatin (native and RGD-modified) coated wells again did not show any significant increase in tumor cell attachment when compared to control wells blocked with BSA alone.

In addition to cell attachment studies, we also examined the direct binding of endostatin to HUVEC by using [^{125}I]-labeled endostatins. Data in Fig. 1D show that about 0.65 pmole of radioiodinated endostatin bound to 10^6 cells, about 1 x 10^4 molecules per cell. Under similar conditions, about 1.2 pmole of [^{125}I]-RGD-endostatin bound to HUVEC (a 2-fold increase in binding). These studies suggest that endostatin binding to endothelial cells can be specifically increased by RGD-modification. Neither amino nor carboxyl terminal modifications caused any steric hindrance to RGD-mediated binding to endothelial cells.

In order to differentiate between RGD-integrins and endostatin-integrin ($\alpha_5\beta_1$) binding, a non-endothelial cell line overexpressing $\alpha_v\beta_3$ was used. Human melanoma cell line WM35, expresses higher levels of $\alpha_v\beta_3$ integrin, but no detectable levels of $\alpha_5\beta_1$ and $\alpha_v\beta_5$ based on flowcytometry analysis (data not shown). Representative photomicrographs of cell attachment to coated wells are shown in Fig. 2B-G. Unlike HUVEC, MW35 cells did not attach to endostatin coated wells by itself (18%, which is similar to BSA blocked control wells) (Fig. 2A, B). However, MW35 cells specifically attached to RGD-endostatin coated wells (60 %) (Fig. 2A, C). In order to determine whether the increased binding of RGD-endostatin was indeed specific, two methods were used. In one experiment, a monoclonal antibody to anti-$\alpha_v\beta_3$ integrin was used to block the interaction. As a control, isotype matched mouse IgG was used at a similar concentration. Preincubation of MW35 cells with the anti-$\alpha_v\beta_3$ integrin antibody completely blocked cell attachment to RGD-endostatin (Fig. 2A, D). The control antibody did not prevent MW35 cells from binding to RGD-endostatin coated wells (Fig. 2A, E). In a second series of experiment, synthetic peptides were used as competitive inhibitors. Inclusion of RGDS peptide in the medium completely prevented attachment of WM35 cells (Fig. 2A, F), whereas a control peptide, RGES, did not affect WM35 cells from attaching to RGD-endostatin coated wells (Fig. 2A, G). Endostatin-RGD was also tested in WM35 cell attachment and showed similar profile as RGD-endostatin (Data not shown).

Inhibition of Endothelial Cell Proliferation. To determine whether the modification of human endostatin affects the biological activity, endothelial cell proliferation assays were carried out by BrdU incorporation. Inhibition of bFGF-induced proliferation was determined in the presence of different concentrations of endostatin preparations. Data in Fig. 3A show that at 1 μM,

endostatin inhibited bFGF-induced BCE cell proliferation by 26.8%. Addition of RGD motif at the amino or carboxyl terminal end of endostatin enhanced the antiproliferative activity. Amino terminal modification of endostatin with RGD sequence showed 76.3 % inhibition of bFGF-induced proliferation. Interestingly RGD-modification at the C-terminal end was more effective and actually inhibited BrdU incorporation below the levels of control cultures grown in the absence of bFGF (125.9% inhibition).

To determine whether the enhanced inhibition of endothelial cell proliferation was due to RGD moiety and endostatin, the effect of synthetic peptides containing RGD sequence was tested under similar conditions. Unlike the RGD-modified endostatins, the synthetic peptides did not inhibit endothelial cell proliferation at 1.0 μM concentration. RGD peptide inhibited endothelial cell proliferation at a concentration of 10 μM. In a parallel set of cultures, RGDS peptide was admixed with unmodified endostatin to determine whether two independent bindings could lead to improved antiproliferative activity. Data shown in Fig. 3B clearly suggest that at the concentrations tested the free peptides either alone or in the presence of endostatin did not significantly change the basal level of inhibition seen with endostatin alone. These studies suggest that RGD-moiety engineered into endostatin molecule acquires enhanced antiproliferative activity, perhaps by cross linking $\alpha_5\beta_1$ and $\alpha_v\beta_3/\alpha_v\beta_5$ integrins.

Increased Inhibition of Endothelial Cell Migration by Endostatin Containing RGD-motif.

To evaluate whether RGD-motif can affect the ability of endostatin to inhibit endothelial cell migration, Boyden chamber based migration assays were performed (Fig. 3C). Basic FGF was used as an inducer of endothelial cell migration. Endostatin treatment at 50 nM inhibited bFGF induced migration by 50.6%. Relative to this, RGD-endostatin and endostatin-RGD showed

statistically significant improvement in the inhibition of cell migration. Cultures treated with RGD-endostatin showed 86.3% inhibition, and endostatin-RGD treated cultures showed almost complete inhibition (101.4%) of bFGF induced cell migration. In a parallel study, RGD containing synthetic peptide was also evaluated for its ability to inhibit cell migration. Free peptide did not show any inhibition at 50 nM. When a mixture of an equimolar concentration of endostatin and peptide was used, there was no enhancement in the basal activity of endostatin. As a negative control, RGES peptide was used, which did not affect cell migration.

These results suggested that the RGD moiety should be a part of endostatin in order to inhibit endothelial cell migration better. This conclusion was further validated by an additional control experiment using RGD containing peptides that were chemically linked to a control protein, BSA, via a thiol group. CGGGRGD peptide has a free thiol group at the aminoterminus. Using a heterobifunctional cross-linking reagent, N-succinimidyl 3-[2-pyridyldithio] propionate (SPDP, Pierce Chemicals, Rockford, IL), CGGGRGD peptide was linked to bovine serum albumin (RGD-BSA). Based on molecular weight shift in SDS-PAGE, an average of 5 RGD moieties were introduced into each BSA molecule. Accessibility of RGD in the BSA conjugate was validated in cell attachment assays (data not shown). Endothelial cells attached to RGD-BSA coated wells very well (84% when compared to gelatin mediated attachment). Cell attachment was similar to RGD-peptide and RGD-endostatin. In spite of high binding to endothelial cells, however, chemically linked RGD-BSA did not inhibit migration of endothelial cells at equimolar concentrations (10-50 nM concentration, data not shown). These studies suggest that the RGD sequence alone at the concentrations tested does not inhibit endothelial cell proliferation and migration, though it enhances the inhibitory activity of endostatin.

Downregulation of Bcl2 mRNA. Endostatin and RGD peptides are independently known to affect apoptotic pathways (16, 17). As a preliminary study, we determined whether RGD modification changes the levels of a key anti-apoptotic molecule, bcl-2. Relative levels of bcl-2 and bax transcripts were determined by RT-PCR in endothelial cells treated with endostatin preparations. Endothelial cells treated with bFGF showed an increase in bcl-2 specific transcripts when compared to control cultures (-bFGF). Treatment with P125A-endostatin at a concentration of 50 nM decreased mRNA levels of bcl2. RGD-modified endostatin also downregulated bcl2 levels significantly when compared to bFGF-treated control cultures (Fig. 3E), but to the same degree as P125A-endostatin. Parallel studies showed no significant change in bax transcript levels in treatment with either of the endostatin preparations (Data not shown).

RGD-modification Increases Tumor Localization of Endostatin. To assess whether the improved endothelial cell binding *in vitro* could translate into enhanced tumor homing *in vivo,* tumor localization studies were carried out. P125A-Endostatin, RGD-endostatin, and endostatin-RGD were injected subcutaneously into human colon cancer bearing athymic mice. Relative levels of endostatin in the tumor tissue when compared to serum levels are shown in Fig. 4A. P125A-endostatin accumulation in tumors considered as 100%. RGD-modified endostatins localized more than two-fold higher when compared to P125A-endostatin (Fig. 4A).

Another pharmacological property that can affect biological efficacy *in vivo* is clearance rate. Therefore, serum half-life was compared. Fig. 4B shows the beta phase of clearance. Both unmodified and RGD-modified endostatin showed a similar half-life. The α phase of P125A-endostatin and RGD-endostatin was 5.3±1.53 min, 2.3±1.14 min respectively, and the β phase of P125A-endostatin and RGD-endostatin was 9.1±2.27 hr, 8.9±2.40 hr respectively (Fig. 4B). The differences seen in the α phase and β phase were not statistically significant. Collectively, these

results suggest that RGD-modification does not alter serum clearance but facilitates tumor tissue accumulation.

Inhibition of Colon Cancer Growth by RGD-modified Endostatin. To test whether RGD modification of endostatin could improve anti-tumor activity, we used a LS174T xenograft model system. LS174T tumors grow very fast, and were allowed to establish for 3 days. At this time, small palpable tumor nodules could be easily seen. Mice were then randomized and divided into groups. RGD-endostatin and P125A-endostatin were administered subcutaneously at a dose of 20 mg/kg/day for a period of 11 days. As shown in Fig. 5, RGD-endostatin inhibited tumor growth significantly better than unmodified endostatin. In this model system, the control tumors reached a size of about 500 mm^3 by day 14. Endostatin treatment inhibited the tumor growth by about 30 % under the conditions tested. In contrast, groups of animals treated with RGD-endostatin significantly decreased the tumor growth by 78 % when compared to the control animals ($p=0.005$).

Effect on Tumor Blood Vessels and Apoptosis. To evaluate the consequence of antiangiogenic therapy, we examined the residual tumors histologically. Frozen tumor sections were stained with anti-CD31 PE conjugate. Both native and RGD-modified endostatin treatment resulted in reduced vessel density (Fig. 6. A-C). The same frozen sections were also analyzed for changes in the apoptosis of tumor cells using a TUNEL assay (Fig 6. D-F). Serial sections of each tumor were also stained by H & E to assess histological changes (Fig 6. G-I). H & E and TUNEL staining revealed that RGD-endostatin induced more apoptosis in tumor tissue (Fig. 6F, I) when compared with control (Fig 6D, G) and P125A-endostatin treated tumors (Fig. 6E, H). A quantitative analysis of

apoptotic index is shown in Fig. 6J. RGD-endostatin treated tumors showed an apoptotic index of 7.91 ± 2.40%. This value is about 45-fold higher than the control tumors (0.176 ± 0.048). Native endostatin treated tumors showed an apoptotic index of 1.32 ± 0.774%, an increase of 7.5-fold over the control tumors.

Slow Release of P125A-Endostatin and Endostatin-RGD by Alginate Beads : Improved Anti-tumor Activity. Initially, we compared the relative effects of amino (RGD-endostatin) and carboxyl (endostatin-RGD) terminal modification. Ovarian cancer cell line, MA148, was subcutaneously injected into female, athymic mice. Groups of 5 mice were treated either with vehicle or with the respective RGD-modified proteins. Mice were injected daily (i.p.) with 20 mg/kg of P125A-endostatin preparations starting on day 7 until day 28. In this study, endostatin alone did not inhibit tumor growth significantly. Amino terminal modification with RGD inhibited tumor growth by 28 % when compared to untreated control group. Carboxyl terminal modification of endostatin with RGD moiety showed a moderate improvement in tumor growth inhibition (57 % inhibition), which, however, was not statistically significant when compared to amino terminal modification (Data not included).

Subsequently, we investigated whether the slow release of P125A-endostatins using alginate microspheres could improve the anti-tumor activity in the ovarian cancer model system. Alginic acid, which is a naturally occurring biopolymer, has been used as a matrix for entrapment and delivery of a variety of biological agents. Ovarian cancer cell line, MA 148, was injected s.c. into the flanks of athymic mice. After seven days, alginate beads containing endostatin preparations were administered to groups of mice. Endostatins were given once a week, four times, at a dose of 20 mg/kg. Control group of mice received vehicle encapsulated alginate beads on a similar

schedule. Unlike bolus, daily injections, administration of P125A-endostatin in alginate formulation showed significant anti-tumor activity (Fig. 7). Tumor growth was significantly inhibited throughout the experiment. For example, 40% of P125A-endostatin treated animals did not show any tumor growth up to 42 days at which time, control animals had a mean tumor volume of 1150 mm^3. Subsequently, the tumors began to grow and reached a size of about 1300 mm^3 by day 60. Interestingly, the endostatin modified with RGD-motif when delivered in alginate beads showed a complete inhibition of tumor growth for 75 days (Fig. 7). Tumor growth was suppressed for a prolonged time even after the cessation of endostatin-RGD treatment. These studies demonstrate that RGD-modification of endostatin can improve the anti-tumor activity of endostatin and that a slow release formulation can be used to inhibit tumor growth very effectively.

DISCUSSION

In the present study, we introduced an integrin binding motif to human endostatin and investigated its effect on biological activity *in vitro* and *in vivo*. Endostatin binds to Glypican and integrins (8, 9, 18). Glypican is believed to sequester endostatin and present it to integrins on endothelial cells. Of the two integrins ($\alpha_5\beta_1$, $\alpha_v\beta_3$) known to interact with endostatin, binding to $\alpha_5\beta_1$ appears to be biologically relevant. Blocking $\alpha_5\beta_1$ integrin mediated interaction with endostatin (immobilized) inhibited endothelial cell migration (9). While retaining this interaction, RGD-modification of endostatin is likely to provide additional binding to integrins, such as $\alpha_v\beta_3/\alpha_5\beta_1$. Both of these integrins play an important role in tumor neovascularization. Interestingly, a recent study using competitive inhibition by peptides showed that endostatin may bind to endothelial cells via RGD dependent manner (19). However endostatin does not have an RGD

sequence. Therefore RGD-dependent direct binding of native endostatin is not possible. Further studies are necessary to characterize this interaction. Independent binding to these integrins can affect the biological activity. Indeed, when endostatin was modified with RGD sequence, there was increased binding to endothelial cells. Increased endothelial cell attachment to RGD-endostatin was highly specific, since it could be completely blocked by a synthetic peptide containing RGD sequence.

The RGD-motif also improved the ability of endostatin to inhibit endothelial cell proliferation and migration. COOH-terminal addition of RGD resulted in enhanced inhibition when compared to NH_2-terminal addition of RGD. These differences can be attributed to peptide folding and presentation of RGD-sequence. Theoretical prediction using Swiss Protein-View software suggests four hydrogen-bonding possibilities when the RGD-sequence was introduced at the carboxyl terminus, compared to three hydrogen bonding with neighboring amino acid residues at the amino terminus (data not shown). The mere presence of the RGD-sequence was not sufficient to enhance activities, since RGD-BSA or RGD mixed with endostatin did not lead to improvement at the concentrations tested. Thus the RGD moiety in the context of endostatin is necessary for enhanced biological activity against endothelial cells.

The mechanism underlying the enhanced activity of RGD-modified endostatin is not known. Endostatin has been reported to decrease bcl2 level in endothelial cells (16, 17), and RGD peptide itself is known to interact with caspases and induce apoptosis when delivered to intracellular sites (20). Studies on the internalization rate and compartmentalization of RGD-endostatin may provide mechanistic insight into the enhanced biological activity. It is possible that these two independent events in combination can account for the pronounced effects seen on endothelial cells. Our studies suggest that RGD-modified endostatin downregulated transcripts for

the antiapoptotic protein, bcl2, without changing the levels of bax, a constituent of proapoptotic signals. The extent of reduction seen in bcl2 levels was greater in RGD-endostatin treated cultures when compared to P125A-endostatin, but the difference was not statistically significant. Therefore, it is likely that changes in other molecules such as bcl-x may be contributing to the increased apoptosis observed in RGD-endostatin treated endothelial cells. Further studies are necessary to understand the mechanism by which increased apoptosis is brought about by RGD-modified endostatins.

Tumor vasculature is known to overexpress $\alpha_v\beta_3$ and $\alpha_v\beta_5$ integrins. Therefore, peptides containing RGD-sequence are very effective in delivering cytotoxic drugs or antibodies to tumor vasculature (21, 22). Increased binding to endothelial cells combined with a potential for targeting by RGD-moiety improved tumor localization and bioavailability of endostatin. RGD-endostatin, for example, accumulated two-fold higher in tumor tissues when compared to endostatin alone. Increased accumulation was achieved without any changes in the serum clearance. Pharmacokinetic studies demonstrated that RGD-modification did not alter the serum half-life. Increased accumulation of RGD-endostatin correlated with greater anti-angiogenic effects. Morphometric analysis revealed that RGD-endostatin treatment reduced vessel density in tumor tissues. A reduced number of blood vessels coincided with increased apoptosis of tumor cells. These results corroborate other recent studies showing improved therapeutic efficacy of many biological response modifiers by genetic modification. TNF-α engineered to contain NGR-sequence, for example, exhibited improved anti-tumor activities (23). RGD-motif introduced into adenoviral coat proteins improved gene transfer efficacy into integrin $\alpha_v\beta_3$ positive cells (24).

Enhanced biological activity and tumor targeting can potentially improve the inhibition of tumor growth. Two different tumor models were used to assess the effect of RGD-endostatins.

LS174T colon cancer cells form rapidly growing tumors in athymic mice. In this model system, administration of RGD-endostatin showed a significant improvement in tumor growth inhibition when compared to unmodified P125A-endostatin given at similar doses.

Consistent with our earlier studies using mouse endostatin, ovarian cancer growth in athymic mice was not significantly affected by bolus injections of human endostatin. RGD modifications showed improvement in antitumor activity. Since recent studies showed that improvement of efficacy of endostatin by slow release administration (25-27), a slow release formulation of endostatin was investigated using ovarian cancer model. P125A-endostatin and RGD-endostatins were encapsulated into alginate beads. While bolus injections of endostatin did not show significant inhibition of ovarian tumor growth (15), slow release preparation was effective. P125A-endostatin treated animals showed significant inhibition of tumor growth when compared to control animals throughout the study. However, tumors began to grow after the discontinuation of treatment. In comparison, endostatin-RGD treatment produced long-term remissions. Tumor growth was completely inhibited for 75 days after tumor cell transplantation. Increased biological activity, enhanced tumor localization and slow release formulation cumulatively contribute to the potent inhibition of tumor growth by endostatin-RGD.

ACKNOWLEDGMENT

This work was supported in part by a grant from the USMRMC (OC980019), Minnesota Ovarian Cancer Alliance (MOCA) and Gynecologic Oncology Group. Authors would like to thank Dr. Robin L. Bliss for statistical analysis.

REFERENCES

1. Folkman, J. What is the evidence that tumors are angiogenesis dependent? J Natl Cancer Inst, *82:* 4-6, 1990.

2. Ferrara, N., Houck, K., Jakeman, L., and Leung, D. W. Molecular and biological properties of the vascular endothelial growth factor family of proteins. Endocr Rev, *13:* 18-32, 1992.

3. Maisonpierre, P. C., Suri, C., Jones, P. F., Bartunkova, S., Wiegand, S. J., Radziejewski, C., Compton, D., McClain, J., Aldrich, T. H., Papadopoulos, N., Daly, T. J., Davis, S., Sato, T. N., and Yancopoulos, G. D. Angiopoietin-2, a natural antagonist for Tie2 that disrupts in vivo angiogenesis. Science, *277:* 55-60, 1997.

4. Friedlander, M., Brooks, P. C., Shaffer, R. W., Kincaid, C. M., Varner, J. A., and Cheresh, D. A. Definition of two angiogenic pathways by distinct alpha v integrins. Science, *270:* 1500-1502, 1995.

5. Brooks, P. C., Klemke, R. L., Schon, S., Lewis, J. M., Schwartz, M. A., and Cheresh, D. A. Insulin-like growth factor receptor cooperates with integrin alpha v beta 5 to promote tumor cell dissemination in vivo. J Clin Invest, *99:* 1390-1398, 1997.

6. Dawson, D. W., Volpert, O. V., Gillis, P., Crawford, S. E., Xu, H., Benedict, W., and Bouck, N. P. Pigment epithelium-derived factor: a potent inhibitor of angiogenesis. Science, *285:* 245-248, 1999.

7. O'Reilly, M. S., Boehm, T., Shing, Y., Fukai, N., Vasios, G., Lane, W. S., Flynn, E., Birkhead, J. R., Olsen, B. R., and Folkman, J. Endostatin: an endogenous inhibitor of angiogenesis and tumor growth. Cell, *88:* 277-285, 1997.

8. Karumanchi, S. A., Jha, V., Ramchandran, R., Karihaloo, A., Tsiokas, L., Chan, B., Dhanabal, M., Hanai, J. I., Venkataraman, G., Shriver, Z., Keiser, N., Kalluri, R., Zeng, H.,

Mukhopadhyay, D., Chen, R. L., Lander, A. D., Hagihara, K., Yamaguchi, Y., Sasisekharan, R., Cantley, L., and Sukhatme, V. P. Cell surface glypicans are low-affinity endostatin receptors. Mol Cell, *7:* 811-822., 2001.

9. Rehn, M., Veikkola, T., Kukk-Valdre, E., Nakamura, H., Ilmonen, M., Lombardo, C., Pihlajaniemi, T., Alitalo, K., and Vuori, K. Interaction of endostatin with integrins implicated in angiogenesis. Proc Natl Acad Sci U S A, *98:* 1024-1029., 2001.

10. Maeshima, Y., Colorado, P. C., and Kalluri, R. Two RGD-independent alpha vbeta 3 integrin binding sites on tumstatin regulate distinct anti-tumor properties. J Biol Chem, *275:* 23745-23750, 2000.

11. Buerkle, M. A., Pahernik, S. A., Sutter, A., Jonczyk, A., Messmer, K., and Dellian, M. Inhibition of the alpha-nu integrins with a cyclic RGD peptide impairs angiogenesis, growth and metastasis of solid tumours in vivo. Br J Cancer, *86:* 788-795, 2002.

12. Yokoyama, Y. and Ramakrishnan, S. Substitution of a single amino acid residue in human endostatin potentiates inhibition of cancer growth. in communication, 2003.

13. Calvo, A., Yokoyama, Y., Smith, L. E., Ali, I., Shih, S. C., Feldman, A. L., Libutti, S. K., Sundaram, R., and Green, J. E. Inhibition of the mammary carcinoma angiogenic switch in C3(1)/SV40 transgenic mice by a mutated form of human endostatin. Int J Cancer, *101:* 224-234, 2002.

14. Ramakrishnan, S., Olson, T. A., Bautch, V. L., and Mohanraj, D. Vascular endothelial growth factor-toxin conjugate specifically inhibits KDR/flk-1-positive endothelial cell proliferation in vitro and angiogenesis in vivo. Cancer Res, *56:* 1324-1330, 1996.

15. Yokoyama, Y., Dhanabal, M., Griffioen, A. W., Sukhatme, V. P., and Ramakrishnan, S. Synergy between angiostatin and endostatin: inhibition of ovarian cancer growth. Cancer Res, *60:* 2190-2196, 2000.

16. Dhanabal, M., Ramchandran, R., Waterman, M. J., Lu, H., Knebelmann, B., Segal, M., and Sukhatme, V. P. Endostatin induces endothelial cell apoptosis. J Biol Chem, *274:* 11721-11726, 1999.

17. Shichiri, M. and Hirata, Y. Antiangiogenesis signals by endostatin. Faseb J, *15:* 1044-1053., 2001.

18. Wickstrom, S. A., Alitalo, K., and Keski-Oja, J. Endostatin associates with integrin alpha5beta1 and caveolin-1, and activates Src via a tyrosyl phosphatase-dependent pathway in human endothelial cells. Cancer Res, *62:* 5580-5589, 2002.

19. Sudhakar, A., Sugimoto, H., Yang, C., Lively, J., Zeisberg, M., and Kalluri, R. Human tumstatin and human endostatin exhibit distinct antiangiogenic activities mediated by alpha v beta 3 and alpha 5 beta 1 integrins. Proc Natl Acad Sci U S A, *100:* 4766-4771, 2003.

20. Buckley, C. D., Pilling, D., Henriquez, N. V., Parsonage, G., Threlfall, K., Scheel-Toellner, D., Simmons, D. L., Akbar, A. N., Lord, J. M., and Salmon, M. RGD peptides induce apoptosis by direct caspase-3 activation. Nature, *397:* 534-539, 1999.

21. Schraa, A. J., Kok, R. J., Moorlag, H. E., Bos, E. J., Proost, J. H., Meijer, D. K., de Leij, L. F., and Molema, G. Targeting of RGD-modified proteins to tumor vasculature: a pharmacokinetic and cellular distribution study. Int J Cancer, *102:* 469-475, 2002.

22. Arap, W., Pasqualini, R., and Ruoslahti, E. Cancer treatment by targeted drug delivery to tumor vasculature in a mouse model. Science, *279:* 377-380, 1998.

23. Curnis, F., Sacchi, A., Borgna, L., Magni, F., Gasparri, A., and Corti, A. Enhancement of tumor necrosis factor alpha antitumor immunotherapeutic properties by targeted delivery to aminopeptidase N (CD13). Nat Biotechnol, *18:* 1185-1190., 2000.

24. Wickham, T. J., Tzeng, E., Shears, L. L., 2nd, Roelvink, P. W., Li, Y., Lee, G. M., Brough, D. E., Lizonova, A., and Kovesdi, I. Increased in vitro and in vivo gene transfer by adenovirus vectors containing chimeric fiber proteins. J Virol, *71:* 8221-8229., 1997.

25. Joki, T., Machluf, M., Atala, A., Zhu, J., Seyfried, N. T., Dunn, I. F., Abe, T., Carroll, R. S., and Black, P. M. Continuous release of endostatin from microencapsulated engineered cells for tumor therapy. Nat Biotechnol, *19:* 35-39, 2001.

26. Kisker, O., Becker, C. M., Prox, D., Fannon, M., D'Amato, R., Flynn, E., Fogler, W. E., Sim, B. K., Allred, E. N., Pirie-Shepherd, S. R., and Folkman, J. Continuous administration of endostatin by intraperitoneally implanted osmotic pump improves the efficacy and potency of therapy in a mouse xenograft tumor model. Cancer Res, *61:* 7669-7674, 2001.

27. Capillo, M., Mancuso, P., Gobbi, A., Monestiroli, S., Pruneri, G., Dell'Agnola, C., Martinelli, G., Shultz, L., and Bertolini, F. Continuous infusion of endostatin inhibits differentiation, mobilization, and clonogenic potential of endothelial cell progenitors. Clin Cancer Res, *9:* 377-382, 2003.

Figure Legends

Fig. 1. Improved endothelial cell attachment by RGD-motif. HUVEC (A, B) or MA148 (C) cells prelabeled with 5(6)-CFDA were added into triplicate wells coated with P125A-endostatins, angiostatin, RGD-peptide at a concentration of 1 nmole / well or 0.2 % gelatin. Bound cells were quantified by a fluorescence plate reader. B, Competitive inhibition of endothelial cell binding to RGD-modified endostatins by RGD peptide. Stippled bars show cell attachment in the presence of RGD-peptide (50 nmole/well). A, B, C, 100 % is equal to the number of cells bound to 0.2 % gelatin coated wells. D, Direct binding of [^{125}I]-P125A-endostatin or [^{125}I]-RGD-endostatin to HUVEC. Data are expressed as a mean (columns)-± SD (bars). Statistical significance was determined using Student's t-test. * $p<0.05$.

Fig. 2. Specificity of RGD-endostatin binding. A human melanoma cell line, WM35, overexpressing $\alpha_v\beta_3$ integrin was used to determine the specificity of RGD-endostatin mediated cell attachment. A. Number of cells attached to wells coated with different reagents was quantified. Cells attached to 0.2% gelatin coated wells were used as 100% to calculate relative number of cells bound to RGD-endostatin coated wells. Data are expressed as a mean (columns) ± SD (bars). Statistical significance of differences was determined using Student's t-test. **$p<0.01$. B-G, The cell attachment was examined by Olympus BX-60 microscope at 100X magnification. Representative field of attached cells are shown. B, P125A-Endostatin; and C-G, RGD-Endostatin coated wells. Binding of WM35 cells to RGD-endostatin coated wells was completely blocked by preincubation with an anti-human $\alpha_v\beta_3$ antibody (D) or RGDS peptide (F). Negative controls include anti-HLA antibody (E) and RGES peptide (G).

Fig. 3. A, Inhibition of endothelial cell proliferation. Purified P125A-endostatin, RGD-endostatin, or endostatin-RGD was added to BCE cultures treated with 5 ng/ml bFGF for 4 days. ❑, P125A-Endostatin; ▲, RGD-Endostatin; ●, Endostatin-RGD. B, Specificity of RGD-modified endostatin mediated inhibition of endothelial cell proliferation. P125A-endostatin, RGD-endostatin, endostatin-RGD, RGDS, or RGES peptide were used at a concentration of 1 μM. As a control, 1 μM RGDS or RGES peptide was mixed with equimolar concentration of P125A-endostatin and added to BCE cells. C, Improved inhibition of endothelial migration by RGD-motif. Effect of P125A-endostatin (open bars), RGD-endostatin (stippled bars), and endostatin-RGD (closed bar) on endothelial cell (HUVEC) migration was determined using Boyden chambers. Basic FGF (25 ng/ml) was used to induce migration of endothelial cells. D, Specificity studies: P125A-endostatin, RGD-endostatin, endostatin-RGD, RGDS, or RGES peptide at a concentration of 50 nM. 50 nM RGDS or RGES peptide was mixed with 50 nM P125A-endostatin and added to HUVEC. The '0%' indicates basal level of migration of HUVEC in the presence of bFGF. E, endostatin-induced changes in bcl2 transcript levels in endothelial cells. Data are expressed as mean (columns) ± SE (bars). Statistical significance was determined using Student's t-test. $^{**}p<0.01$, $^{*}p<0.05$.

Fig. 4. Tumor uptake and half life studies. A, Human colon carcinoma cells (LS174T) were injected s.c. into female athymic nude mice. When the tumor size was around 500 mm^3 (10 days after inoculation), endostatin preparations were injected at a dose of 20 mg/kg subcutaneously. Endostatin levels are expressed as a percent of serum levels, and tumor tissue accumulation of P125A-endostatin was considered as 100%. B, Half life (β phase) of P125A-endostatin (empty bar)

and RGD-endostatin (solid bar) are shown. Data are expressed as mean percentage of injected dose. Statistical significance was determined using Student's t-test. **p<0.01, *p<0.05.

Fig.5. Improved inhibition of human colon cancer growth by RGD-endostatin. Human colon carcinoma cell line LS174T was injected s.c. into female athymic mice. After tumor establishment (3 days), mice were randomized and treated with P125A-endostatin or RGD-endostatin subcutaneously about 2 cm away from tumor sites at a dose of 20 mg/kg/day. Treatment was continued for 11 days. ❑, Control, PBS; ▲, P125A-Endostatin; ●, RGD-Endostatin. Mean tumor volume of control is shown. Statistical significance was determined by repeated measurement analysis of variance. The error bars indicate SE.

Fig. 6. Histochemical Analysis. Residual tumors from P125A-endostatin and RGD-endostatin treated groups were resected 1 day after the completion of treatment. A-C show vessel staining by anti-mouse CD31-PE conjugate; D-F show TUNEL staining for apoptotic cells and G-I show histology (H and E staining). Yellow bars = 250 μm. A, D and G, control; B, E and H, P125A-endostatin treated tumor sections; C, F and I, RGD-endostatin treated tumor sections. Quantification of apoptotic cells showed a marked increase in RGD-endostatin treated animals (J). Statistical significance was determined using Student's t-test. * p<0.05. The error bars indicate SE.

Fig. 7. Improved inhibition of human colon cancer growth by endostatin-RGD. Inhibition of ovarian cancer growth by endostatin-RGD encapsulated into alginate beads. Arrows represent treatment schedule. ❐, Alginate bead control; ▲, P125A-Endostatin; △, Endostatin-RGD. Mean

tumor volume of control is shown. Statistical significance was determined by repeated measurement analysis of variance.

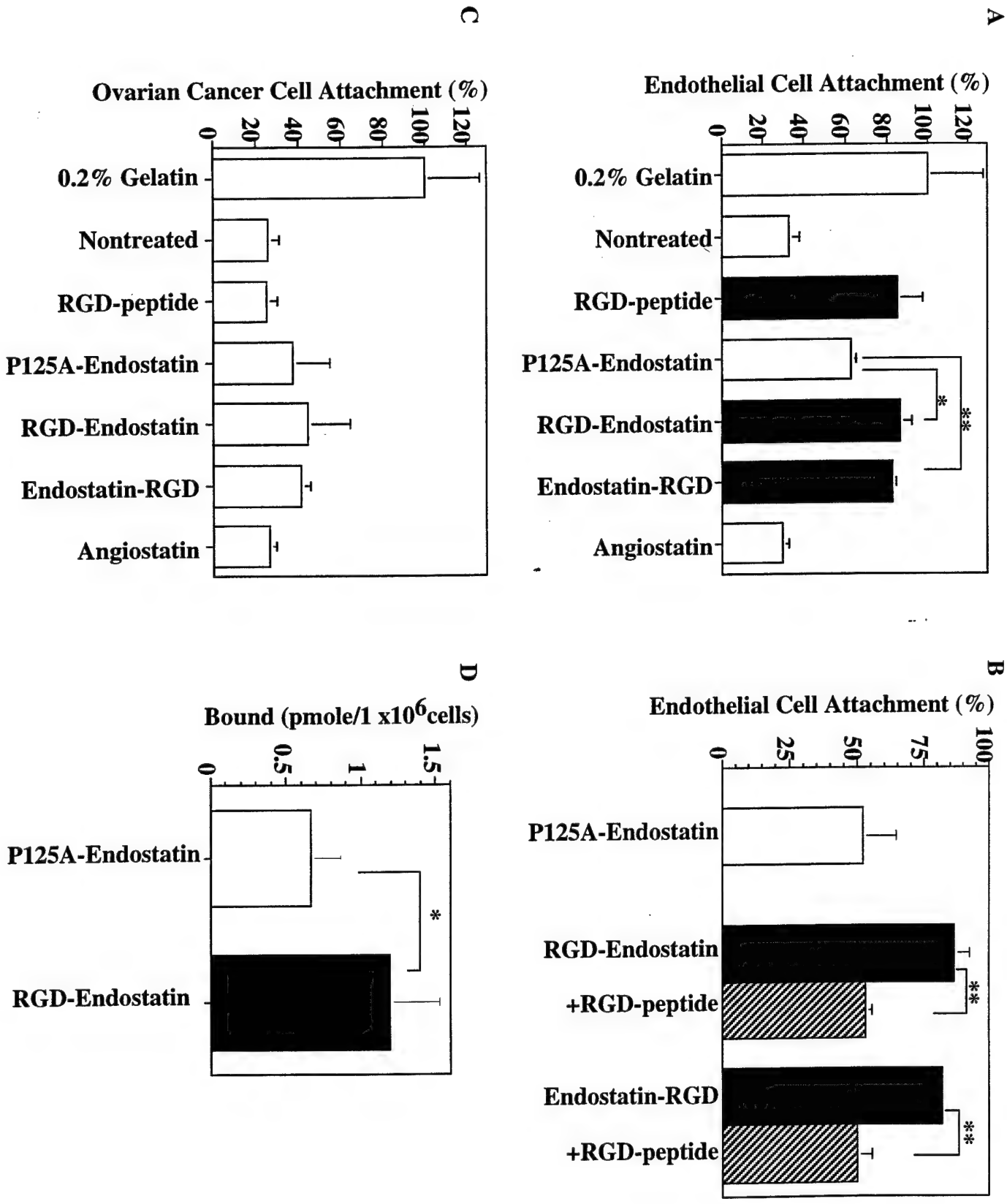
A
Endothelial Cell Attachment (%)
0
20
40
60
80
100
120
0.2% Gelatin
Nontreated
RGD-peptide
P125A-Endostatin
RGD-Endostatin
Endostatin-RGD
Angiostatin
*
**
B
Endothelial Cell Attachment (%)
0
25
50
75
100
P125A-Endostatin
RGD-Endostatin
+RGD-peptide
Endostatin-RGD
+RGD-peptide
**
**
C
Ovarian Cancer Cell Attachment (%)
0
20
40
60
80
100
120
0.2% Gelatin
Nontreated
RGD-peptide
P125A-Endostatin
RGD-Endostatin
Endostatin-RGD
Angiostatin
D
Bound (pmole/1 x10^{6}cells)
0
0.5
1
1.5
P125A-Endostatin
RGD-Endostatin
*

Figure 1

A

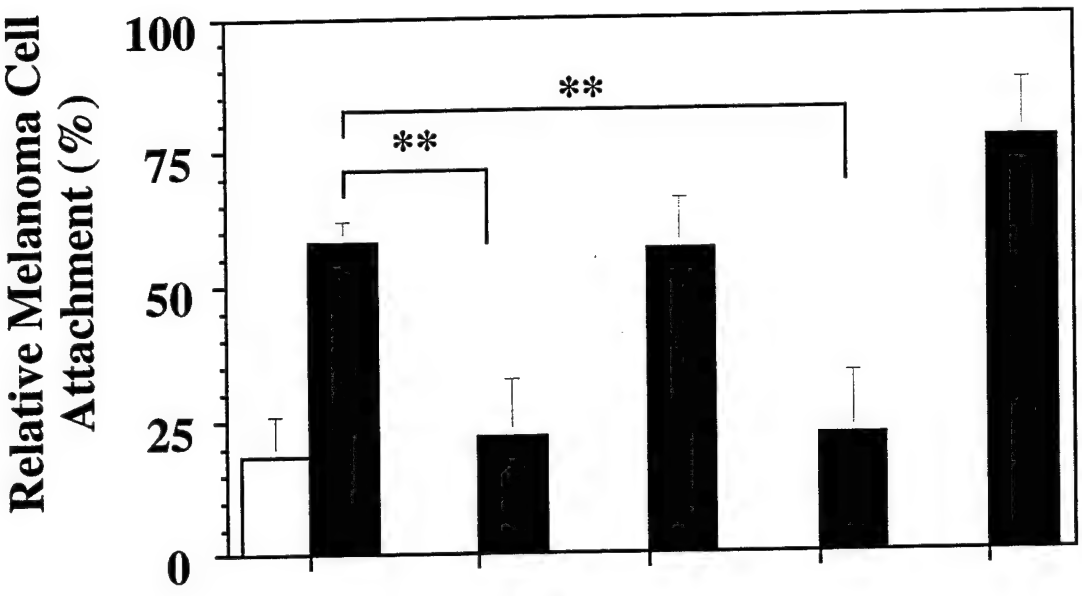

P125A-Endostatin	+	-	-	-	-	-
RGD-Endostatin	-	+	+	+	+	+
anti αvβ3	-	-	+	-	-	-
control IgG	-	-	-	+	-	-
RGDS	-	-	-	-	+	-
RGES	-	-	-	-	-	+

Figure 2-A

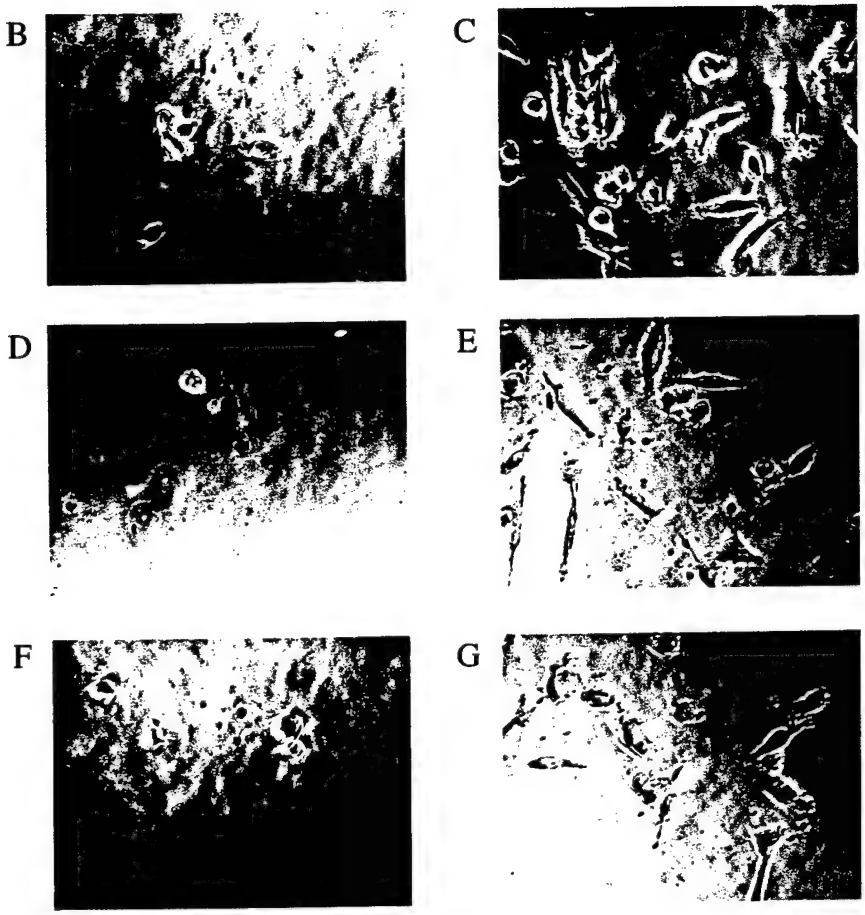

Figure 2-B

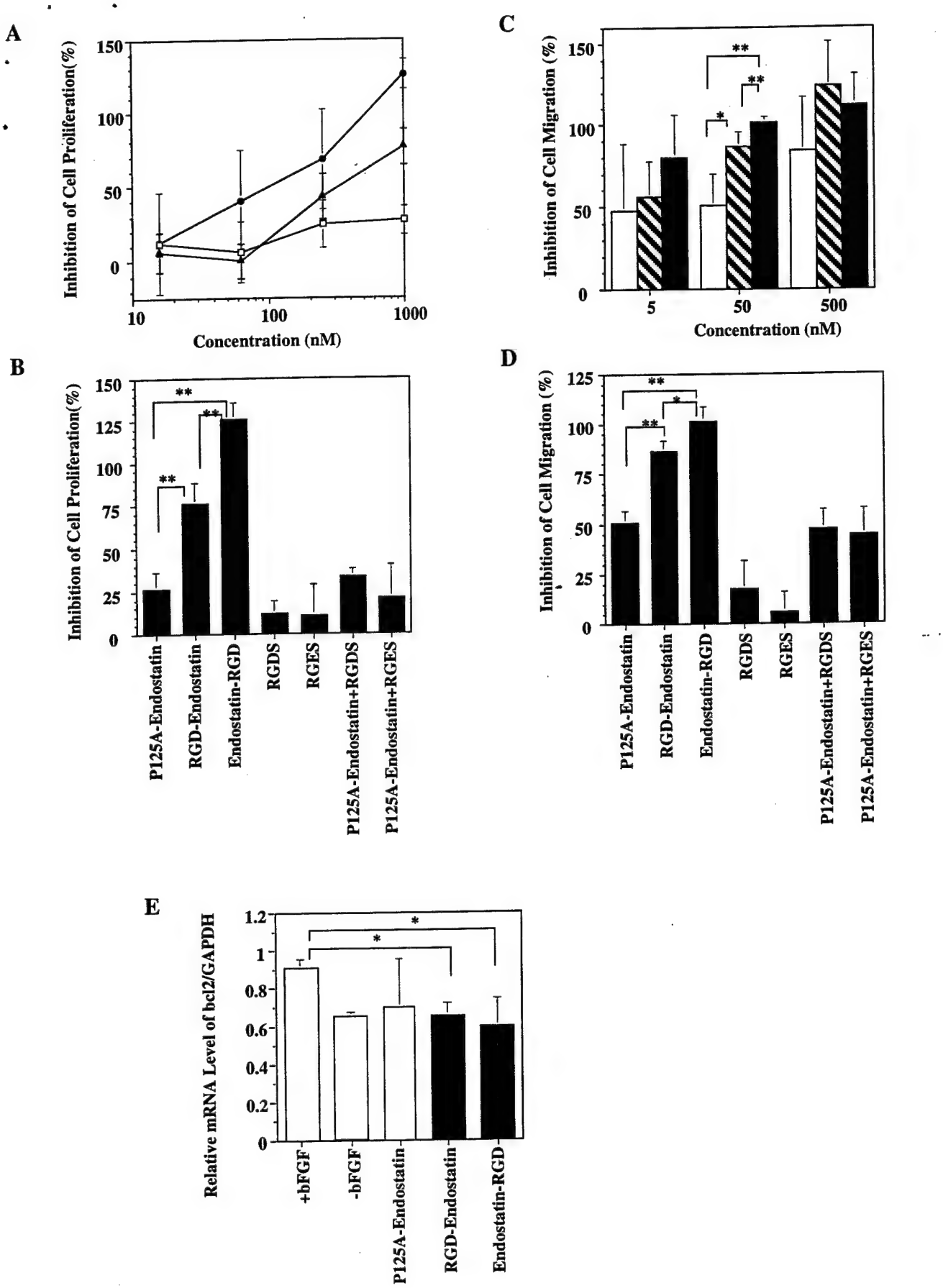
A
Inhibition of Cell Proliferation(%)
150
100
50
0
10
100
1000
Concentration (nM)
C
Inhibition of Cell Migration (%)
150
100
50
0
5
50
500
Concentration (nM)
B
Inhibition of Cell Proliferation(%)
150
125
100
75
50
25
0
P125A-Endostatin
RGD-Endostatin
Endostatin-RGD
RGDS
RGES
P125A-Endostatin+RGDS
P125A-Endostatin+RGES
D
Inhibition of Cell Migration (%)
125
100
75
50
25
0
P125A-Endostatin
RGD-Endostatin
Endostatin-RGD
RGDS
RGES
P125A-Endostatin+RGDS
P125A-Endostatin+RGES
E
Relative mRNA Level of bcl2/GAPDH
1.2
1
0.8
0.6
0.4
0.2
0
+bFGF
-bFGF
P125A-Endostatin
RGD-Endostatin
Endostatin-RGD

Figure 3

A

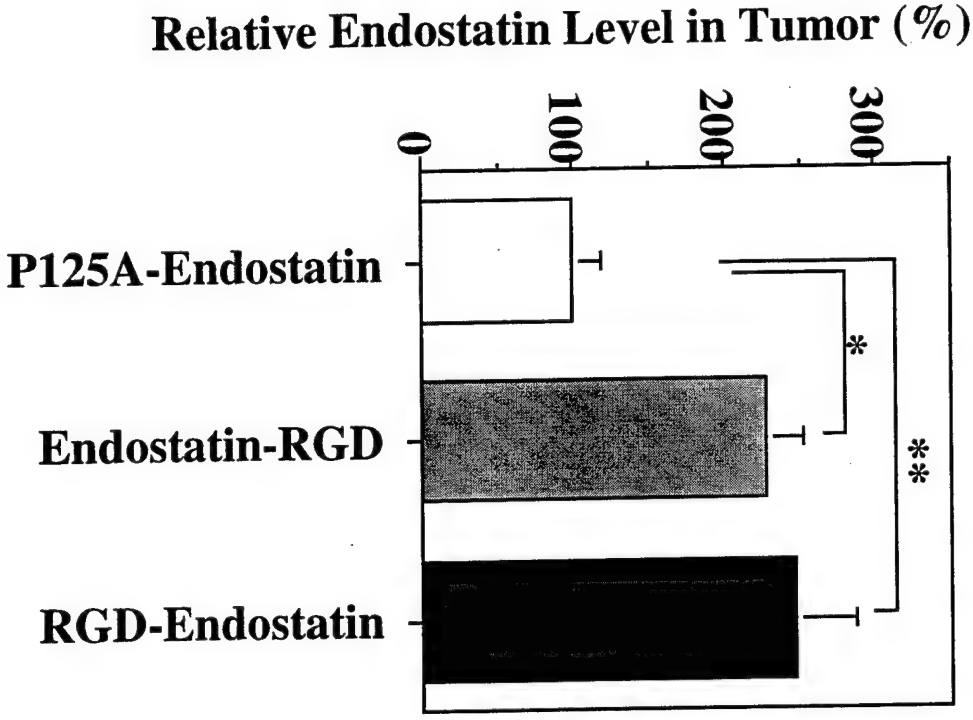
Relative Endostatin Level in Tumor (%)
0
100
200
300
P125A-Endostatin
Endostatin-RGD
RGD-Endostatin
*
**

B

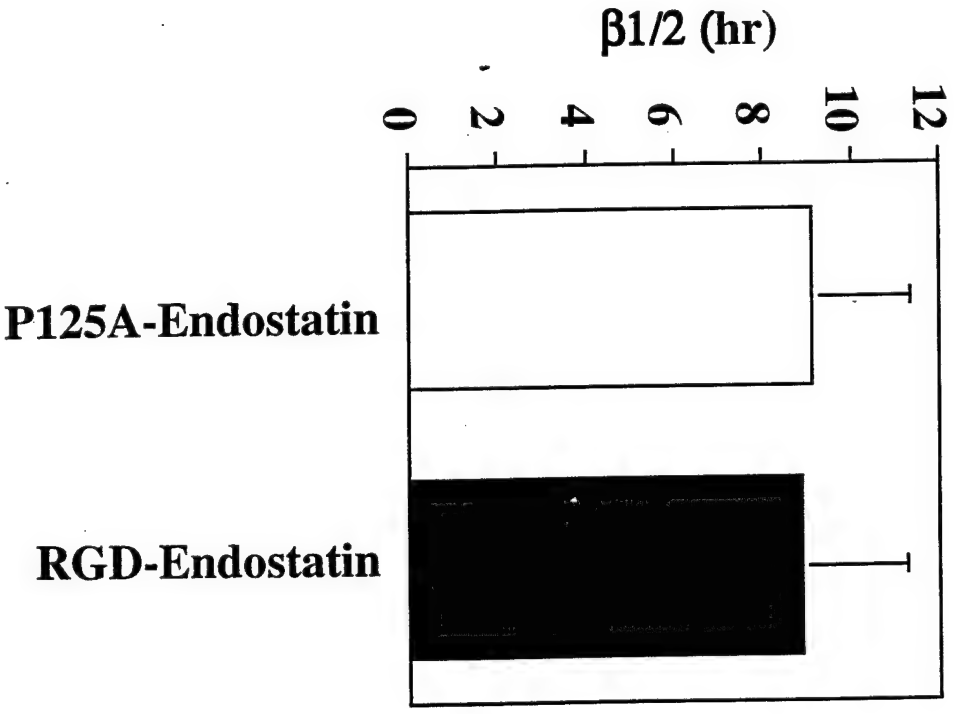
β1/2 (hr)
0
2
4
6
8
10
12
P125A-Endostatin
RGD-Endostatin

Figure 4

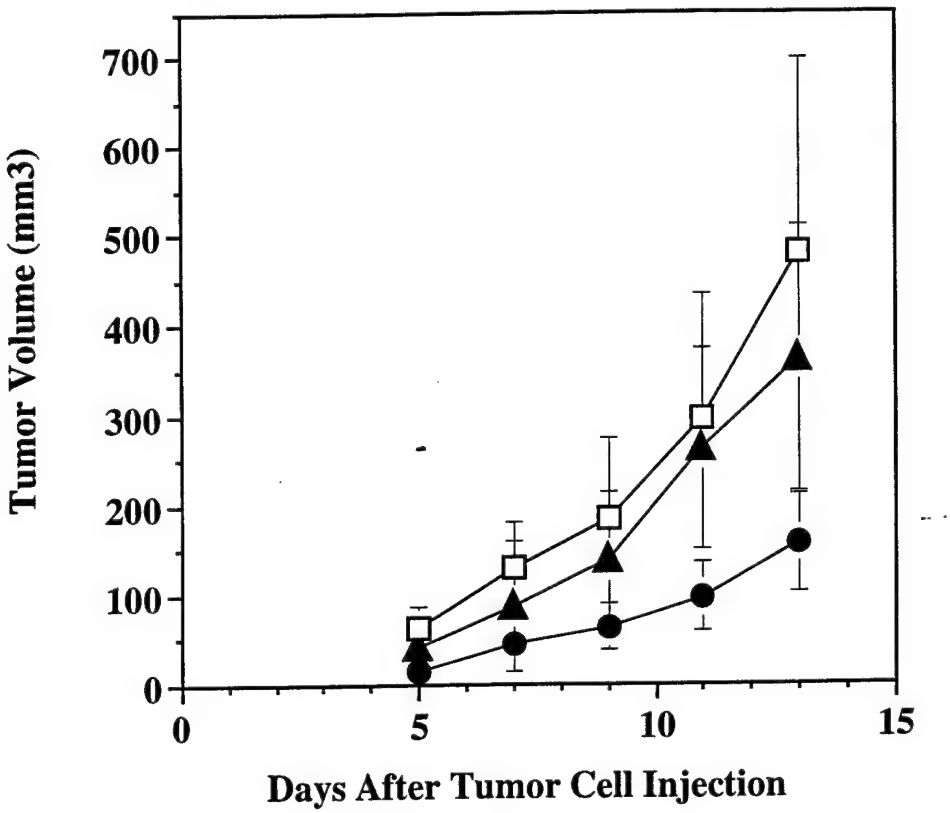
Tumor Volume (mm3)
700
600
500
400
300
200
100
0
0
5
10
15
Days After Tumor Cell Injection

Figure 5

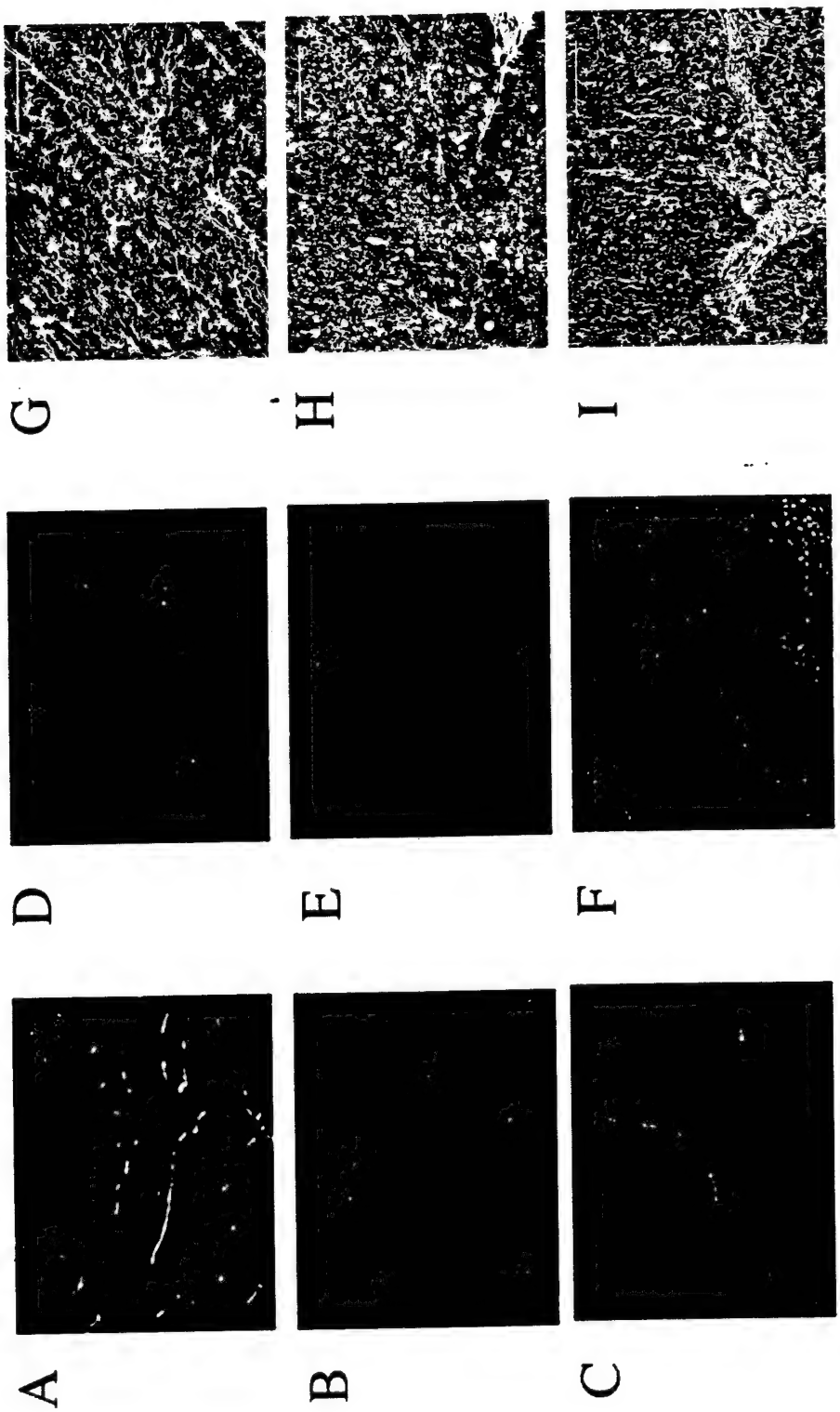

Figure 6 (A-I)

J

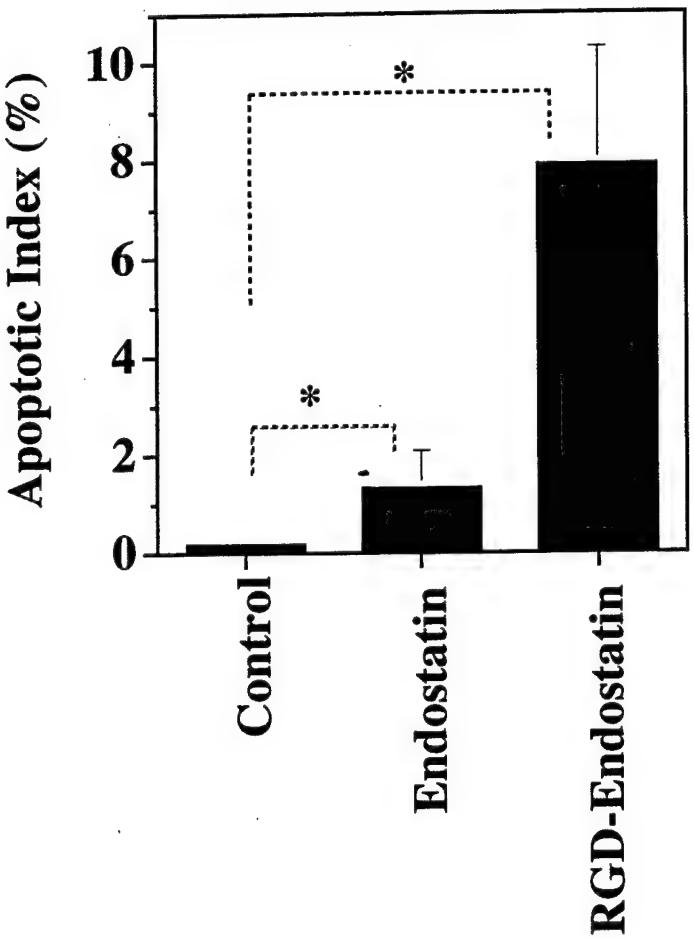
Apoptotic Index (%)
10
8
6
4
2
0
*
*
Control
Endostatin
RGD-Endostatin

Figure 6 (J)

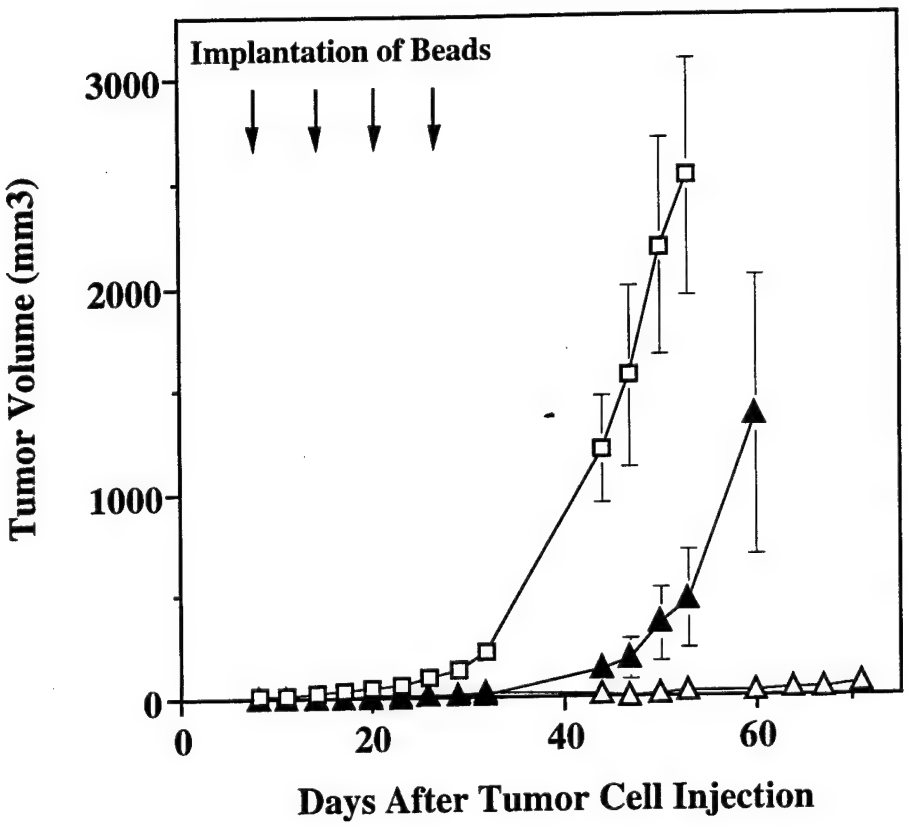
Implantation of Beads
3000
2000
1000
0
Tumor Volume (mm3)
0
20
40
60
Days After Tumor Cell Injection

Figure 7

Improved biological activity of a mutant endostatin containing a single amino acid substitution

Yumi Yokoyama[1] and S. Ramakrishnan[1, 2,3]

Department of Pharmacology [1], Obstetrics and Gynecology [2], Comprehensive Cancer Center [3], University of Minnesota, Minneapolis, MN

Running Title: Mutant Endostatin

Corresponding author: S. Ramakrishnan

6-120 Jackson Hall,

321 Church Street, S.E.,

Department of Pharmacology,

University of Minnesota, Minneapolis, MN 55455

Ph: (612) 624 1461

Fax : (612) 625 8408

Email: sunda001@umn.edu

Key Words: endostatin, point mutation, tumor angiogenesis, ovarian cancer, colon cancer

Abbreviations: HUVEC, human umbilical vein endothelial cell; bFGF, basic fibroblast growth factor; BCE, Bovine adrenal gland capillary endothelial; VEGF, vascular endothelial growth factor; PMSF, phenylmethylsulfonyl fluoride

ABSTRACT

Human endostatin has an internal NGR-motif at position 126-128 following a proline at position 125. NGR-containing peptides have been shown to target tumor vasculature and inhibit aminopeptidase N activity. We previously compared the *in vitro* and *in vivo* biological activities of native endostatin and endostatin with a proline to alanine mutation (P125A-endostatin). P125A-endostatin exhibited greater inhibition of both endothelial cell proliferation and human ovarian cancer growth compared to native endostatin. Here we explore further the effects on biological activity of the P125A mutation, and show that aminopeptidase N is not involved.

To determine whether the increased biological activity of the mutant was due to unmasking of downstream NGR-sequence, effect of endostatin on aminopeptidase N activity was investigated. Neither the native nor the P125A-endostatin inhibited aminopeptidase N. However, synthetic peptides consisting of the S118-T131 region of endostatin inhibited aminopeptidase N. These results suggest that the internal NGR-site in native or mutant endostatin is not accessible to aminopeptidase N, and that this activity is not involved in the enhanced biological activity of the P125A form.

P125A-endostatin bound to endothelial cells more efficiently than native endostatin and exhibited greater inhibition of not only proliferation but also migration of endothelial cells. P125A-endostatin also localized into tumor tissue to a higher degree than the native protein, and displayed greater inhibition of growth of colon cancer in athymic mice. Both proteins inhibited tumor cell-induced angiogenesis effectively. Real Time PCR analysis showed that both native and P125A-endostatin decreased expression

of key proangiogenic growth factors. VEGF and angiopoietin 1 were downregulated more by the mutant. These studies suggest that the region around P125 can be modified to improve the biological activity of endostatin.

INTRODUCTION

Endostatin is a proteolytic fragment of the non-collagenous domain of collagen type XVIII (O'Reilly et al., 1997), a component of the basement membrane. Endostatin inhibits growth factor induced proliferation and migration of endothelial cells *in vitro* and angiogenesis *in vivo*. A number of independent studies have shown that endostatin treatment inhibits tumor growth by blocking angiogenesis (Boehm et al., 1997; Dhanabal et al., 1999; O'Reilly et al., 1997). Endostatin binds to at least two distinctive sets of molecules on the endothelial cell surface, $\alpha_5\beta_1/\alpha_v\beta_3$ integrin (Rehn et al., 2001; Wickstrom et al., 2002) and glycosyl-phosphatidylinositol (GPI) anchored heparin sulphate proteoglycan (HSPG), or Glypican (Karumanchi et al., 2001). Glypican is believed to sequester endostatin and present it to the integrins, thereby forming a receptor-signaling complex. Binding to integrins is linked to phosphorylation of SH2 containing Shb adaptor protein, which is implicated in the apoptotic cascade (Dixelius et al., 2000). Such interactions can activate intracellular signaling leading to inhibition of endothelial cell proliferation and migration (Rehn et al., 2001; Shichiri & Hirata, 2001). A recent study showed that wnt-signaling pathways might also be modulated by endostatin (Hanai et al., 2002). In addition to these direct actions, endostatin has been shown to bind and inactivate metalloproteinases *in vitro* (Kim et al., 2000). These studies collectively imply that the mechanism of endostatin action is diverse and complex. Understanding the structure/function of endostatin therefore will help in improving its efficacy to inhibit tumor growth.

Human endostatin containing a point mutation at position 125 has been identified during expression cloning (Calvo et al., 2002). Proline 125 is followed by a tripeptide,

Asn-Gly-Arg (NGR), a sequence that is known to target endothelial cells (Pasqualini et al., 2000). In fact, chemical linkage of doxorubicin to NGR peptides inhibited tumor growth efficiently (Arap et al., 1998). NGR sequence has also been shown to bind and inhibit aminopeptidase N localized on vascular endothelial cells of tumors. The P125A-mutation is not a conservative change and would be expected to alter peptide folding around the mutation site. However, we were able to express P125A-endostatin in yeast in fully soluble form, and showed that it has similar gross secondary structures as native endostatin. P125A-endostatin inhibited *in vitro* endothelial cell proliferation and *in vivo* growth of ovarian cancer more effectively when compared to native endostatin (Calvo et al., 2002).

In this study we have further explored the differences between native and P125A-endostatin. We report that the mutant protein binds more effectively to endothelial cells and is more effective in inhibiting not only endothelial cell proliferation but also migration *in vitro*. P125A-endostatin also displayed improved inhibition of colon cancer growth in athymic mice, and greater down regulation of human Vascular Endothelial Growth Factor (VEGF) and human Angiopoietin 1 (Ang1) from tumors. Neither native nor mutant endostatin inhibited aminopeptidase N activity. These studies suggest that structural changes in endostatin can be used to improve the biological activity of human endostatin.

MATERIALS AND METHODS

Cell lines and culture conditions

Bovine adrenal gland capillary endothelial (BCE) cells were obtained from Clonetics Inc. (San Diego, CA). Culture conditions of human umbilical vein endothelial cells (HUVEC) have been published previously (Ramakrishnan et al., 1996). Human colon carcinoma cell line, LS174T, was obtained from American Type Culture Collection (ATCC, Rockville, MD). LS174T cells were cultured in RPMI-1640 (GIBCO BRL, Gaithersburg, MD) supplemented with 10% FBS, 100 U/ml penicillin, 100 μg/ml streptomycin, and 2 mM L-glutamine.

Cloning, expression and purification of mutant human endostatin

The following primers were used to amplify the C-terminal end of collagen type XVIII (183 amino acid residues) by RT-PCR:

Up : GGGGAATTCCACAGCCACCGCGACTTCCAG

Down : GGGGCGGCCGCCTACTTGGAGGCAGTCATGAAGCT.

The PCR product was cloned into pPICZ-αA vector (Invitrogen, Carlsbad, CA) and sequenced. Selected clones were electroporated into X-33 host strain of *Pichia pastoris* (Invitrogen). Previously published methods were followed for expression and purification of endostatin (Yokoyama et al., 2000).

Structural analysis by circular dichroism (CD)

CD studies of endostatin and P125A-endostatin were carried out in a JASCO J-710 spectropolarimeter. Protein samples were prepared in PBS at a concentration of 100

μg/ml. Path length of the cell was 0.1 cm. CD spectra and molar ellipticity were obtained over the wavelength range of 195-260 nm.

Cell attachment assay

One nmole/well of endostatin preparations or 0.2% gelatin were used to coat 96 well plates. Plates were incubated at 4°C overnight, and then blocked with 2 % BSA in PBS at 37°C for 2 hr. HUVEC were harvested by 2 mM EDTA in PBS and prelabeled with a vital, fluorescence dye, 5 μM 5-(and-6)-carboxyfluorescein diacetate, succinimidyl ester (5(6)-CFDA) (Molecular Probes, Eugene, OR) for 10 min at 37°C. After washing with Hank's balanced salt solution (HBSS), the labeled cells were resuspended in M199 medium (GIBCO BRL) supplemented with 10 % FBS. Cells were added to wells at a density of 40,000 cells / well. After one hour-incubation at 37°C, plates were washed twice with HBSS to remove unbound cells. Fraction of bound cells was determined by a fluorescence plate reader (Cyto Fluor II; PerSeptive Biosystems, Framigham, MA) (excitation; 485 nm, emission; 530 nm).

Aminopeptidase N activity

Aminopeptidase N was extracted from HUVEC by lysis buffer (20 mM Tris/HCl (pH 7.6), 150 mM NaCl, 2 mM PMSF, 10 μg/ml leupeptin, 0.5 mM o-vanadate, 20 mM N-ethyl-maleimide and 2% Triton X-100) and the enzymatic activity was assayed using alanine p-nitroanilide (Sigma-Aldrich, St. Louis, MO) as a substrate (Arap et al., 1998). HUVEC lysate (10 μg protein) was used as a source of aminopeptidase N and incubated with 0.225 mg (0.9 μmole) substrate in a reaction buffer (10 mM Tris/HCl (pH 7.6), 150

mM NaCl) in the presence and absence of inhibitors at 37°C for 2 hr. Aminopeptidase N activity was detected by absorbance at 405 nm.

Endothelial cell proliferation assay

Essentially, the method described by O'Reilly *et al.* was used (O'Reilly et al., 1997). Logarithmically growing BCE cells were trypsinized, and resuspended in M199 medium with 2 % FBS. Cells were then seeded into gelatinized, 96-well culture plates at a density of 5000 cells per well. After 24 hours, different concentration of native or P125A-endostatin was added. Twenty minutes later, cultures were treated with 5 ng/ml of basic fibroblast growth factor (bFGF; GIBCO BRL). The viability of the control and the treated cells was determined by the 3-(4,5-dimethylthiazol-2yl)-2,5-diphenyl-2,4-tetrazolium bromide (MTT; Sigma-Aldrich) assay (Carmichael et al., 1987) after 72 hrs of incubation. This assay has been previously used to evaluate endothelial cell proliferation (Yoon et al., 1999).

Endothelial cell migration assay

The migration of endothelial cells was determined by using Boyden chambers (Neuro Probe, Gaithersburg, MD). Polycarbonate filters (pore size; 12 μm) were coated with 0.2% gelatin for 1 hour at 37°C. HUVEC were harvested by 2 mM EDTA in PBS. HUVEC were prelabeled with 5 μM 5(6)-CFDA for 10 min at 37°C. Cells were resuspended in 0.5% FBS, M199 medium and then preincubated with native or P125A-endostatins for 60 min at 37°C. Basic FGF (25 μl of 25 ng/ml 0.5% FBS, M199 medium) was added to lower chambers. HUVEC (200,000 cells / ml, control and treated) were

added to upper chambers. After 4 hours of incubation at 37°C, endothelial cells that had migrated to the bottom side of the membrane were counted. Cells that remained on the upper side of the membrane were removed by cotton swabs. Migrated cells were counted using a fluorescence microscope (Olympus) using FITC filters (magnification 200 X). Three independent experiments were carried out.

Tumor localization

LS174T cells were injected subcutaneously at right and left sides of the flanks of athymic nude mice. Tumor size reached about 500 mm^3 on day 10. Tumor bearing mice were randomized into 2 groups. Endostatin or P125A-endostatin was injected at a dose of 20 mg/kg subcutaneously. Tumor tissues and representative normal tissues were surgically removed after 19 hrs. This time point was chosen to minimize overwhelming serum levels from obscuring the tissue bound endostatin. For comparison, serum samples were also collected from the mice. Tissues were snap frozen, and homogenized in RIPA buffer containing proteinase inhibitors (PBS, 1% NP40, 0.5% sodium deoxycholate, 0.1% SDS, 10 μg/ml PMSF), maintained at 4°C for 45 min, and cleared by centrifugation. Human endostatin concentrations in serum and tissue lysates were measured using an enzyme linked immunoassay (Cytimmune, College park, MD) according to the manufacturer's instructions. Statistical significance was determined by Student's t-test.

Matrigel plug assay

Matrigel plug assay was used to determine inhibition of tumor cell-induced angiogenesis *in vivo* (Zhang et al., 2000). Matrigel (ECM gel) was purchased from Sigma-Aldrich.

LS174T cells were trypsinized, and resuspended in serum free RPMI1640 medium at a density of 2 x10^6 cells per 167 μl. Cell suspension was mixed with 333 μl of matrigel on ice, and this mixture was injected into nude mice subcutaneously. Mice were treated with native endostatin or P125A-endostatin at a dose of 20 mg/kg/day subcutaneously at a distant site near the neck. Control mice were treated with an equal volume of sterile PBS at similar schedule. Treatment was started just after the matrigel implantation and continued for one week. One day after the last treatment, the matrigel was removed. A part of the matrigel was used to prepare cryostat sections and another part of the samples was used for Real Time PCR analysis. Frozen sections (10 μm) of matrigel samples were treated with PBS containing 10 % fetal bovine serum to block non-specific binding (background). Sections were then incubated with 1: 50 dilution of an anti-CD31 monoclonal antibody conjugated to phycoerythrin (MEC 13.3, BD PharMingen, San Diego, CA). Following one-hour incubation at room temperature, sections were washed thoroughly with PBS and then examined under an Olympus BX-60 fluorescence microscope at 200 X magnification. Images were captured by a Spot Camera (Diagnostic Instrument). Vessel density, length, branch points and ends were quantified by a method previously reported by Wild *et al.* (Wild et al., 2000). Serial frozen sections were used to localize VEGF by indirect immunoflourescence method using a polyclonal antiserum made against recombinant human $VEGF_{165}$ (Olson et al., 1996). FITC-labeled goat anti-rabbit IgG was used as a secondary antibody. After one hour incubation at room temperature, sections were washed with PBS, and examined by a fluorescence microscope. A mounting solution including 1 μg/ml DAPI was used to stain nuclei.

Another part of the matrigel samples were fixed in 10 % neutral buffered formalin and processed for hematoxylin and eosin (H&E) staining.

Quantitative real time PCR analysis

Total RNA was extracted from frozen matrigel samples using the RNeasy Mini kit (Qiagen, Valencia, CA) according to the manufacturer's protocol. Reverse transcription was performed with the SuperScript II kit (Invitrogen) using 1 μg of total RNA. Real Time PCR was carried out by using SYBR Green PCR Master Mix (Applied Biosystems, Foster City, CA) in an ABI PRISM 7700 Sequence Detection System (Applied Biosystems) (TaqMan). Primer sequences described by Gerber *et al.* (Gerber et al., 2000) were used (Table 1) to amplify proangiogenic factors related messages from the human tumor cells and relevant target receptors on endothelial cells of mouse origin. Following conditions were used for PCR: 50 °C for 2 min, 95 °C for 10 min, and 40 cycles at 95°C for 0.15 min, 60°C for 1 min. Negative controls included omission of the template. SYBR Green dye intercalation into the minor groove of double-stranded DNA reaches an emission maximum at 530 nm. Relative RNA equivalents for each sample were calculated by either comparing to human or mouse GAPDH levels. Five to six samples per group were run in duplicate. Statistical analysis was performed by Student's t-test.

Preparation of alginate beads encapsulated endostatins and tumor growth inhibition studies

Alginic Acid extracted from *Macrocystis pyrifera* was purchased from Sigma Chemicals. Four percent (w/v) of alginic acid in water was sterilized by autoclaving. Endostatin

preparations or PBS (control) made in 1.5 % alginic acid were dropped gently into 0.1 M $CaCl_2$ solution using a fine needle under aseptic conditions. Beads were kept at 4°C overnight and were washed with sterile water before the subcutaneous implantation into tumor bearing mice. Entrapment efficiency was calculated by determining the amount of protein remaining outside the beads from the total protein using BCA protein assay kit (Pierce, Rockford, IL). Logarithmically growing LS174T cells were harvested by trypsinization and suspended in serum free medium at a density of 1 x 10^7 cells/ml. One hundred μl of the single cell suspension were then subcutaneously injected into the flanks of female athymic mice (6 to 8 wks old). When the tumors became visible (3 days after inoculation), mice were randomized into groups and treated with endostatin encapsulated alginate beads (five animals per group). Endostatins were implanted at a distant site (about 2 cm away) at a dose of ~20 mg/kg once a week. Tumor growth was monitored by periodic caliper measurements. Tumor volume was calculated by the following formula. Tumor volume (mm^3) = $(a \times b^2)/2$ Where 'a' = length in mm, 'b' = width in mm. Statistical significance between control and treated groups was determined by Student's t-test.

RESULTS

Preparation and structural analysis of P125A endostatin

Native human endostatin and a mutant with a proline to alanine substitution at position 125 were cloned and expressed in *Pichia pastoris*. The P125A mutation did not change the binding of endostatin to heparin. Like native human endostatin, P125A-endostatin

bound to a heparin-ceramic column and eluted at around 300 mM NaCl concentration, indicating similar binding strength to heparin (data not included).

An NGR-sequence capable of targeting endothelial cells is located immediately following the P125A-mutation site. Conformational features surrounding the mutation site are shown in Fig. 1A. Crystallographic data published by Ding *et al.* (Ding et al., 1998) show that P125 is located in a loop flanked by two β-sheets. In order to determine whether the mutant protein was folded properly, gross secondary structural analysis of the P125A mutant was compared to the native protein made in the same expression system. The CD spectra of native and P125A human endostatin showed identical profiles, indicating that the two proteins have similar gross secondary structures (Fig. 1B).

P125A mutation enhanced endothelial cell binding

The biological characteristics of P125A-endostatin were compared to those of the native protein in a number of assays. As a first step, the ability to bind endothelial cells was assessed using cell-attachment assays. Gelatin (0.2 %) coated wells were used as a control, with the number of cells (HUVEC) attached to gelatin coated wells taken as 100 % to calculate relative binding. By this standard, 38.5% of HUVEC attached to endostatin-coated wells. Under similar conditions, a significantly higher number of HUVEC (71%) bound to wells coated with P125A-endostatin (Fig. 1C) (P=0.005). The observed differences in cell attachment are not due to variation in coating efficiencies, which were determined by ELISA method.

Inhibition of endothelial cell migration

A possible consequence of increased binding is increased biological activity. Previously we showed that P125A-endostatin inhibited endothelial cell proliferation more efficiently than native endostatin did (Calvo et al., 2002). Endothelial cell migration assay is a more sensitive parameter to assess the biological activity of endostatin. Therefore, bFGF induced migration of endothelial cells was determined in the presence of native and P125A-endostatin. Similar to the proliferation assays, this mutant endostatin was more effective than native protein in inhibiting cell migration (Fug. 1D). At all three concentrations tested, P125A-endostatin inhibited endothelial cell migration more efficiently than native endostatin.

Tumor localization is improved by P125A-mutation

To assess whether the improved endothelial cell binding *in vitro* can translate into enhanced tumor homing *in vivo,* tumor localization studies were performed. Endostatin and P125A-endostatin were injected subcutaneously into human colon cancer-bearing athymic mice. Tumor, lung, liver and serum samples were collected. Relative levels of endostatin in the tissues are shown in Fig. 1E. Native endostatin accumulated in the tumor tissues at a level of 3.0 % when compared to serum levels. P125A-endostatin, on the other hand, was found at a more than 3-fold higher concentration in the tumor tissue (10.22% compared to serum levels). This difference was statistically significant ($p=0.03$). While the liver showed negligible amounts of endostatins, lung tissues had significant accumulation of both native and mutant endostatin. However, lung tissues did not show any statistical difference between native and P125A-endostatin accumulation.

Effect of endostatin and P125A-endostatin on aminopeptidase N activity

As the mutation site is immediately followed by NGR motif, we next tested whether the mutant endostatin has aminopeptidase N inhibitory activity. Cellular extracts of aminopeptidase N enzyme were prepared from HUVEC. These cells express 8-10 times higher levels of aminopeptidase N compared to cancer cells such as B16F10 (mouse melanoma), U937 (human monocytic leukemia cell line), MA148 (human ovarian cancer cell line) and LS174T (human colon carcinoma cell line). Confluent HUVEC lysate showed about 3 times higher activity than proliferating HUVEC lysate (data not shown).

The data in Fig. 2A show the effect of endostatin and its mutant on aminopeptidase N activity. As a positive control, the same concentration of bestatin, a known inhibitor of aminopeptidase N, was included. Bestatin inhibited 35 % of the enzymatic activity under the experimental conditions used. Leupeptin, a negative control, did not inhibit the enzyme. Interestingly, neither the native nor the P125A mutant showed any inhibition of aminopeptidase N activity even at 5 μM concentration.

In a separate experiment we tested whether synthetic peptides consisting of the amino acid sequence flanking the normal or mutated position 125 (S118-T131) could inhibit aminopeptidase N (Fig. 2B). Interestingly both peptides (native and mutant) inhibited aminopeptidase N activity more effectively than bestatin. At a concentration of 5 μM, the mutant and native peptide inhibited aminopeptidase N by 71.2% and 69.2% respectively. These studies suggest that the NGR-motif in intact endostatin molecules constructs may not be accessible to interact with aminopeptidase N.

To confirm our findings we characterized the interaction between endostatins and aminopeptidase N in an immunoabsorption assay using antibodies to human aminopeptidase N enzyme. Both synthetic peptides (125A and 125P) corresponding to the region S118-T131 were capable of binding to aminopeptidase N, to similar levels. However, intact proteins (native and P125A-endostatin) did not show any detectable binding to aminopeptidase N (data not included). These results further confirm that the NGR motif in endostatin is not accessible for binging to aminopeptidase N.

Antiangiogenic activity of P125A-endostatin

Next we determined the ability of endostatin and P125A-endostatin to inhibit human colon cancer cell-induced angiogenesis *in vivo* using matrigel plug assays. Both endostatin and P125A-endostatin inhibited angiogenesis stimulated by LS174T colon carcinoma cells (Fig. 3). Histological investigation of matrigels from control and treated (native or mutant endosttain) animals showed higher tumor cell density interspersed with well developed blood vessels in control matrigels when compared to endostatin treated groups. Endostatin treated groups showed some of the tumor cells organized into islands. (Fig. 3 B, C, E, and F) when compared to control group treated with PBS (Fig. 3 A, D). Anti-CD31 staining of frozen sections showed quantitative difference between control and treated groups (Fig. 4).

The overall indicators of angiogenesis, such as microvessel density (MVD), number of blood vessel ends (Ends), Nodes (branch points), and length, showed that both endostatin and P125A-endostatin treatment significantly inhibited angiogenesis *in vivo* (Fig.3 H, I, Fig. 4). Furthermore, endostatin treatment seemed to alter angiogenic growth

factor expression in the tumor cell microenvironment. Cryostat sections of matrigels showed reduced amounts of VEGF in immunofluorescence studies using a polyclonal antibody made against human $VEGF_{165}$ (Fig. 3 K, L). Reduced VEGF levels may be a reflection of reduced number of tumor cells in the matrigel following endostatin treatment or due to an indirect effect of endostatin mediated changes in the microenvironment.

Downregulation of angiogenic factors and receptors by native and P125A-endostatin

Previously we showed that the mammary gland of P125A-endostatin treated C3(1)/SV40 transgenic mice exhibited decreased mRNA levels of VEGF, Angiopoietin-2, flk-1, flt-1, tie-1 and cadherin-5 when compared to PBS treated control. In the present study, a different model system was used to determine selective changes in tumor induced neovascularization. Matrigel plugs do not contain any other host cells or vasculature at the beginning of the experiment. Therefore this model system is good to assess changes in tumor cell microenvironment following antiangiogenic therapy. To determine whether endostatin treatment altered RNA levels of proangiogenic factors from tumor and host receptors in newly formed blood vessels, Real Time PCR was performed using total RNA isolated from the matrigel samples. Proangiogenic factors were detected by human gene specific primers, and receptors were detected by mouse gene specific primers (Table 1).

Results shown in Fig. 5 demonstrate that mRNA levels of major proangiogenic growth factors (tumor cell derived) and receptors expressed on host endothelial cells were downregulated by endostatin or P125A-endostatin treatment. Moreover, Vascular

Endothelial Growth Factor (VEGF) and Angiopoietin 1 (Ang1) expression were significantly decreased by P125A-endostatin when compared to native endostatin. Angiopoietin 2 transcript was not detected in any of the samples analyzed. Basic FGF related transcript levels were equally decreased by both the native and mutant endostatin.

Target receptors for the tumor derived angiogenic factors are located on the host vascular endothelial cells. Therefore, mouse specific primers were used to study the levels of receptor molecules for VEGF and Ang-1. These studies showed that both native and P125A-endostatin decreased mRNA levels of flt-1, flk-1, tie-2 and endoglin, a coreceptor for TGF-beta. Although native endostatin showed a slightly better effect when compared to the mutant protein in decreasing flk-1 and flt-1, the differences were not statistically significant.

Inhibition of tumor growth by endostatin and P125A-endostatin

Microencapsulated endostatin is more effective than bolus administration. In our previous studies we showed that alginate beads of P125A-endostatin was more effective in inhibiting MA148 ovarian cancer growth when compared to the native protein given under similar condition (Calvo et al., 2002). These results were confirmed in a human colon cancer model system (Fig. 6). LS174T colon cancer cell line, which was used in the previous matrigel plug assay, grows aggressively in athymic mice and visible tumors can be seen as early as 3 days after subcutaneous injection. Endostatins encapsulated in alginate beads were given twice on day 3 and 10 at a dose of 20 mg/kg. Although native endostatin exhibited only a marginal inhibition of LS174T tumor growth, P125A-endostatin treatment resulted in significantly enhanced antitumor activity. At the end of

the experiment native endostatin showed 30 % inhibition of tumor growth, but P125A-endostatin decreased tumor size by 75% when compared to PBS treated control animals. These studies confirm that P125A-endostatin inhibits tumor growth more effectively than the native protein.

DISCUSSION

Human endostatin is a proteolytic fragment of collagen type XVIII (O'Reilly et al., 1997) and is generated *in situ* by elastase (Wen et al., 1999) and in the corneal epithelial cells by the action of matrilysin, MMP-7 (Lin et al., 2001). The α-1 chain of collagen XVIII is characterized by 10 domains of typical, triple-helical collagenous repeats separated by short non-collagenous regions (Oh et al., 1994). The carboxyl terminus 315 or 313 residues (mouse and human respectively) are non-collagenous and form the NC1 domain. Proteolytic processing of this domain results in the release of the C- terminal 183 or 181 residues of the NC1 domain, endostatin. Collagen XVIII and its three splice variants are expressed in a tissue specific manner and localized to the perivascular basement membrane. Endostatin like sequence is also found at the C-terminal end of α-1 chain of collagen type XV (Ramchandran et al., 1999). Protein fragments from the NC1 domains of α-1 chain (arrestin), α-2 chain (canstatin) and α-3 chain (tumstatin) of collagen type IV, are also effective in inhibiting angiogenesis and tumor growth (Kamphaus et al., 2000).

Recombinant mouse and human endostatins have been cloned and expressed (Dhanabal et al., 1999). In a number of model systems endostatin treatment either inhibited or regressed experimental tumors (O'Reilly et al., 1997). In some studies only

moderate inhibition was observed (Dhanabal et al., 1999; Yokoyama et al., 2000). Understanding the basis for these discrepancies may help in the successful clinical development of endostatins. Alternatively, structure/function studies can be used to generate more potent angiogenic inhibitors. Proline125 is located in a β-hairpin loop between the beta sheets K and L of human endostatin. An endothelial cell homing motif, NGR, is located immediately following this mutation site in human endostatin. In mouse endostatin, however, the SGR sequence is seen in place of NGR. The NGR motif was originally identified while mining for sequences capable of homing to tumor vasculature using Phage display libraries (Pasqualini et al., 2000). In spite of the non-conservative substitution of a proline to alanine, the mutant protein was expressed in soluble form and was biologically active. The CD spectrum showed that P125A-mutation did not cause major structural change. NGR containing peptides are known to inhibit endothelial cell membrane-associated aminopeptidase N activity. However, neither the native nor the mutant protein showed any detectable inhibition of aminopeptidase N. Though synthetic peptides corresponding to this region showed potent inhibition of aminopeptidase N. These studies suggest that the internal NGR sequence in endostatin is constrained and not accessible to bind aminopeptidase N. Furthermore, inhibition of this enzyme may not be directly relevant to the biological activity of endostatin since mouse and human endostatin have different sequences (SGR and NGR respectively).

Endostatin binds to two distinct classes of proteins on the endothelial cell surface. $\alpha_5\beta_1/\alpha_v\beta_3$ integrins and heparin sulphate-glycosaminoglycan component of the Glypican have been reported to be direct targets for endostatin. The domains of endostatin, which are involved in binding the target molecules on endothelial cell surface, have not been

completely characterized. The heparin binding domain of endostatin is composed of a number of positively charged arginine residues (Yamaguchi et al., 1999). There are 15 arginine residues in mouse endostatin of which 14 are conserved in human endostatin. In fact, synthetic peptides emcompassing these arginine regions showed antiangiogenic properties (Kasai et al., 2002). Other reports showed that mutagenesis of some of the arginine residues either individually or in pairs changed their affinity to heparin. These changes, however, did not affect the biological activity significantly (Sasaki et al., 1999; Yamaguchi et al., 1999). Our studies show that the P125A-mutation does not affect heparin binding. This conclusion is based on the NaCl concentration required to elute native and mutant protein from heparin affinity column.

However, cell attachment assays showed that P125A-endostatin bound more avidly than native endostatin. Enhanced binding to endothelial cells led to improved biological activity, indicated by the results of endothelial cell proliferation and migration assays. In the both assays the P125A-mutation increased bioactivity of endostatin. Enhanced binding to endothelial cells also led to improved tumor localization of endostatin. The homing specificity of endostatin to tumors compared to lung or liver tissue was also improved by P125A-mutation. It is interesting that only tumor accumulation was changed by P125A mutation. These results suggest that the target molecule for P125A is perhaps upregulated in tumor vasculature thereby facilitating higher binding.

Higher tumor homing also coincided with better *in vivo* activity in matrigel plug assay. Treated matrigels showed tumor cells forming glandular structures. Recently Hajitou *et al.* also reported a similar finding. Endostatin or angiostatin delivered by

adenoviral vectors inhibited local invasion and tumor vascularization of transplanted murine malignant keratinocytes (Hajitou et al., 2002).

Real Time PCR data showed that mRNA levels of proangiogenic factors and receptors were downregulated by endostatin treatment, with VEGF and Ang1 downregulated more by P125A-endostatin when compared to native endostatin. Histochemical analysis also showed that VEGF protein levels were decreased in endostatin or P125A-endostatin treated tumor tissues. Our results are in agreement with those of Calvo *et al.* who showed, in the C3(1)/SV40 transgenic mouse model, that P125A-endostatin treatment suppressed mRNA and protein levels of VEGF (Calvo et al., 2002). Female C3(1)/SV40 mice treated with P125A-endostatin for a three week period showed significant delay in tumor development, reduced tumor burden and increased survival (Calvo et al., 2002). Hajitou *et al.* also showed 3- to 10-fold down regulation of VEGF mRNA expression in endostatin treated aortic ring (Hajitou et al., 2002). These results indicate endostatin affects proangiogenic factor expression in the tumor microenvironment.

Slow release of endostatin by alginate encapsulation was used to determine antitumor efficacy. Unlike the bolus injection protocol, alginate entrapped endostatin was given once a week. This method reduced the cumulative dose to be given to each mouse by seven-fold. Kisker *et al.* also showed that continuous administration using a mini-osmotic pump increased the potency of endostatin therapy (Kisker et al., 2001). Present studies clearly demonstrate that P125A-endostatin inhibits colon carcinoma growth more effectively when compared to the native endostatin.

In summary, these studies show that human endostatin can be genetically modified to improve its ability to bind and inhibit endothelial cells. Higher binding also coincided with changes in potency in inhibiting cell proliferation and migration, and in homing to tumors. Such differences in tumor homing properties can contribute to improved anti-tumor activity of mutant endostatin.

The mechanism of enhanced binding to endothelial cells of P125A-endostatin still not entirely clear. It is likely that binding to glypican (supported by heparin binding data) is not altered by P125A mutation. However, the P125A mutation may expose cryptic determinants in endostatin, which can in turn bind to novel target molecules on endothelial cells. Such an interaction may enhance binding of P125A-endostatin to endothelial cells. We initially hypothesized that aminopeptidase N could be a potential target for P125A-endostatin. However, our current studies clearly demonstrated that P125A-endostatin did not bind to aminopeptidase N. Further work will be necessary to understand the molecular target and mechanism of enhanced binding of P125A-endostatin to endothelial cells.

ACKNOWLEDGEMENTS

This work was supported in part by a grant from the USMRMC (DAMD17-99-19564), Gynecologic Oncology Group and Minnesota Ovarian Cancer Alliance. Authors would like to thank Dr. Robin L. Bliss, Comprehensive Cancer Center, for statistical analysis, and Ms. Shaoying Li for technical assistance. Dr. Thao Yang and Anna Maria Piras helped in the CD spectral analysis of proteins.

REFERENCES

Arap, W., Pasqualini, R. & Ruoslahti, E. (1998). Cancer treatment by targeted drug delivery to tumor vasculature in a mouse model. *Science*, **279,** 377-80.

Boehm, T., Folkman, J., Browder, T. & O'Reilly, M.S. (1997). Antiangiogenic therapy of experimental cancer does not induce acquired drug resistance. *Nature*, **390,** 404-7.

Calvo, A., Yokoyama, Y., Smith, L.E., Ali, I., Shih, S.C., Feldman, A.L., Libutti, S.K., Ramakrishnan, S. & Green, J.E. (2002). Inhibition of the mammary carcinoma angiogenic switch in C3(1)/SV40 transgenic mice by a mutated form of human endostatin. *Int J Cancer*, **101,** 224-34.

Carmichael, J., DeGraff, W.G., Gazdar, A.F., Minna, J.D. & Mitchell, J.B. (1987). Evaluation of a tetrazolium-based semiautomated colorimetric assay: assessment of chemosensitivity testing. *Cancer Res*, **47,** 936-42.

Dhanabal, M., Ramchandran, R., Volk, R., Stillman, I.E., Lombardo, M., Iruela-Arispe, M.L., Simons, M. & Sukhatme, V.P. (1999). Endostatin: yeast production, mutants, and antitumor effect in renal cell carcinoma. *Cancer Res*, **59,** 189-97.

Ding, Y.H., Javaherian, K., Lo, K.M., Chopra, R., Boehm, T., Lanciotti, J., Harris, B.A., Li, Y., Shapiro, R., Hohenester, E., Timpl, R., Folkman, J. & Wiley, D.C. (1998). Zinc-dependent dimers observed in crystals of human endostatin. *Proc Natl Acad Sci U S A*, **95,** 10443-8.

Dixelius, J., Larsson, H., Sasaki, T., Holmqvist, K., Lu, L., Engstrom, A., Timpl, R., Welsh, M. & Claesson-Welsh, L. (2000). Endostatin-induced tyrosine kinase signaling through the Shb adaptor protein regulates endothelial cell apoptosis. *Blood*, **95,** 3403-11.

Gerber, H.P., Kowalski, J., Sherman, D., Eberhard, D.A. & Ferrara, N. (2000). Complete inhibition of rhabdomyosarcoma xenograft growth and neovascularization requires blockade of both tumor and host vascular endothelial growth factor. *Cancer Res*, **60,** 6253-8.

Hajitou, A., Grignet, C., Devy, L., Berndt, S., Blacher, S., Deroanne, C.F., Bajou, K., Fong, T., Chiang, Y., Foidart, J.M. & Noel, A. (2002). The antitumoral effect of endostatin and angiostatin is associated with a down-regulation of vascular endothelial growth factor expression in tumor cells. *FASEB J*, **16,** 1802-4.

Hanai, J., Karumanchi, S.A., Kale, S., Tank, J., Hu, G., Chan, B., Ramchandran, R., Jha, V., Sukhatme, V.P. & Sokol, S. (2002). Endostatin is a potential inhibitor of Wnt signaling. *J Cell Biol*, **158,** 529-39.

Kamphaus, G.D., Colorado, P.C., Panka, D.J., Hopfer, H., Ramchandran, R., Torre, A., Maeshima, Y., Mier, J.W., Sukhatme, V.P. & Kalluri, R. (2000). Canstatin, a novel matrix-derived inhibitor of angiogenesis and tumor growth. *J Biol Chem*, **275,** 1209-15.

Karumanchi, S.A., Jha, V., Ramchandran, R., Karihaloo, A., Tsiokas, L., Chan, B., Dhanabal, M., Hanai, J.I., Venkataraman, G., Shriver, Z., Keiser, N., Kalluri, R., Zeng, H., Mukhopadhyay, D., Chen, R.L., Lander, A.D., Hagihara, K., Yamaguchi, Y., Sasisekharan, R., Cantley, L. & Sukhatme, V.P. (2001). Cell surface glypicans are low-affinity endostatin receptors. *Mol Cell*, **7,** 811-22.

Kasai, S., Nagasawa, H., Shimamura, M., Uto, Y. & Hori, H. (2002). Design and synthesis of antiangiogenic/heparin-binding arginine dendrimer mimicking the surface of endostatin. *Bioorg Med Chem Lett*, **12,** 951-4.

Kim, Y.M., Jang, J.W., Lee, O.H., Yeon, J., Choi, E.Y., Kim, K.W., Lee, S.T. & Kwon, Y.G. (2000). Endostatin inhibits endothelial and tumor cellular invasion by blocking the activation and catalytic activity of matrix metalloproteinase. *Cancer Res*, **60,** 5410-3.

Kisker, O., Becker, C.M., Prox, D., Fannon, M., D'Amato, R., Flynn, E., Fogler, W.E., Sim, B.K., Allred, E.N., Pirie-Shepherd, S.R. & Folkman, J. (2001). Continuous administration of endostatin by intraperitoneally implanted osmotic pump improves the efficacy and potency of therapy in a mouse xenograft tumor model. *Cancer Res*, **61,** 7669-74.

Lin, H.C., Chang, J.H., Jain, S., Gabison, E.E., Kure, T., Kato, T., Fukai, N. & Azar, D.T. (2001). Matrilysin cleavage of corneal collagen type XVIII NC1 domain and generation of a 28-kDa fragment. *Invest Ophthalmol Vis Sci*, **42,** 2517-24.

O'Reilly, M.S., Boehm, T., Shing, Y., Fukai, N., Vasios, G., Lane, W.S., Flynn, E., Birkhead, J.R., Olsen, B.R. & Folkman, J. (1997). Endostatin: an endogenous inhibitor of angiogenesis and tumor growth. *Cell*, **88,** 277-85.

Oh, S.P., Kamagata, Y., Muragaki, Y., Timmons, S., Ooshima, A. & Olsen, B.R. (1994). Isolation and sequencing of cDNAs for proteins with multiple domains of Gly-Xaa-Yaa repeats identify a distinct family of collagenous proteins. *Proc Natl Acad Sci U S A*, **91,** 4229-33.

Olson, T.A., Mohanraj, D. & Ramakrishnan, S. (1996). In vivo neutralization of vascular endothelial growth factor (VEGF)/vascular permeability factor (VPF) inhibits ovarian carcinoma-associated ascites formation and tumor growth. *International Journal of Oncology*, **8,** 505-511.

Pasqualini, R., Koivunen, E., Kain, R., Lahdenranta, J., Sakamoto, M., Stryhn, A., Ashmun, R.A., Shapiro, L.H., Arap, W. & Ruoslahti, E. (2000). Aminopeptidase N is a receptor for tumor-homing peptides and a target for inhibiting angiogenesis. *Cancer Res*, **60,** 722-7.

Ramakrishnan, S., Olson, T.A., Bautch, V.L. & Mohanraj, D. (1996). Vascular endothelial growth factor-toxin conjugate specifically inhibits KDR/flk-1-positive endothelial cell proliferation in vitro and angiogenesis in vivo. *Cancer Res*, **56,** 1324-30.

Ramchandran, R., Dhanabal, M., Volk, R., Waterman, M.J., Segal, M., Lu, H., Knebelmann, B. & Sukhatme, V.P. (1999). Antiangiogenic activity of restin, NC10 domain of human collagen XV: comparison to endostatin. *Biochem Biophys Res Commun*, **255,** 735-9.

Rehn, M., Veikkola, T., Kukk-Valdre, E., Nakamura, H., Ilmonen, M., Lombardo, C., Pihlajaniemi, T., Alitalo, K. & Vuori, K. (2001). Interaction of endostatin with integrins implicated in angiogenesis. *Proc Natl Acad Sci U S A*, **98,** 1024-9.

Sasaki, T., Larsson, H., Kreuger, J., Salmivirta, M., Claesson-Welsh, L., Lindahl, U., Hohenester, E. & Timpl, R. (1999). Structural basis and potential role of heparin/heparan sulfate binding to the angiogenesis inhibitor endostatin. *Embo J*, **18,** 6240-8.

Shichiri, M. & Hirata, Y. (2001). Antiangiogenesis signals by endostatin. *Faseb J*, **15,** 1044-53.

Wen, W., Moses, M.A., Wiederschain, D., Arbiser, J.L. & Folkman, J. (1999). The generation of endostatin is mediated by elastase. *Cancer Res.*, **59,** 6052-6.

Wickstrom, S.A., Alitalo, K. & Keiski-Oja, J. (2002). Endostatin associates with integrin alpha5beta1 and caveolin-1, and activates Src via a tyrosyl phosphatase-dependent pathway in human endothelial cells. *Cancer Res*, **62,** 5580-9.

Wild, R., Ramakrishnan, S., Sedgewick, J. & Griffioen, A.W. (2000). Quantitative Assessment of Angiogenesis and Tumor Vessel Architecture by Computer-Assisted Digital Image Analysis: Effects of VEGF-Toxin Conjugate on Tumor Microvessel Density. *Microvasc Res*, **59,** 368-376.

Yamaguchi, N., Anand-Apte, B., Lee, M., Sasaki, T., Fukai, N., Shapiro, R., Que, I., Lowik, C., Timpl, R. & Olsen, B.R. (1999). Endostatin inhibits VEGF-induced endothelial cell migration and tumor growth independently of zinc binding. *Embo J*, **18,** 4414-23.

Yokoyama, Y., Dhanabal, M., Griffioen, A.W., Sukhatme, V.P. & Ramakrishnan, S. (2000). Synergy between angiostatin and endostatin: inhibition of ovarian cancer growth. *Cancer Res*, **60,** 2190-6.

Yoon, S.S., Eto, H., Lin, C.M., Nakamura, H., Pawlik, T.M., Song, S.U. & Tanabe, K.K. (1999). Mouse endostatin inhibits the formation of lung and liver metastases [In Process Citation]. *Cancer Res*, **59,** 6251-6.

Zhang, L., Yu, D., Hu, M., Xiong, S., Lang, A., Ellis, L.M. & Pollock, R.E. (2000). Wild-type p53 suppresses angiogenesis in human leiomyosarcoma and synovial sarcoma by transcriptional suppression of vascular endothelial growth factor expression. *Cancer Res*, **60,** 3655-61.

Table 1. Primer Sequences used for Real-time PCR

Probe Name	Forward Primer	Reverse Primer
Human VEGF	AATGACGAGGGCGTGGAGT	TTGATCCGCATAATCTGCATG
Human bFGF	TGAATCACTAACTGACTGAAAATTGA	GAAGGGTCTCCCGCATACT
Human Angiopoietin-1	CCTTCCAGCAATAAGTGGTAGTT	CAAACGGCTCCAGATTCA
Human IL-8	TTTAGCATAGCTGGACATTAAAGAG	GCAAATATGCTTAGGCTTTAACC
Human GAPDH	CCACCCATGGCAAATTCCATGGCA	TCTACACGGCAGGTCAGGTCCACC
Mouse flt-1	GTCGGCTGCAGTGTGTAAGT	TGCTGTTCTCATCCGTTTCT
Mouse flk-1	TGTCAAGTGGCGGTAAAGG	CACAAAGCTAAAATACTGAGGACTTG
Mouse tie-2	CGGCCAGGTACATAGGAGGAA	CCCCCACTTCTGAGCTTCAC
Mouse Endoglin	GCAGGCAAGAACTCAGACAT	AGCTCCCTCAGCTTCTGTTT
Mouse GAPDH	ATGTTCCAGTATGACTCCACTCACG	GAAGACACCAGTAGACTCCACGACA

FIGURE LEGENDS

Figure 1 Characterization of P125A-endostatin – Increased binding and biological activity. A: Structural details surrounding the mutation site are shown. Swiss PDB Viewer program was used to generate the figure based on the structural information published by Ding *et al.* (Ding et al., 1998). P125 is followed by N126, G127, and R128. B: Circular Dichroism Spectroscopy of endostatin (---) and P125A-endostatin (——). C: Cell attachment assay. Single cell suspension of HUVEC, prelabeled with 5(6)-CFDA, was added into triplicate wells coated with either endostatin or P125A-endostatin at a concentration of 1 nmole / well. Wells coated with 0.2 % gelatin were used as maximum attachment (100%). Bound cells were quantified by a fluorescence plate reader. Values represent mean of 2 independent experiments. Data are expressed as a mean (columns) ± SD (bars). Statistical significance was determined by Student's t-test. $^{**}p<0.01$. D: Effect of endostatin (open bars) and P125A-endostatin (closed bars) on endothelial cell (HUVEC) migration. Basic FGF (25 ng/ml) was used to induce migration of endothelial cells. Data are expressed as a mean (columns) ± SE (bars). Statistical significance was determined using Student's t-test. $^{*}p<0.05$, $^{**}p<0.01$. E: Tumor Localization. Human colon carcinoma cells (LS174T) were injected s.c. into female athymic nude mice. When the tumor size was around 500 mm^3 (10 days after inoculation), Endostatin (open bars) or P125A-endostatin (closed bars) was injected at a dose of 20 mg/kg subcutaneously. Endostatin levels were determined by ELISA. Endostatin levels are expressed as a percent of serum levels.

Figure 2 Effect of endostatin and synthetic peptides on aminopeptidase N activity.

A: Aminopeptidase N was extracted from HUVEC cultures. Bestatin was used as a positive control, and leupeptin treatment served as a negative control. Values represent mean of two independent experiments. B: Two polypeptides containing 14 amino acid residues (S118-T131) spanning the mutation site P125 were synthesized. One of the peptides had the native sequence and the other contained P to A substitution. Both peptides included the NGR-motif. ●, SR1 peptide (P125A); ○, SR2 peptide (native sequence); ▲, bestatin.

Figure 3 Histological analysis of matrigel plugs. Matrigel plugs containing LS174 human colon cancer cell line were used to determine the effect of endostatin and P125A-endostatin on angiogenesis. A-F show H&E staining; A-C, x100 magnification, D-F, x400 magnification, Green squares in A-C indicate the area of the images in x400 magnification of D-F. G-I show vessel staining with anti-CD31 antibody (red) and nuclei staining with DAPI (blue) x 200 magnification; J-L VEGF expression detected by indirect immunofluorescence using FITC conjugated antibodies (green) with DAPI (blue). A, D, G and J, control; B, E, H and K; native endostatin treated Matrigel sections; C, F, I and L; P125A-endostatin treated Matrigel sections.

Figure 4 Inhibition of angiogenesis by native and mutant endostatin. Seven to ten frames of matrigel sections stained with anti-mouse CD31-PE were captured per sample and then analyzed for microvessel density. A, pixel density; B, blood vessel ends (Ends); C, branch points (Nodes); D, vessel length. Statistical significance was determined using Student's t-test. **, $p<0.01$; *, $p<0.05$. The error bars indicate SE.

Figure 5 Downregulation of proangiogenic growth factors and receptors by endostatin treatment. Real Time PCR data were normalized by mRNA level to GAPDH. Data show relative mRNA levels. Messenger RNA of human proangiogenic factors (VEGF, bFGF, Angiopoietin1 and IL8) and mouse receptors (flt-1, flk-1, tie2 and Endoglin) in Matrigel plugs were downregulated by endostatin and P125A-endostatin treatment.

Figure 6 Improved inhibition of tumor growth by P125A-Endostatin. Human colon carcinoma cell line, LS174T was injected s.c. into female athymic mice. After tumors reached a palpable size, mice were treated with endostatin and P125A-endostatin encapsulated in alginate beads (s.c.) at a dose of 20 mg/kg/week. Endostatins were administered two times one week apart to colon cancer bearing mice. Arrows denote time points at which microencapsulated endostatins were administered. Two endostatin treatments were given one week apart. ❐, Alginate bead control (PBS); ○, Endostatin; ●, P125A-Endostatin. Mean tumor volume of control and treated groups are shown. Statistical significance was determined using Student's t-test. *$p<0.05$, **$p<0.01$. The error bars indicate SE.

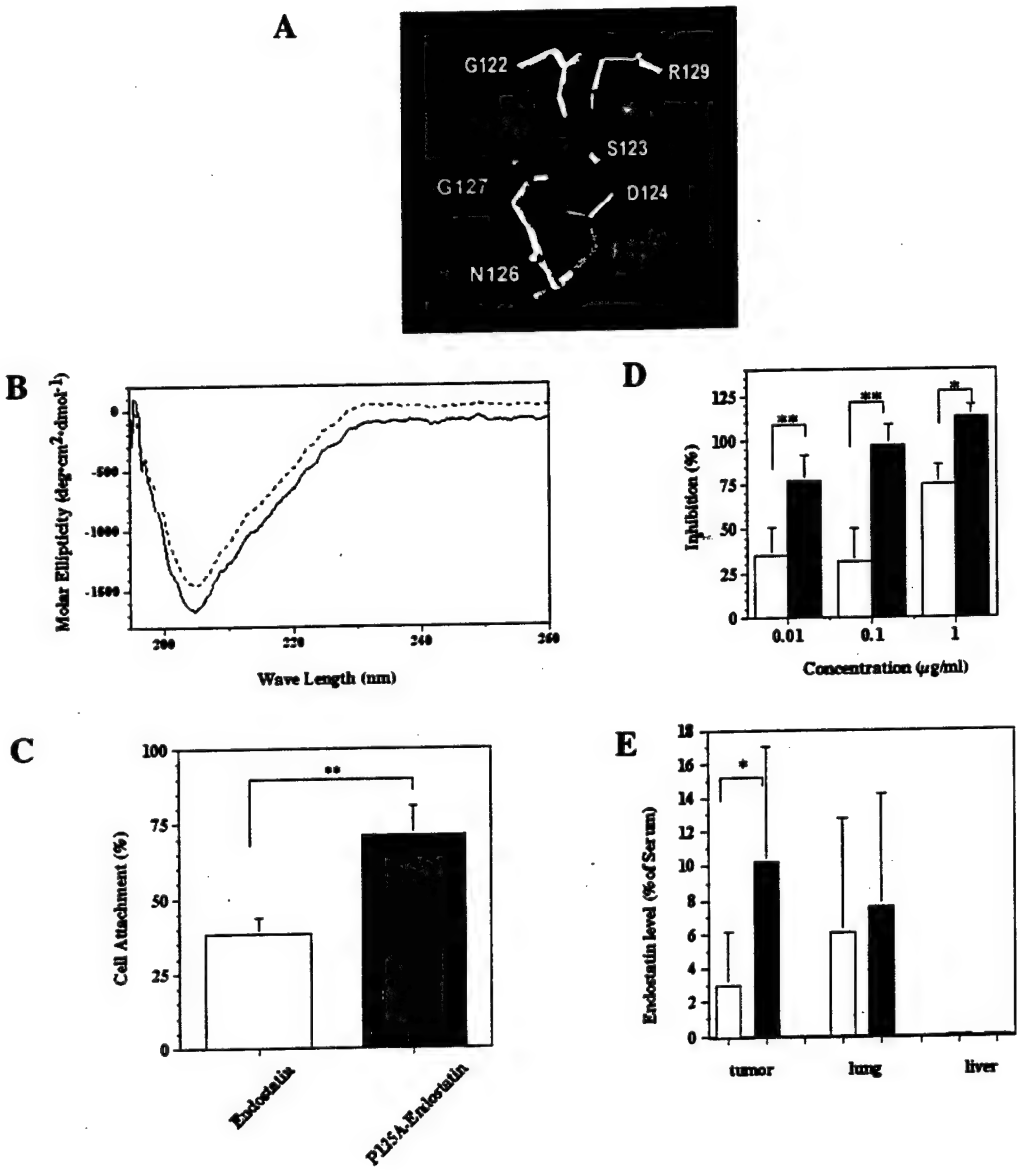
A
G122
R129
S123
G127
D124
N126
B
Molar Ellipticity (deg·cm²·dmol⁻¹)
0
-500
-1000
-1500
200
220
240
260
Wave Length (nm)
D
Inhibition (%)
125
100
75
50
25
0
**
**
*
0.01
0.1
1
Concentration (μg/ml)
C
Cell Attachment (%)
100
75
50
25
0
**
Endostatin
P125A-Endostatin
E
Endostatin level (%of Serum)
18
16
14
12
10
8
6
4
2
0
*
tumor
lung
liver

Figure 1

A

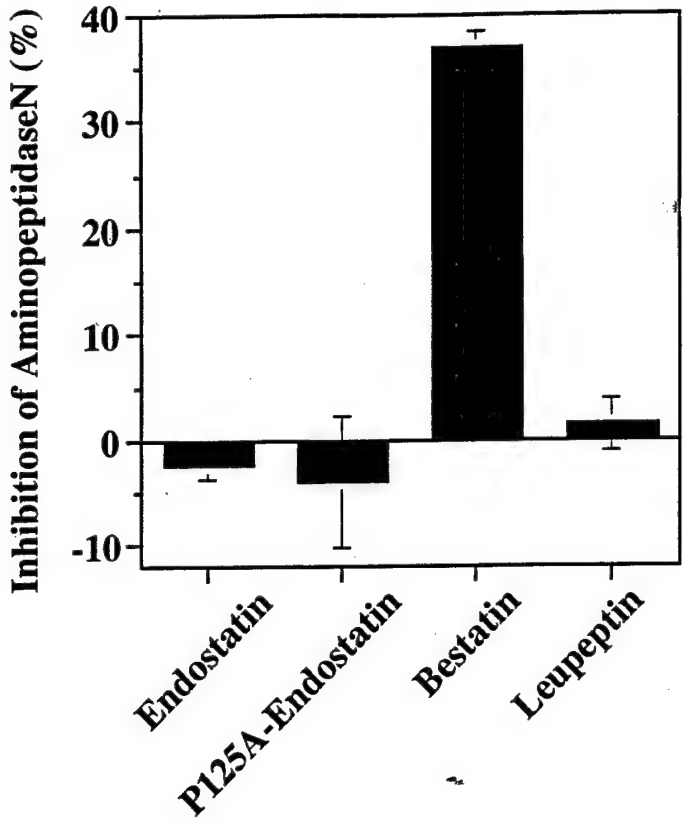
Inhibition of AminopeptidaseN (%)
40
30
20
10
0
-10
Endostatin
P125A-Endostatin
Bestatin
Leupeptin

B

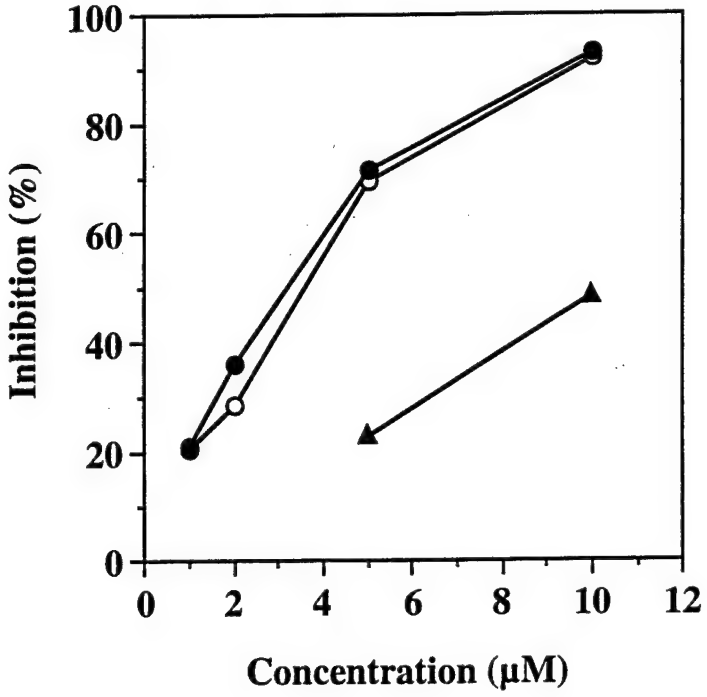
Inhibition (%)
100
80
60
40
20
0
0
2
4
6
8
10
12
Concentration (μM)

Figure 2

Figure 3

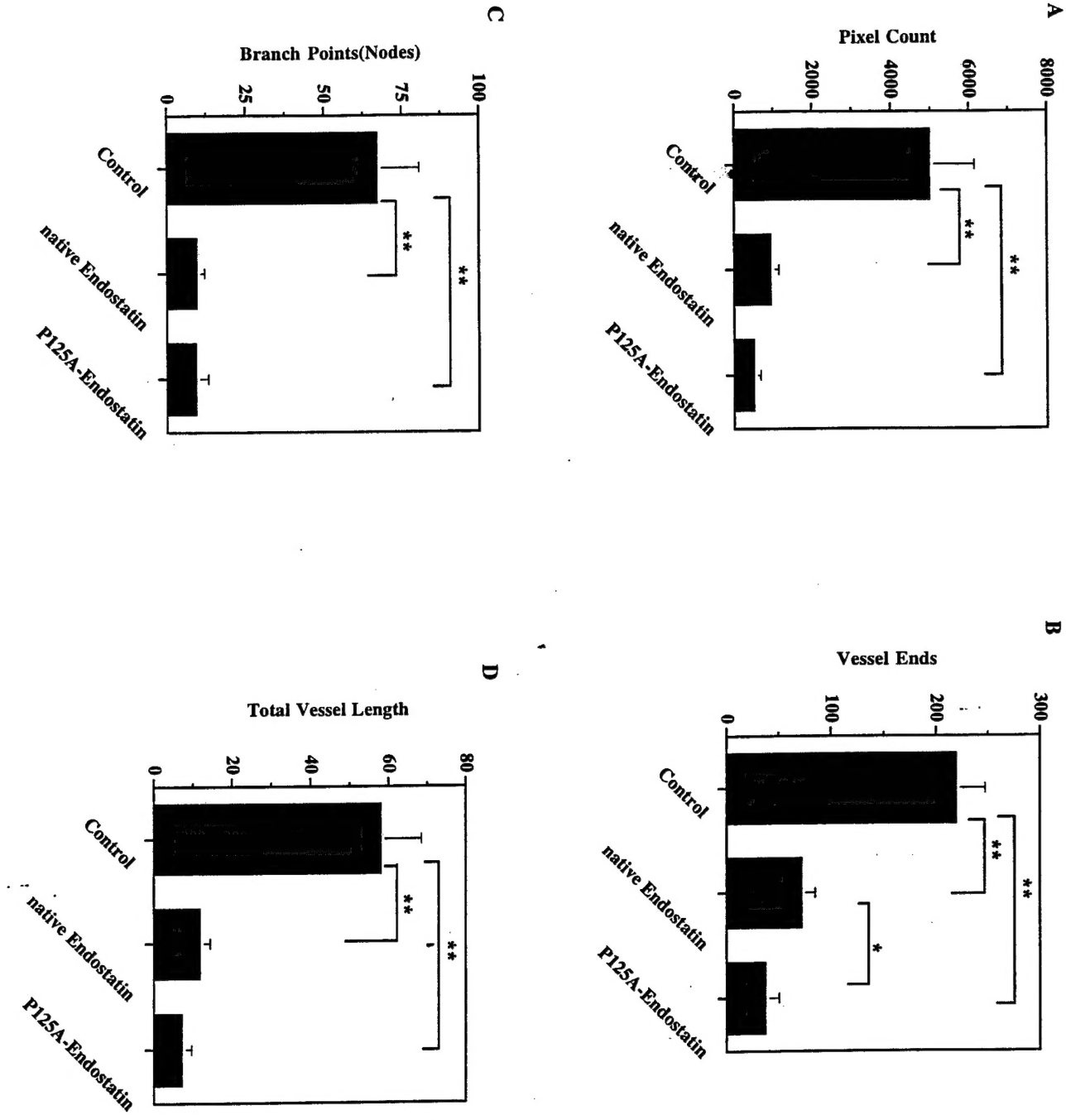
A
Pixel Count
0
2000
4000
6000
8000
Control
native Endostatin
P125A-Endostatin
**
**
B
Vessel Ends
0
100
200
300
Control
native Endostatin
P125A-Endostatin
**
*
**
C
Branch Points(Nodes)
0
25
50
75
100
Control
native Endostatin
P125A-Endostatin
**
**
D
Total Vessel Length
0
20
40
60
80
Control
native Endostatin
P125A-Endostatin
**
**

Figure 4

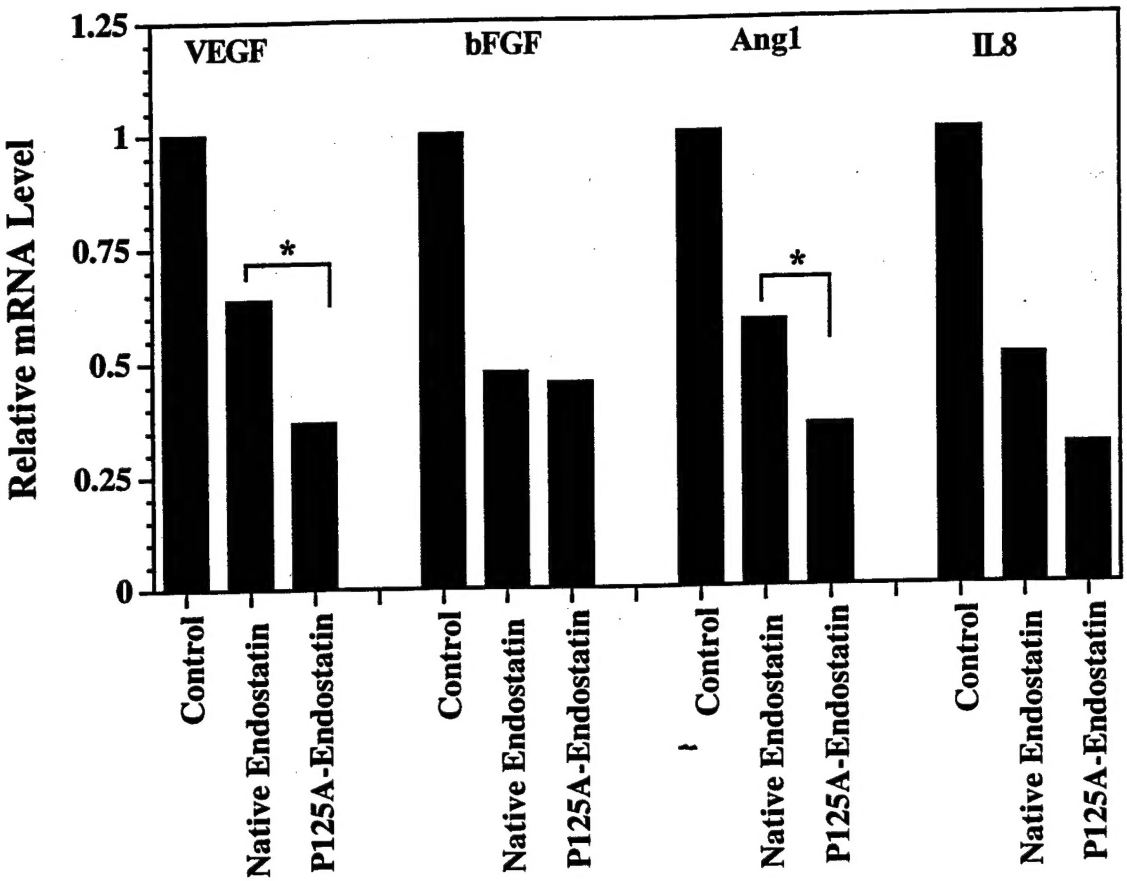
VEGF
bFGF
Ang1
IL8
Relative mRNA Level
1.25
1
0.75
0.5
0.25
0
*
*
Control
Native Endostatin
P125A-Endostatin
Control
Native Endostatin
P125A-Endostatin
Control
Native Endostatin
P125A-Endostatin
Control
Native Endostatin
P125A-Endostatin

Figure 5

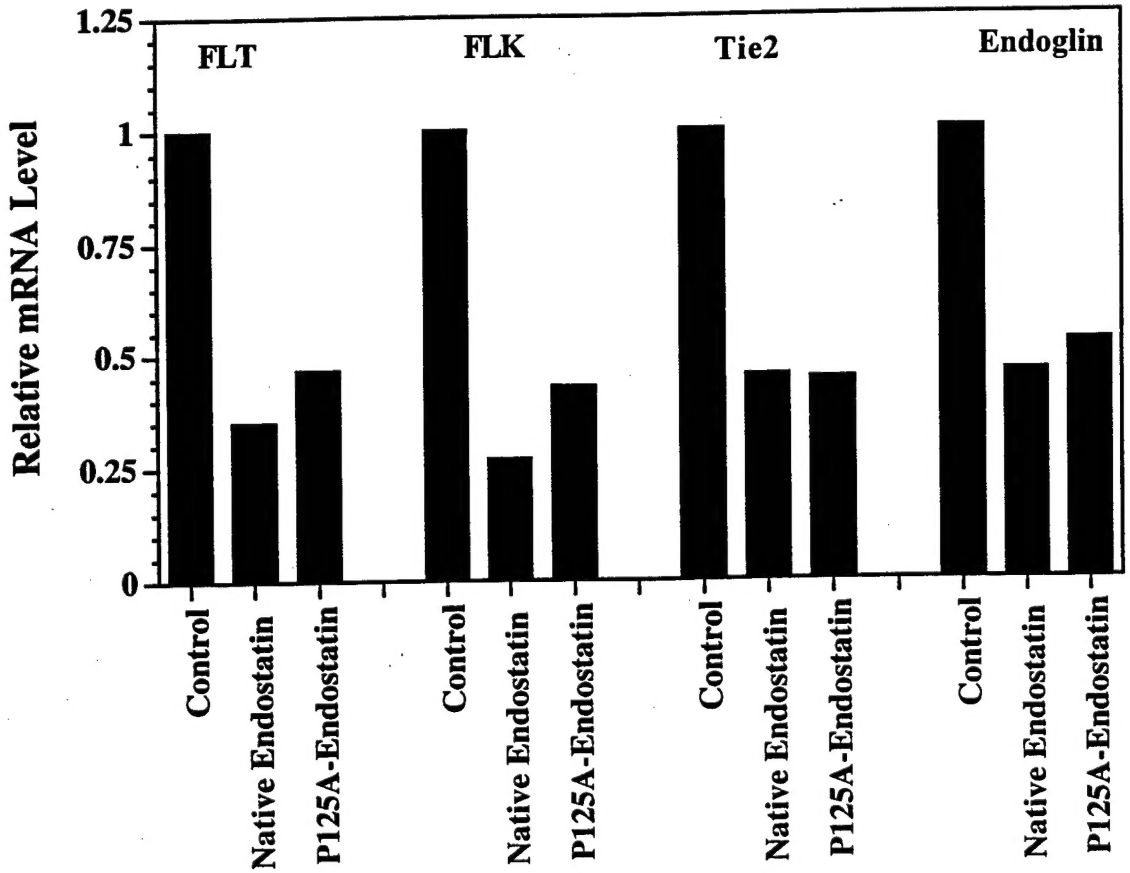
FLT
FLK
Tie2
Endoglin
Relative mRNA Level
1.25
1
0.75
0.5
0.25
0
Control
Native Endostatin
P125A-Endostatin
Control
Native Endostatin
P125A-Endostatin
Control
Native Endostatin
P125A-Endostatin
Control
Native Endostatin
P125A-Endostatin

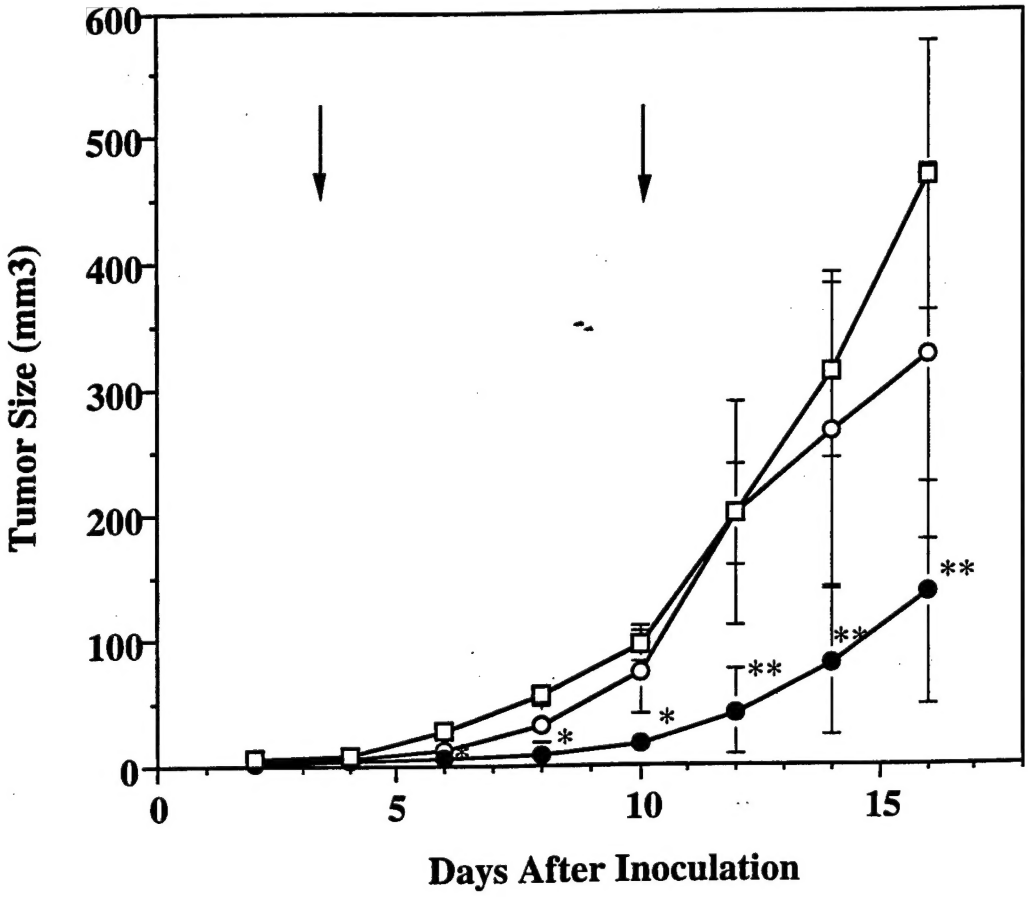
600
500
400
300
200
100
0
Tumor Size (mm3)
0
5
10
15
Days After Inoculation
*
*
**
**
**

Figure 6